Master thesis

On tip-split wind turbine blades

H. T. Verheul

This thesis is confidential and cannot be made public until November 21, 2023.

TU Delft Delft University of Technology

LM WIND POWER
a GE Renewable Energy business

Challenge the future

Master thesis

On tip-split wind turbine blades

by

H. T. Verheul

to obtain the degree of

Master of Science
in Aerospace Engineering

at the Delft University of Technology,
to be defended publicly on Wednesday November 21, 2018 at 14:00.

Student number:	4391047	
Project duration:	May 1, 2017 – November 21, 2018	
Supervisor	Dr. Ir. J.J.E. Teuwen	TU Delft
	Ir. H.P. Minnee	LM Windpower
Thesis committee:	Prof. C.A. Dransfeld	TU Delft
	Dr. Ir. C.J. Simao Ferreira	TU Delft

This thesis is confidential and cannot be made public until November 21, 2023.

TU Delft

LM WIND POWER
a GE Renewable Energy business

Summary

To achieve the goals set in the Paris agreement, it is required to replace fossil energy by renewable energy. One source of renewable energy, also used extensively at the start of the industrial revolution, is the wind. Unfortunately, utilizing wind energy bears substantial investment costs as the capital cost of a wind turbine are the largest cost for a wind energy project. Since 1980 the cost of wind energy has reduced significantly due to technological improvements and upscaling of wind turbines. As a result, the transportation of wind turbine blades can now be a substantial cost. These could be reduced if the blades can be manufactured in multiple pieces and assembled at or near the final turbine installation area. LM Wind Power is investigating with the Hyller project if it is possible to build a tip split wind turbine blade. Next to reducing the transportation cost, this project also focusses on reducing the manufacturing cost by using different production processes for the root and tip sections. The root section was produced with the traditional two-shell production process and the tip section was produced with a new one-shot infusion and cure production process. This process should not only produce the parts at lower cost, it should also improve part quality. In this thesis, three main subjects related to the alignment of the wind turbine blade sections are reviewed.

The first is the alignment process itself, for this a low-cost tool was build which could be manipulated easily in an all six degrees of freedom. This tool and lasers were used with actual size parts in alignment trials. When the alignment error could not be reduced further, 3D scans were made to determine the accuracy of this alignment process. These scans revealed that the tip section was misaligned $< \pm 3$ mm & $< \pm 0.15°$ relative to the designed position. These results were obtained with accurate reference points on the blade sections. To determine if mould marks could be used to generate accurate reference points, their relative positional accuracy was measured on several wind turbine blade laminates. It was expected that mould marks move due to chemical and thermal shrinkage. Therefore, thin CLT was used to predict the movement strains. For most measurements the predicted strain was higher than the measured strain. As the measurement error was relatively high compared to the measured deviations, more accurate measurements are required to determine if the strains are indeed lower than would be expected from chemical and thermal shrinkage. All of this was combined in the production of the Hyller test article. Unfortunately, some problems in the production of both blade sections prevented correct alignment of both sections. This resulted in the achieved alignment deviations being larger as compared to the deviations in the alignment trials ($< \pm 25$ mm & $< \pm 0.5°$).

The second subject that is reviewed in this thesis is the impact of angular alignment deviations on the aerodynamics. This was done with the help of a lifting line simulation program. It was assumed and verified, that the twist angle is the most critical alignment angle with respect to the power output (this is a rotation of the tip section over the length axis). With simulations, the relationship between the twist angle alignment deviation of the tip section and power output was established, for wind turbine blades containing small manufactured twist errors. For an increasing twist angle deviation, the power output will reduce with an increasing rate. Whereas a negative twist angle deviation will result in a small increase in power output. With additional simulations the relation between the variance in power output and the average twist angle error of the tip section was reviewed. This revealed an exponential relationship, and that the variance in power output can be reduced significantly relative to single piece wind turbine blades that contain similar manufactured twist errors.

The third subject reviewed in this thesis is the variation in profile thickness, in the web region, due to different blade production processes. In order to calculate the joint strength, it is required to know this variation. Since it is unknown if there is a variation or what the cause for this variation is, a review was made. This revealed that for the two-shell production process the bondline thickness is most influential, whereas the web position has a small, almost negligible, influence. For the one-shot infusion production process, it was found that the profile thickness varies with ± 4 mm. This is caused in part by a variation in mould geometry due to the mould closure process, which has an influence $< \pm 2$ mm on the profile thickness. Furthermore, the measurement data indicated potentially a relation between the trailing edge web position and the profile thickness for the one-shot production process.

Preface

This thesis was done in cooperation with LM Wind Power on the Hyller project. The goal of this project is to build a tip-split wind turbine blade for off-shore usage in wind farms at sites with a predominant wind direction. The acronym Hyller, which stands for 'high yield low loads extended rotor', gives a basic summery of the topic of this research project. The idea is to enlarge the rotors which are in the wake of other turbines. This should give an improved energy output without increasing the wind loads on the wind turbine blade. Then by optimizing the weight of the tip section the rotor size could be enlarged without increasing the blade mass. To also reduce the transportation cost, the separate wind turbine blade sections have to be aligned and joined on-site. This led to the master graduation assignment from LM Wind Power which can be summarized as followed: 'Required tolerances to safeguard the structural as well as the aerodynamic behaviour of the resulting blade as compared to a one-piece blade with the same dimensions and loads'. As this is too big of an assignment for a master thesis, the research was focused on three major topics: the alignment of a tip-split blade, aerodynamic effects of angular deviations on power output and lastly the influence of blade production processes on the variation in profile thickness. I hope that you will enjoy reading this report as much as I enjoyed doing all the tests!

During this thesis I got to spend half a year in Denmark, working at the technology centre of LM Wind Power in Lunderskov. I would like to thank Hans Minnee and all other people at LM for giving me this possibility. I would also like to extent my gratitude to Jesper Thuesen for help he gave as the day to day supervisor from LM wind power, and of course also to all other LM employees which were involved in the Hyller project. I would also like to thank my university supervisor, Julie Teuwen, for all the time she put in supervising me during this master graduation project. Furthermore, I want to thank Ard Flier for providing me with a desk to work at after I moved back to the Netherlands. I like to extend my gratitude to Maarten Frijling & Brendon de Raad for their help. Lastly, I would also like to thank my girlfriend, fiancé, wife and parents for providing a listening ear and all other people that have helped me during this project.

H. T. Verheul
Dordrecht, November 2018

Contents

List of symbols & abbreviations

Symbols

°C = Temperature in degrees Celsius
ΔP = Difference in power
α = Angle of attack / Angle of twist
β = Flapwise angle
γ = Edgewise angle
ρ = Air density
Cl = Coefficient of lift
Cd = Coefficient of drag
z = Position along blade length, 0 at the root

Abbreviations

2D = two dimensional 3D = three dimensional
ABS = Absolute
AEP = Annual Energy Production, the amount of energy produced in one year
AOA = Angle Of Attack, Angle relative to local airspeed
AVG = Average
CAD = Computer-Aided Design
CCS = Coefficient of Chemical Shrinkage
CFD = Computational Fluid Dynamics
CLT = Classical Lamination Theory
CNC = Computer Numerically Controlled
CTE = Coefficient of Thermal Expansion
DOF = Degree/Degrees Of Freedom
DW = Down Wind, the profile side closest to the tower
FEM = Finite Element Method FRBM = Flapwise Root Bending Moment LE = Leading Edge
LM = LM Windpower
LSL = Lower Specified Limit
m = Meter
mm = Millimetre
SD = Standard Deviation
TA = Test Article
TE = Trailing Edge
UD = Uni-Directional
UW = Up Wind, the profile side directly in the wind
USL = Upper Specified Limit
VARTM = Vacuum Assisted Resin Transfer Moulding

1 Introduction

The eighteenth century is known most notably by the industrial revolution in the Western world. It began with water and wind powered machines but this quickly changed to fossil powered machines [1]. In the following centuries, the western world became highly dependent on this fossil energy. This form of energy results in high carbon-dioxide emissions. On the fourth of November, 2016 the Paris agreement came into force [2]. With this agreement 89% of the countries connected to the United Nations, agreed to reduce the usage of fossil energy to significantly reduce the carbon-dioxide emissions. In order to achieve this, fossil energy needs to be replaced by renewable energy. This is energy with much lower carbon-dioxide emissions. One source of renewable energy, also used extensively at the start of the industrial revolution, is the wind [1]. Unfortunately, utilizing wind energy bears high investment costs as the capital cost of a wind turbine is between 75%-85%[1] of the total cost for a wind energy project [3], with offshore wind projects being more expensive than onshore projects. Therefore, the cost for 75%-85% of the energy which will be produced by a wind turbine in 25 years has to be paid upfront. Since 1980 the cost of wind energy has reduced significantly due to technological improvements and upscaling of wind turbines. This allows for the first subsidy free wind energy projects to start operation in the near future [4]. However, according to Michael Guldbrandtsen, an energy market analyst, this is more the exception than the norm [5]. Therefore, the cost of wind energy has to be reduced further to make it economically possible to achieve the goals set in the Paris agreement.

1.1. Reducing cost of wind energy by building split wind turbine blades

The transportation cost of wind turbine blades rises sharply for blades over 46 meters long [6]. As a result, the transportation costs are about 2% of the total cost of an onshore wind turbine with 61 meter long blades [7]. Another jump in the transportation costs comes for blades with lengths over 61 meters [6], and these blades are more likely to not be able to reach potential wind sites. For example, LM Wind Power produced a 88.4 meter long prototype blade in 2016, at the moment the longest in the world [8]. This blade had to be transported 217 km over public roads, requiring one year of planning. Due to the large dimensions of the blade, road signs, guardrails and trees had to be (temporarily) removed to allow the blade to pass. Now, two years later, the next biggest blade is in development and has grown to 107 meters long, with planned demonstration in 2019 [9][2]. As can be expected, transporting these large blades leads to high transportation costs. These could be reduced if the blades can be manufactured in multiple pieces and assembled at or near the final turbine installation area. Producing a blade in multiple pieces does provide more opportunities for cost reductions. For example, using the most optimal production processes for each part might result in a lower production cost. Furthermore, if the tip parts remains smaller than 40 feet (12 meters), they can easily be shipped in standard containers. Allowing for one blade to be produced in different continents, possibly leading to additional cost savings. As a result, the total cost of a blade at the final turbine installation area could be reduced greatly. Another possibility in which tip-split blades can reduce the cost of energy is in wind farms with a predominant wind direction. This is what the Hyller project of LM is investigating, where Hyller stands for: High yield low loads extended rotor. The idea is to enlarge the rotors of the turbines that are in the wake

[1] The variable cost of a wind turbine is generally around 20% of the total project cost. These variable cost include operation & maintenance, insurance, land rent, taxes and the employee costs [3]

[2] This blade is designed for off-shore usage and is built in a harbour to reduce the transportation cost

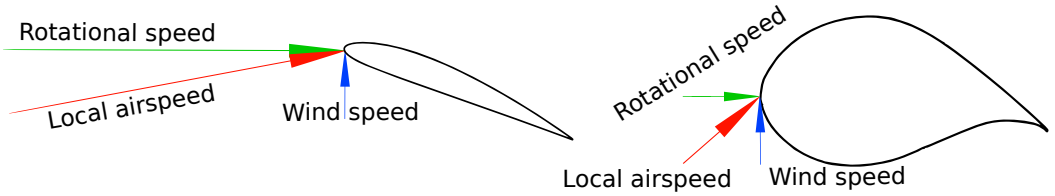

Figure 1.1: Different speeds on wind turbine blade near the tip (left) and near the root (right), inspired by [17].

of other turbines to increase the amount of energy that is produced by the wind farm. And as these enlarged rotor are in the wake of other turbines, it is assumed that the loads on the blade do not increase. So the same root can be used to accommodate tip sections with different lengths.

In 1982 the first split wind turbine blade was built, it was a 11.58 meter long blade which was split in the middle and joined on-site with bolts. This blade worked successfully for a number of years, although the maintenance was problematic [10]. Then in 2000, two different root split blades where build and structurally tested by LM Wind Power and its research partners [11–13]. One being a 13.4 meter long blade with a tube connection and the other a 23.3 meter long blade joined with bolts. However, the conclusion of these projects was that the cost would increase 15%-20% (mainly due to an increase in production cost), while the transportation cost would only be reduced by 5% on average for a 60 m blade. The first commercial split blade came in 2007 from Enercon. A 59 meter long blade split at 40% of the blade length and connected with bolts. This blade was not a game changer as it was not installed often [14]. In the meantime other commercial split wind turbine blades have been released as well. However, according to Nielsen, a wind turbine industry market analyst [15], there are no cost effective split wind turbine blades on the market. However, the large number of possibilities and benefits of split blades will at some point allow for cost effective blades for very large offshore or onshore wind turbines [6].

All commercial and research projects to date now made the split in the middle, or closer to the root [10–14]. To determine the best location to split a wind turbine blade, the effect of the split location on the thriving design criteria at the split location must be known. On wind turbines the two most important design criteria are the aerodynamics and the structure. For aerodynamics, the local airspeed is important as it influences how much lift, and thus power, can be produced locally. Due to the rotation of wind turbine blades, the local airspeed differs along the length of the blade. At the root the rotational speed is low. Here the local airspeed is roughly equal to the wind speed. Moving to the blade tip, the rotational speed increases. At the tip, the local airspeed can be an order of magnitude larger than the wind speed. This is illustrated in figure 1.1. As the local airspeed is roughly equal to the wind speed near the root, no significant lift is produced for up to 10% of the blade length and maximum lift is produced at 85% of the blade length due to the higher local airspeed [16].

For the loads it is the opposite, on the blade tip they are low compared to the loads on the root. Although much more lift is present at the tip, the accumulated loads are much lower. These accumulated loads are the driving design requirement for the root of a wind turbine blade. In figure 1.2, the importance of the aerodynamic versus the structural requirements is illustrated as was stated by Schubel et al. [17]. From this figure it can be seen that in the tip region (67-100% of blade length), a good aerodynamic outer geometry is most important. Although maximum lift occurs at 85% of the blade length, the absolute blade tip is aerodynamically most important due to the highest local velocities and the presence of a tip vortex[3]. Whereas the aerodynamics can almost be neglected for a split in the root region (0-33% of blade length). As the structural importance of a wind turbine blade is opposite of the aerodynamic importance, the structural requirements for a tip split joint are minimal. While the structural requirements are most important for a blade split in the root region. It is also possible to split a blade in the middle region (33-67% of blade length), this maximizes the reduction in transportation length. In this region the aerodynamic and structural requirements are roughly balanced. The loads to be transferred are quite high, but not as high as with a split closer to the root. While any distortions to the aerodynamic profile and misalignments are more important than with a root split, they are less important than for a tip split. Therefore, this might be a somewhat more forgiving region to the distortions that will be created due to a split in the blade.

[3]The tip vortex is a three-dimensional flow that creates drag, this airflow is caused by air flowing from the higher pressure (on the wind side of the blade) to the lower pressure side (on the tower side of the blade).

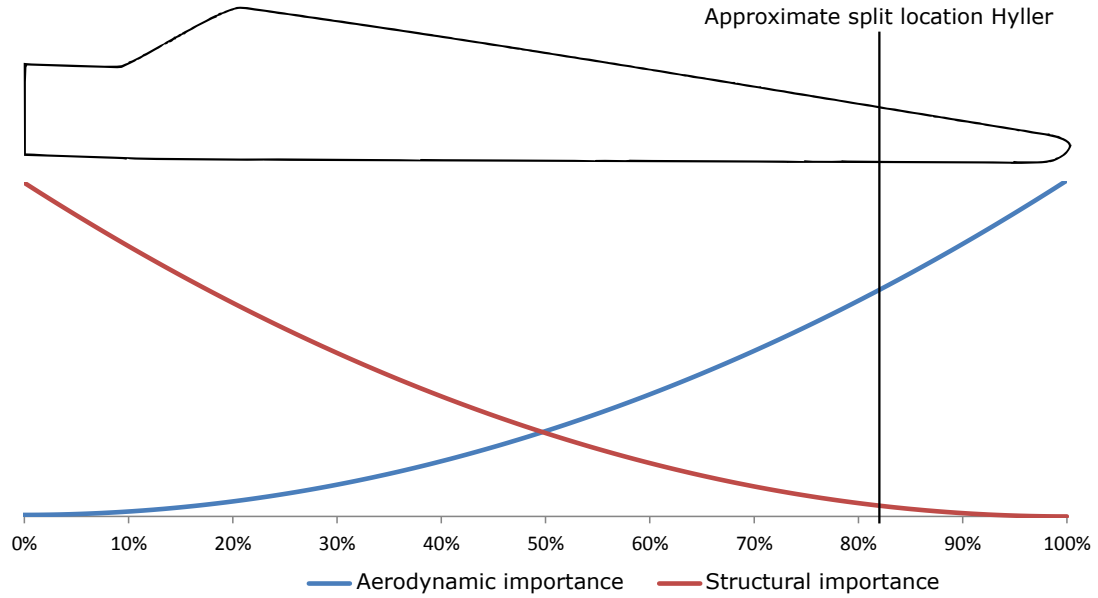

Figure 1.2: Importance of aerodynamics and structural requirements along a wind turbine blade, inspired by [17].

So coming back to determining the optimal split location, Qin et al. [14] determined that balancing the structural, manufacturing, and assembling requirements the best split location is 20% from the blade root for bolted connections. However, this project is part of the Hyller project from LM Wind Power, a project in which it is tried to make a blade split at 80% of the length from the root. Furthermore, the prerequisites are different as where used by Qin et al. For example, different manufacturing processes will be used for the production of tip and root sections. Using these different manufacturing processes for the different parts should lead to equal or lower production cost as compared to a single piece blade with the same length. Also, the tip sections should have a more consistent geometry due to the used manufacturing process. This should result in a more consistent aerodynamic behaviour and thus a higher power output on average. Furthermore, the blade will be joined with a full composite joint. This should result in a lower weight joint as compared to bolted joints, where the lower weight of the joint in the tip region should keep the additional loads for the root part to a minimum. This results in different prerequisites as were used by Qin et al. [14] and in the previous split blade projects from LM [11–13]. Therefore, it could be possible that with these prerequisites the optimal split location is in the tip region. If this is true, then the cost of wind energy can be lowered by building wind turbine blades that are split in the tip region, both for onshore and offshore wind turbines.

1.2. Scope of thesis

To lower the cost of wind energy by making a tip-split blade, the assembly costs should be lower than the reduction in transportation cost, while the performance of the blade remains similar. In order to solve this problem, the following objective is formulated:

The objective of this research is to investigate if wind turbine blade sections, of a tip split blade and produced with different production processes, can be aligned and joined on-site to yield a similar power output at rated speed as single-piece wind turbine blades while using mould marks as reference points and low cost alignment tooling. This is done by determining the relative positional accuracy of mould marks and the blade to blade variation in profile thickness in the joining region due to the different production processes. Furthermore, the aerodynamic effects of angular misalignments will be simulated at rated speed to determine the most critical angle for power output, as well as the relation of this angle to the differences in power output compared to single piece wind turbine blades.

To fulfil this objective, several research questions were defined. These questions are split into three groups, the first is alignment (section 1.2.1). The second group covers the aerodynamics (section 1.2.2) and the third group of questions follows from the structural connection requirements (section 1.2.3).

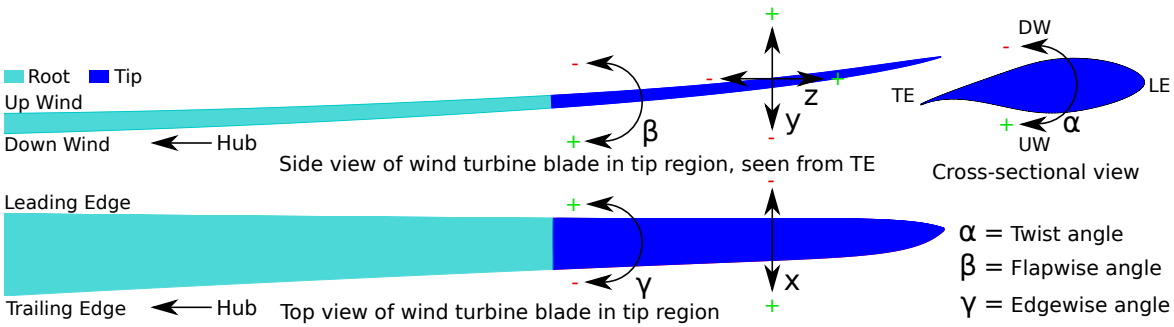

Figure 1.3: Definition of directions as used by LM Wind Power

1.2.1. Alignment research question

Although a tip-split wind turbine blade will not yield a transportation cost reduction as high as a blade that is split in the middle. Joining a tip-split blade on-site near the final turbine installation area will result in lower transportation cost as compared to transporting a single piece blade with the same length. Especially considering that there are substantial increases in transportation cost if the blade becomes longer than 46 and 61 meters [6]. This means that aligning, joining and verifying a correct outer geometry needs to be done on-site. Therefore, the position and orientation of each section has to be determined on-site so parts can be positioned correctly. LM Wind Power uses mould marks to provide reference points on their wind turbine blades, these are used to correlate an in-mould position to an out of mould position. The mould marks are used to mount aerodynamic add-ons that improve the power output, such as vortex generators. Since composite parts are known to not necessarily have the same geometry as the mould in which they were produced [18], for example due to shrinkage. This could mean that the mould marks might not be in the desired position. However, it is unknown what this change in geometry does to the relative position of mould marks. As the required positional accuracy of vortex generators is not extremely critical [19, 20], they can be used as reference points for mounting these devices. At LM Wind Power the most commonly used laminates are made from glass fibre and polyester. So to determine if mould marks on glass polyester laminates can also be used to provide reference points for aligning split wind turbine blades, the following research question was formulated:

Research question 1:

What is the relative positional accuracy in x & z directions of mould marks on glass fibre polyester wind turbine blade laminates?

1.2.2. Aerodynamic research questions

As is explained in section 1.1, the aerodynamics dictate the design in the tip region. So when the parts are aligned and joined on-site, the tip can deviate from the designed position in all six degrees of freedom (DOF). Three DOF describe the position: x, y & z and three DOF describe the angle: α, β & γ. This is visualised in figure 1.3 with the positive and negative directions indicated as used by LM. Insight in how deviations in these DOF influence the aerodynamic performance, and thus the power output, is vital to the development of tip split wind turbine blades. The six DOF can be split into two groups, misplacements (x, y & z) and misalignments (α, β & γ), which these be reviewed in the following sections.

From a global perspective it is assumed that the placement errors in x & y only have a local effect on the aerodynamics. Furthermore, it is assumed that the blade joint makes the transition from root to tip smooth. Therefore it is assumed in this project that if these deviations remain small ($< \pm 20$ mm), the effects of errors in x & y are negligible with respect to the power output. Whether this is a correct assumption would require Computational Fluid Dynamics (CFD) analysis, which is out of scope for this project. If this assumption is not valid, then the power output of a tip-split wind turbine blade will deviate more than is described in this project. For a deviation that makes the blade length longer or shorter (z), the blade will capture more or less wind respectively. On a site with the most energetic wind, EIC class 1 [21], a ± 20 mm variation on a 42.1 meter long blade will result in $\pm 0.10\%$ difference in power. For the angular alignment errors, it cannot be assumed that the effects are only local as the entire tip section will be misplaced. According to literature the effects of angular deviations are as followed:

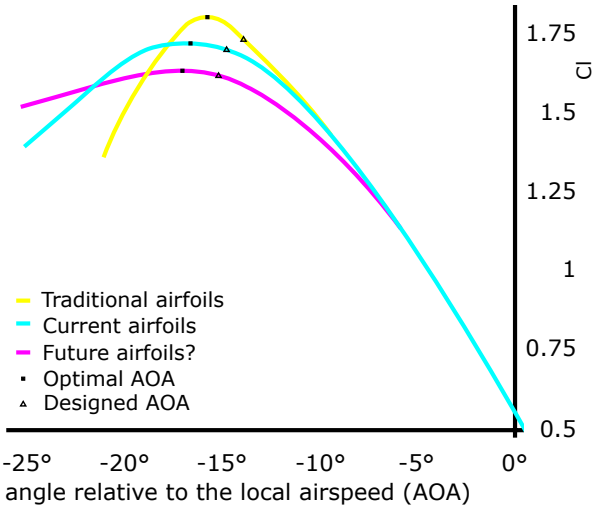

Figure 1.4: Plot of three different $C_L - \alpha$ curves, with indication of optimal & designed α. Inspired by [24].

- Twist angle (α):
  A twist misalignment results in a different angle of attack which is directly related to the coefficient of lift (C_L) and thus the lift and power production [22]. Most power is produced when the blade is operated at $C_{L_{max}}$ [23], but due acoustic and structural requirements the blade is operated a slightly higher α. As the precise shape of the $C_L - \alpha$ curve is strongly dependent on the aerofoil [24], the power loss/gain of a deviation is dependent on the used aerofoil. To illustrate this, three different $C_L - \alpha$ curves are shown in figure 1.4[4], in which a number of things are visualised. The yellow line shows the traditional aerofoils, which were designed for a high $C_{L_{max}}$. However, if the twist angle would deviate slightly from this angle, then the C_L value, and thus the power output, would decrease quickly. As can be seen, for the newer wind turbine blade aerofoils the value of $C_{L_{max}}$ has decreased somewhat and a plateau region has been formed around $C_{L_{max}}$. Resulting in less variation in the power output for varying twist angles as with the traditional aerofoils. This is a trend which is expected to continue [24], and is visualised with the purple line in figure 1.4. Furthermore, the optimal twist angle ($C_{L_{max}}$) and the designed twist angle are also visualised on each line.

- Flapwise angle (β):
  During operation of wind turbines, the wind will deform the blade tip towards the tower. In order to keep enough space in-between the blade tip and tower, the blades are designed with a pre-bend away from the tower [25]. Therefore the swept area, and thus power output, are smaller compared to a straight blade with the same curved length. Attaching the tip with a positive or negative flapwise angle will result in a respectively larger or smaller swept area, meaning more or less power captured respectively. However, the larger swept area might cause the blade to hit the tower and could result in higher loads.

- Edgewise angle (γ):
  Connecting the blades with an edgewise angle deviation results in a blade with a forward or rearward sweep. On aeroplanes a rearward sweep is used to lower the drag of the aeroplanes at transonic and supersonic speeds [22]. Although wind turbines operate in the subsonic regime, the energy output of a wind turbine blade with a negative edgewise angle can be increased. If this is completely optimized the annual energy production (AEP) can increase by up to 10% [26]. However, for large blades (>5 MW) and an edgewise angle of about 6° this could cause flutter[5] to occur [27].

So for each angular misalignment, literature describes if a power loss or gain can be expected in each direction for small angular alignment deviations. Only it does not describe how a twist angle deviation compares to a flapwise or edgewise angular deviation in terms of power output. However, looking at blade geometry, it is likely that the twist angle is by far most critical for on-site alignment. This because the twist angle

[4] Note that the direction definition of α is reversed compared to the aeronautical definition.
[5] Flutter is a potentially destructive self-feeding motion caused by aerodynamic forces.

mismatch is the angular misalignment of the chord[6], which is ±1 meter long. Whereas the flapwise and edgewise angles are the misalignment of the blade tip with a correctly placed root of the tip section, which is ±7 meters long. If one is capable of aligning reference points with an accuracy of ±10 millimetres, then the twist angle can deviate with ±0.57° whereas the flapwise and edgewise angles can only deviate ±0.08°. Wherefore the effect on power output of flapwise or edgewise deviations has to be much stronger in order to have the same effect on power output as a twist angle deviation. To determine if the critical alignment angle is indeed the twist angle, the following research question was formulated:

Research question 2:

How do the differences in power output of twist angle deviations compare to the differences in power output due to flapwise and edgewise angular deviations?

Following the description in the previous section, it will be assumed that the twist angle is most critical for power output. If this assumption is incorrect, then this will be shown by the answer of the last research question. Following the assumption that the twist angle is critical, the twist angle will be reviewed more closely. On the large wind turbine blades in use today, a twist that varies along the length of the blade is build-in to optimize the power output [28]. Furthermore, the entire blades are also rotated in the hub to control the power output with blade pitch systems, this further optimizes the power output [29]. However, the blade manufacturing processes will cause twist deviations to be present on blades. According to Petrone et al. [30], these manufactured twist angle deviations are normally distributed and range up to ±2°. Due to these errors the average power output will deviate -0.78% compared to the nominal power output. A twist alignment deviation will cause a step change in the twist angle. This deviation is added on top of the already present manufactured twist errors. In order to gain more understanding in the relation between the twist angle of the tip section and the variation in power output on blades containing manufactured twist deviations, the following research question is defined:

Research question 2.1:

What is the relation between the twist angle at the tip and the resulting variation in power output on a tip-split blade containing small twist errors due to manufacturing and misalignments?

The goal of the alignment process is to position the parts as close as possible to the designed position. If this is done correctly, then this should lead to the aerodynamics being equal to that of a single piece blade. However, as shown by Petrone et al. [30], the power output of single piece wind turbine blades is already variable due to manufacturing twist errors. Campobasso et al. [31] demonstrated that if the presence of these deviations is incorporated in the blade design, the variation in AEP due these deviations can be reduced. They optimized a blade with a random normally distributed twist variation of 2.5° and a chord length variation of ±1 cm. On the optimized blade the AEP of the blade design reduced with 1.21 %, which makes it look like a lesser blade. However, due to the presence of manufacturing deviations, the average AEP of a group of blades is always lower than the AEP of a designed blade. So if the average AEP of the optimized blade is compared to the non-optimized blade, the AEP actually increases with 1.83% and the standard deviation reduces with 44.32%. Wherefore the average energy produced by a blade increases, which could result in a lower cost of wind energy. So if the manufactured twist deviations are taken into consideration during the alignment process, can the additional freedom of a split in the tip region allow for a reduction in power output variation? This might be possible because the manufactured twist errors on the tip section could possibly be reduced by placing the tip section such that the average twist angle error of the tip section is reduced, as compared to single piece blades with the same manufactured twist deviations. In order to determine if it is indeed possible to make the power output of tip split blades more constant compared to the single piece counterparts, the following research question is defined:

Research question 2.2:

What is the relation between the variance in power output, due to twist errors, and the absolute average twist error of the tip section after joining?

[6]The chord is the longest straight line on an aerofoil from leading edge (LE) to trailing edge (TE)

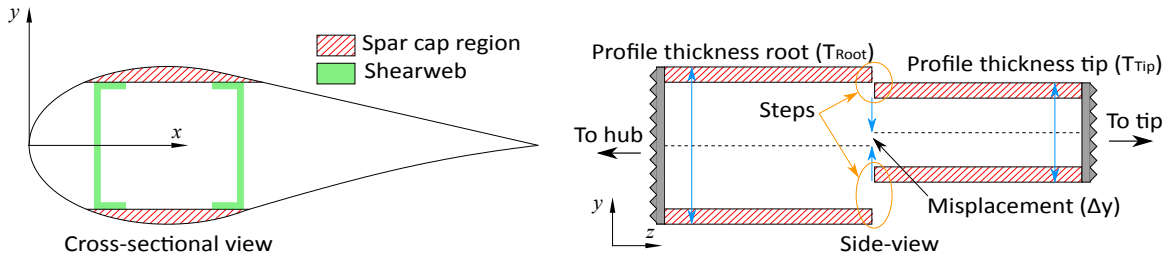

Figure 1.5: Left: Visualisation of spar cap regions and webs on wind turbine blade section [17], right: side-view of spar caps at split location.

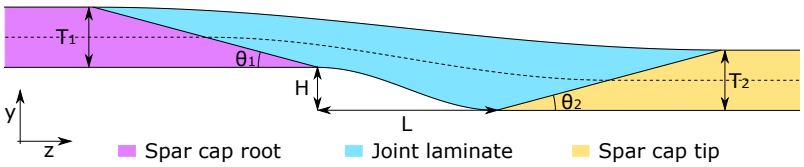

Figure 1.6: Detailed overview of geometrical parameters of upper step visible in figure 1.5.

1.2.3. Structural joining research questions

As is visualised in figure 1.2 the structural aspects are much less of a concern in the tip region [17]. However, it is still important to make a proper joint which will last the lifetime of the blade. From a structural perspective, a wind turbine blade section consists out of two spar caps, two webs and an aerodynamic casing. The spar caps are located at the thickest part of the aerofoil, illustrated in figure 1.5 on the left, and consist out of UD fibres going in the z direction of the wind turbine blade. These spar caps carry most of the bending loads and the webs carry most of the shear loads [17]. The bending loads in the flapwise direction are critical for wind turbine blade design as the loads are highest and the available building height is limited due to the aerodynamics. On the right in figure 1.5, a side view of the spar caps of the root and tip sections at the split location is visualised. Since the blade sections will be produced with different manufacturing processes and at different locations, it is possible that the profile thickness at the split location of both sections is not the same. This could cause two steps to be present in the spar caps. Furthermore, improper alignment of the parts will also increase/decrease these steps. This is highlighted in the orange ellipses in figure 1.5.

In figure 1.6 a more detailed overview of the top step visible in figure 1.5 is shown. The exact joining method for the two blade sections has not yet been selected. However, for the first test article (TA) of the Hyller project the spar caps of both parts are tapered down and on-site a tailor fit joint laminate will be made that fills the gap in between the two parts to form a structural connection. In the sketch of figure 1.6 a high taper angle is shown, in reality the taper angle will be much lower to reduce the peak stresses [32]. The loss in strength due to this step in the spar caps is dependent on the specific geometry [33]. When this geometry is known, the allowable alignment deviations can be calculated using a Finite Element Method (FEM) [34, 35]. Therefore, the blade joint is out of scope for this project, but a review of the geometrical variations and factors influencing this geometry is in scope. As these must be known to do the joint design of a joint that lasts the lifetime of the blade. With figure 1.6 the following geometric parameters are found:

- T_1 & T_2:
  Both spar caps will be produced using a vacuum assisted resin transfer moulding (VARTM) process. According to Yenilmez et al. [36] the thicknesses of VARTM laminates is depend on the following factors: thickness and areal weight of ply stack, duration and level of initial vacuuming & gelation, resin pressure and resin shrinkage. By controlling these parameters the variation of part thickness can be controlled. So the variation in the values of T_1 & T_2 could be minimized to an acceptable variation for the spar cap joint.

- θ_1 & θ_2:
  The taper angles come from the design and depend on the maximum allowable peak stresses. To create these angles, accurate milling will be used to make the right taper on the spar caps. Therefore, the taper angles depend on the design and the accuracy of the used milling process.

- L:
  To allow for joining the webs with one-another, a gap in between the two parts is designed to be present. Due to misplacements of the tip section relative to the root, this gap can become larger or smaller. However, to make the web joint only small deviations of L can be accepted. Therefore, the variation of L, and thus the allowable alignment deviation in the z-direction, is known from the design and the allowable tolerances of the web joints.

- H:
  The parameter H represents the height of the step. The size and variation of the step is depended on: profile thickness of the root (T_{Root}), the profile thickness of the tip (T_{Tip}) and the misplacement in y-direction[7].

So reviewing the variation in the geometrical parameters of the spar cap joint, the remaining unknowns for the geometry of the spar cap joint in the flapwise direction are: the profile thicknesses of the root & tip and misplacement in the in the y-direction. In order to determine with what accuracy the blade sections can be placed and aligned with one-another, a low cost tool was build and alignment trials with actual size parts were performed. From these trials the achievable placement accuracy of the blade sections can be determined. These trials are described in chapter 2. To determine how the profile thickness of the root varies, one has to review the used manufacturing process. In the Hyller project the root is produced with a two-shell production process. This wind turbine blade production process is already used by LM Wind Power for many years. As part of quality checks, the profile thickness is measured at several positions along the length of the blade. From this measurement data it is known that the profile thickness varies from blade to blade on blades produced with a two-shell production process. However, no literature is available on how the thickness & position of each component influences the profile thickness locally. As the spar caps are only in the web region, see figure 1.5, the following research question is formulated to study this:

Research question 3:

What is the influence of component thickness & position on the local profile thickness in the web region for a two shell wind turbine blade production process?

The tip section in the Hyller project is produced with a one-shot infusion and cure production process. This is a new production process for LM, therefore it is unknown if there are variations in profile thickness on blades produced with this process and the used materials by LM. However, in essence the laminates are still produced by a VARTM process, only then in a matched-die mould. Since it is known that the thickness of composite parts produced with a VARTM process varies [36] and matched-die moulds have a certain closure accuracy, it is likely that the profile thickness of the tip section varies. Therefore the following research question is formulated:

Research question 4:

What is the blade to blade profile thickness consistency in the web region of wind turbine blade tip sections produced with a one-shot infusion and cure production process?

One of the possible causes for a variation in the profile thickness of blade sections produced with a one-shot production process, is a variation in the mould geometry due to the closure process of the matched-die moulds. To investigate how consistent the mould geometry is during the closure process, the following research question is formulated:

Research question 4.1:

What is the blade to blade profile thickness consistency in the web region due to closing the matched-die Hyller mould in the one-shot production process?

[7] To be complete, a twist misalignment would also cause a variation in step height over the length of the blade. By defining the maximum step in y as the point of rotation, the step height would be smaller at all other locations. So with this definition, the maximum step size in y is not dependent on the twist angle deviation.

In the one-shot production process not only the glass for the upwind (UW) and downwind (DW) shells are infused and cured at once, the two webs are also infused and cured in the same process. So when placed into the mould, the webs are still flexible which could allow for the webs to deform during the mould closure process. With the first research question in this section one of the things to be investigated is whether the position of the webs has an influence on the profile thickness in the two shell production process. Since the webs are still flexible when placed in the mould and during mould closure, it might be possible that the position of the webs in the one-shot process does have an influence on the blade profile thickness. Furthermore, the web angle and height might also have an influence on the profile thickness. Therefore the following research question is defined:

Research question 4.2:

> *What is the influence of web location, -angle and -height on the profile thickness of wind turbine blade tip sections produced with a one-shot production process?*

Answering all these questions should fulfil the objective and will give additional information to the viability of lowering the cost of wind energy by building tip split wind turbine blades.

1.3. Outline of report

During this thesis a total of three subjects have been investigated. The first is how well sections of a tip split wind turbine can be positioned relative to one another with low cost alignment tooling. For doing this, a tool was build that can be manipulated in all six DOF, named the six-axis manipulator. The design, build and validation process of this tool is described in chapter 2. In chapter 3 a review of the relative positional accuracy of mould marks is described. As these could be used to create reference points on the blade sections, which are necessary for correctly positioning both parts on-site. All of this was used in the production of the Hyller test article, this is also described in chapter 3. The second subject to be reviewed is the effects of the angular deviations on the power output and this is described in chapter 4. As is described in section 1.2.3, FEM can be used to determine the effect of the deviations on the structural life of the blade. However, in order to be able to do this, it is necessary to know how the geometry of both parts and how much it varies from blade to blade. So the third subject is a review of the blade to blade variation in profile thickness, with the influential factors for this variation. This is described in chapter 5 for the two-shell production process and in chapter 6 for the one-shot infusion production process. Then all of this is concluded in chapter 7, with all recommendations for further work.

2

Design, build and validation process of alignment tools

As is described in the objective, the use of low-cost alignment tooling is required for the on-site placement of the tip section relative to the root. In order to get an idea of what alignment accuracies are achievable, low tooling was built and a process was designed for the alignment of tip split wind turbine blade sections. The design and build process of this alignment tool, named the six-axis manipulator, is described in section 2.1. To gain experience with the alignment process and to improve the process & tooling, alignment trials were held with actual sized parts. The lessons learned during these trials and the improvements are described in section 2.2. After these initial alignment trials, the alignment precision was verified with accurate 3D scanning. The results of these scans can be found in section 2.3. The chapter is ended with a discussion of the achieved alignment results in section 2.4.

2.1. Design and build process of a six-axis manipulator

LM Wind Power plans to use a mobile joining factory to provide a dry and temperature controlled environment for joining blades on-site. This mobile factory will most likely have the same dimensions as a standard shipping container to allow for low cost transportation. Only the tip of the root part will be inside the mobile factory. Meaning that the largest part of the blade will be laying in the field. Depending on the length of the tip section, it might also be partially outside the mobile joining factory. However, the tip section will be placed on a six-axis manipulator, a tool which can be freely adjusted in all six DOF. A picture of this tool is visible in figure 2.1. To allow for easy manipulation in the x-z plane, LM Wind Power plans to place the mobile joining factory such that the floor is level. With enough money sophisticated tools can be made to align parts with a near perfect accuracy, as for example is done in the latest generation of gravitational wave detectors [37]. Only, using the most sophisticated tooling will likely result in high joining cost, as the depreciation of high cost equipment is in general higher than the depreciation of low-cost equipment. Therefore, the six-axis manipulator was developed as a low-cost tool which allows for a ± 1 mm adjustment precision. The design considerations and the solutions for a tool that should be accurately adjustable in 3D space are as followed:

- Six-axis manipulator to be used on a similar sized area as a standard shipping container
  The mobile joining factory which is described above will require operation of the six-axis manipulator inside a space limited area. Furthermore, there should always be enough room to allow technicians to freely move around the tip section. Therefore, the six-axis manipulator can only be a meter wide and two meters long. If in the future the blades are too wide to fit into one shipping container, then two or three containers will be but side by side to create a larger mobile factory.

- Tip sections to be placed on six-axis manipulator in any orientation
  The six-axis manipulator allows for the tip to be placed in any orientation on top of the tool. Therefore, the six-axis manipulator has a 'table top' on which supports can be placed to fixate the tip in the desired orientation. For example, in figure 2.1 the tip section is placed with DW up and in figure 2.2 the tip section is placed with UW up on the same six-axis manipulator.

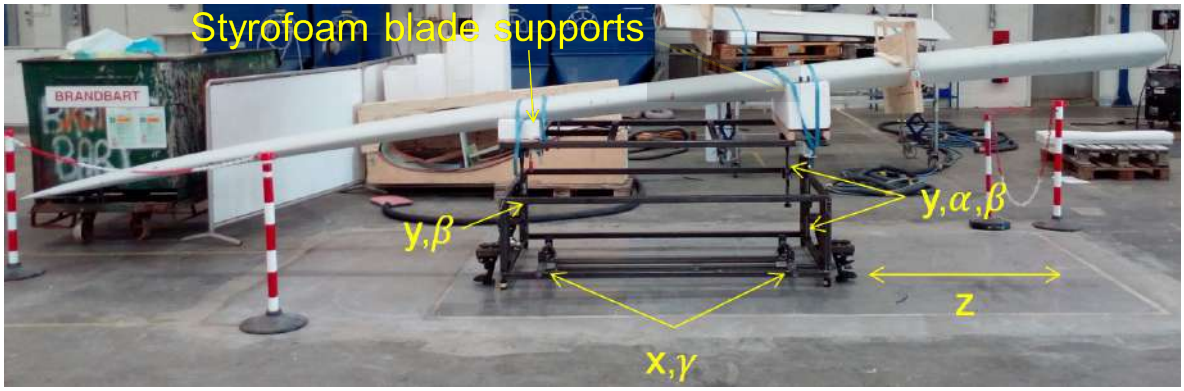

Figure 2.1: Picture of six-axis manipulator with actual size Hyller tip and adjustment location for each degree of freedom.

- Table top supported on three legs
  Something with which everyone is probably familiar, is a wobbling table. To resolve the wobbling, one usually puts something underneath the shortest table leg. However, if a table is supported on three legs it will never wobble. This is because to define a plane in 3D space three different vectors are required. A table top can also be seen as a plane in 3D space and the table legs as the vectors describing the plane. More vectors/table legs can be used to describe the same plane. However, the fourth vector will be a multiple of the other vectors, resulting in an over constrained situation. Therefore, supporting a table top by three legs can only result in one plane wherefore the tool does not become over constrained.

- Non-swivelling wheels to move over floor
  If one wishes to easily move a cart in every direction over a floor, it is common to put swivelling wheels under the cart. As the name suggest, theses wheels swivel first in the same direction as the cart is moved to. However, if one only wishes to move the cart in for example the x direction, this swivel will also slightly move the cart in the z direction while the wheels align with the movement direction. This makes it difficult to make small adjustments in multiple directions. Therefore, using revolving balls as wheels, one can move the tool accurately in all directions of the floor.

- Two threaded rods connected to guidance rail on ground
  In order to allow for accurate positioning of the x position and the edgewise angle (γ), the bottom frame of the six-axis manipulator is connected to a guidance rail on the ground with two threaded rods, see figure 2.1. Therefore, accidentally hitting the six-axis manipulator will not change the x and γ. The ground adjusters are more clearly visible in figure 2.2.

- Brakes instead of guidance rail & threaded rod in z direction
  Initially a thread on a guidance rail was added with the idea to use it for accurately manipulating the z position. However, for this to work, this slider has to be placed exactly perpendicular to the other guidance rail. Furthermore, the slider on the guidance rail should have no manually noticeable play to allow for easy manipulation, like the linear sliding guide blocks used in computer numerically controlled (CNC) machines. However, the low-cost sliders used in this project did have about one mm of play. Therefore, this didn't work for the z direction. With the low mass of the tip (<200 kg), and the floor being level, little effort is required to move the six-axis manipulator accurately. To prevent movement in the z direction when it is not desired, brakes were added.

2.2. Alignment trials with actual size parts

To determine the accuracy of the six-axis manipulator, alignment trials with actual size parts were held. For this a scrapped tip section of a LM42.1 wind turbine blade[1], the reference blade for the Hyller project, was used. This tip is also visible in figure 2.1. The tip section of the received scrapped tip was ten meters long whereas the Hyller tip is only seven meters long. So, after cutting the tip section at the appropriate location, a three-meter-long root section was created. However, before the blade was cut into two parts, numerous

[1] The tip section of this blade was according to specifications, the blade was scrapped due to defects closer to the blade root.

Figure 2.2: Picture of aligned LM42.1 tip, cut position is in between six-axis manipulator and stack of pallets.

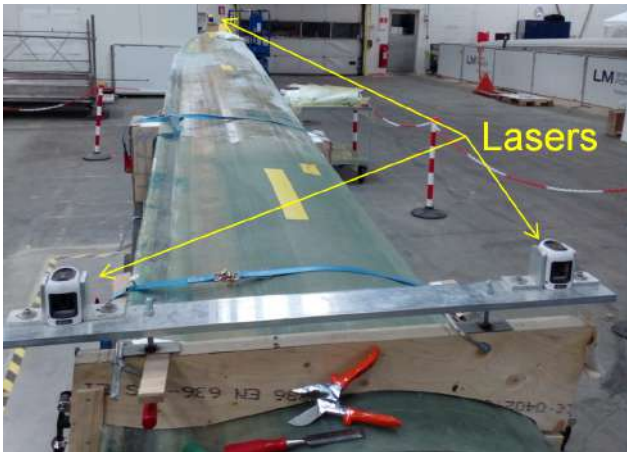

Figure 2.3: Picture of Hyller tip on six axis manipulator with three lasers mounted.

marks were made on the part to serve as reference points for the alignment process. These reference points were scratches in the surface of the blade starting at the root and finishing at the tip. If the parts would be aligned properly, then all these scratches would line up perfectly which gives a good visual confirmation of how well the alignment is. For the joining of the following process was used:

1. Align with UW up, sketch a in figure 2.4
2. Join webs
3. Join UW shell
4. Turn blade and align with DW up, sketch b in figure 2.4
5. Join DW shell

During the alignment the 3-meter-long root piece was placed with a crane in approximately the right position on Styrofoam blade supports, after which it was rigidly fixed. This is like the on-site conditions, where the high mass and length of the root do not allow for easy and accurate positioning with the available tools. In order to simplify the alignment during the trials, the supports of the root were placed such that they mimic the root laying in the mould, for now called the level position. By positioning it as such, the standard LM42.1 drawings could be used. Positioning the root differently is possible, only this would require re-dimensioning of the drawings in the on-site coordinate system. This could be done, but a due to the high amount of work required, this was not done. During the alignment trials low density wire cut Styrofoam supports were used to place the blade sections on, see figure 2.1. However, it was noticed that these could not support the mass of the blade sections. Also, they are somewhat flexible which resulted in subtle movements of the tip section when the six-axis manipulator was manipulated. Therefore, new plywood supports were made for the joining process of the TA. These supports provided the required rigidity and are visible in figure 2.2. However, for the initial trial alignments only the Styrofoam blade supports were used.

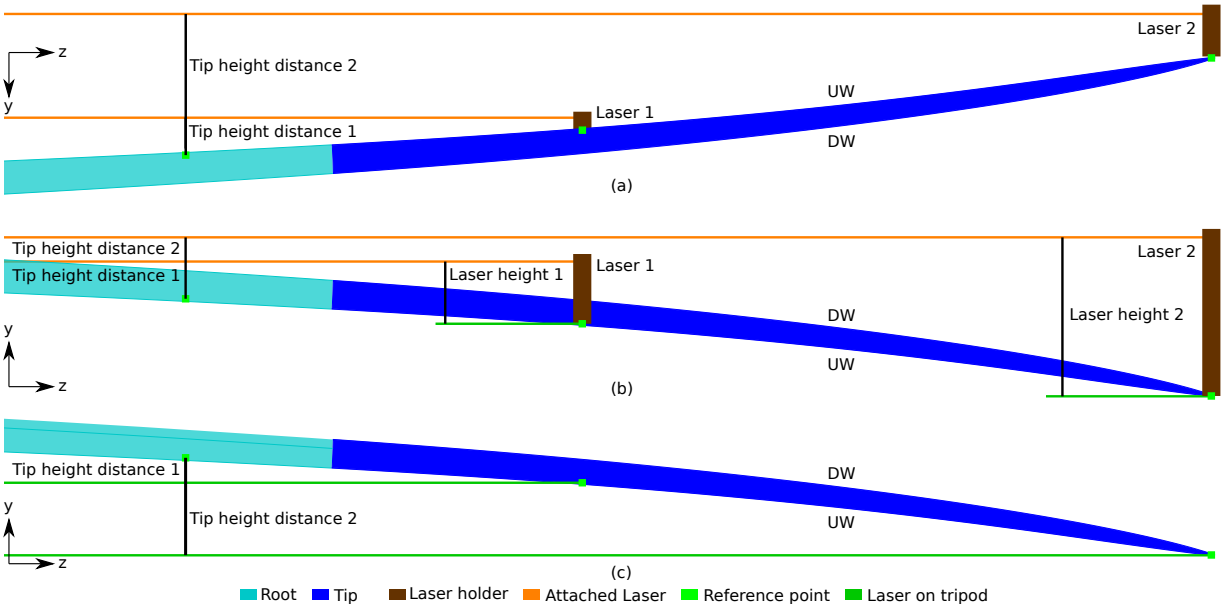

Figure 2.4: Side view sketches of root and tip sections with lasers, viewed from the TE. (a) shows the alignment with UW up, (b) shows the alignment with lasers on the part with DW up, (c) shows the alignment with DW up and external lasers on tripods.

The alignment itself was done with the help of four self-levelling lasers. Three of the lasers were placed on the tip section, see figure 2.3. The fourth laser was placed on a tripod which could be placed anywhere around the tip. These lasers projected a level plane at the height to which they were set. Due to the self-levelling nature and the root part being supported in the level position, aligning these planes is not necessary. However, for the alignment of x & γ, the vertical planes projected by these lasers have to be parallel to the y axis of the blade, which needs to be aligned manually. To do this, the laser on the tripod and additional reference points were used. In figure 2.4 sketch a shows how this alignment of the tip section with UW up was done. A total of three reference points on the tip, and two reference points on the root were used (In figure 2.4 two reference points are invisible as they are on the LE).

To correctly align the height of the tip section (DOF y) with respect to the root, the height between the line of laser 1 and the reference point on the root has to be equal to the designed height. When this is not the case, the table top of the six-axis manipulator is raised until this is the case. Next the flapwise angle (DOF β) can be aligned. This is achieved by angling the table top until the designed 'tip height distance 2' is achieved. A similar method is used to align the other directions (DOF x, z, α, γ). This alignment method is useful when aligning with UW up. However, aligning with DW up is somewhat cumbersome, in sketch b of figure 2.4 this is visualised. First, with this alignment method the lasers will have to shine above the product, so the laser line is visible near the reference point on the root. Due to the high pre-bent in the tip region, the laser holders have to be high in order to visualise the laser line above the blade sections. Visualising this line on the UW side of the blade section (with DW up) is also impractical as the absolute tip is close to the ground and the supports can also block the laser light. Furthermore, working that close to the ground is also not ergonomic.

Secondly, the geometry of wind turbine blade sections is also varying from blade to blade (This is reviewed more in-depth in chapters 5 & 6). This means that the holders which are placed around the blade sections, visible in figure 2.3, need to be adjustable in order to fit around every blade. As a result of adjusting the laser holder, one would first have to use the laser on the tripod to determine the height of each laser with respect to the reference point, see laser height 1 & 2 in sketch b of figure 2.4 (A step that is also necessary when aligning with UW up). A faster and more convenient alignment method, when aligning with self-levelling lasers, is not using laser holders on the tip section. Instead, placing the lasers on tripods and using those to create a level plane at the reference point on the tip. The height difference in-between the reference points can then be measured at the reference point on the root. This visualised in sketch c of figure 2.4 with tip height distance 1 & 2.

2.3. Verification of alignment with accurate 3D scanning

In order to determine how accurate the alignment is with the method described above, a 3D surface scan of the parts was made. This scan was then compared with the 3D model to determine with what accuracy the two blade sections were aligned with one-another. The 3D scanner itself has a measurement accuracy of ±0.04 mm [38], and is therefore considered accurate. By doing a scan a 3D point cloud is made of the scanned parts. By making a best fit of this point cloud with the 3D model of the LM42.1 it is possible to determine the deviations. However, as the tip section of a scrapped wind turbine blade was used for the alignment trials, the blade geometry does already have some variation relative to the design as a result of manufacturing tolerances. So even if the parts would be aligned without any deviations, then the scan would still reveal the manufactured deviations. Therefore, it was considered initially to use 3D wire cut foam piece in the alignment trials, as this would eliminate the manufactured twist deviations. Only this was relatively expensive, especially considering that a scrapped tip section of a LM42.1 blade was free to use for alignment trials. As a result, the manufactured twist deviations have to be subtracted from the deviations measured by the 3D scanner to find the alignment deviations. A best fit of the 3D scan data on the root section model shows all the deviations of the tip section relative to the root. Similarly, a best fit of the 3D scan on the tip section model shows all the manufacturing deviations of the tip section. Subtracting the latter from the first will result in the alignment deviations.

A picture of the aligned tip and root before the first scan is visible in figure 2.2. As can be seen from a distance, all lines seem smooth and it is also almost impossible to see the split line in between the six-axis manipulator and the stack of pallets. With this alignment, the lasers alignment method described in section 2.2 indicated that there were no deviations in DOF x, y, z, α, β. However, it was observed that the tip was placed with a small negative edgewise deviation[2] ($\Delta\gamma \approx -0.16°$). Correcting γ would require adjusting threads one and two, visible in figure 2.2, by different amounts. However, these rods were not completely parallel to the global γ axis, so making this adjustment would also influence the alignment of the other DOF. Therefore, to let perfect not be the enemy of good, a scan was made with this known misalignment present. The 3D scan could then reveal how correct the measurement of the misalignment was.

The colour plot results of the first alignment are visible in Appendix A in figure A.1. As can be seen for the alignment on the root, most of the surface seems to be off by more than -5 mm in the tip region. However, the plot with the alignment on the tip shows that the tip itself is already 2 mm too thin in the tip region. Meaning that the misalignment is only 3 mm. In table 2.1 the measured alignment deviations relative to the 3D computer-aided design (CAD) model are visualised. This shows that it is understandable that the alignment process with lasers indicated no deviations in all DOF except for DOF γ. Also, some observed misalignments can also come from the difference in measuring methods. If the misalignments are measured with the lasers, only three points on the tip are used[3]. Whereas the 3D scanner reviews the entire surface of the tip-section. On this surface, it generates an equal amount of reference points per surface area. As a result of this, more data points are in the LE region compared to the TE region due more surface being in the LE region. For the best fit alignment of the 3D scan, all data points are taken as to be equally important. This results in a good alignment of the LE being slightly favourable over a best fit alignment of the entire tip section due to more reference points in this region

The scan also showed that $\Delta\gamma = -0.12°$, which confirms that the two different measuring methods show a similar deviation for $\Delta\gamma$ ($-0.16°$&$-0.12°$). With the data from the scan, the exact deviations at each adjustment point for γ could be found. This showed that ground thread two, see figure 2.2, had to be adjusted by 9.9 mm, and ground thread one had to be adjusted by 6.5 mm. An effort was made to adjust these two ground threads by these specific amounts after which another 3D scan was made. The data from this second scan revealed that ground thread two, see figure 2.2, was adjusted 0.7 mm too much, and ground thread one was moved 1.4 mm too much. In table 2.1 the results of the second scan are also visible. These show that although only the ground adjusters were moved, of which the goal was to only change γ, all other values have changed as well. This was also visible with the lasers. In order to further improve the alignment, the LE leg of the table top, see figure 2.1, was moved down by 2 mm. The results from the third scan, visible in table 2.1 show that it was difficult to further improve the alignment. The first 3D scan showed with what order of accuracy the

[2] being off by 20 mm on a distance of 7 m ≈ 0.16°

[3] The three used reference points are: LE & TE at z=36.5 and TE at z=41

	3D Scan 1	3D Scan 2	3D Scan 3
Δx	$2.3\ mm$	$-3.0\ mm$	$-1.75\ mm$
Δy	$-0.15\ mm$	$-2.3\ mm$	$-0.15\ mm$
Δz	Could not be measured with this 3D scan		
$\Delta\alpha$	$0.07^{\circ}{}^{+0.03^{\circ}}_{-0.03^{\circ}}$	$0.11^{\circ}{}^{+0.05^{\circ}}_{-0.02^{\circ}}$	$-0.02^{\circ}{}^{+0.02^{\circ}}_{-0.00^{\circ}}$
$\Delta\beta$	$0.02^{\circ}{}^{+0.01^{\circ}}_{-0.02^{\circ}}$	$0.05^{\circ}{}^{+0.06^{\circ}}_{-0.02^{\circ}}$	$0.01^{\circ}{}^{+0.00^{\circ}}_{-0.00^{\circ}}$
$\Delta\gamma$	$-0.12^{\circ}{}^{+0.00^{\circ}}_{-0.00^{\circ}}$	$-0.04^{\circ}{}^{+0.00^{\circ}}_{-0.00^{\circ}}$	$-0.01^{\circ}{}^{+0.00^{\circ}}_{-0.00^{\circ}}$

Table 2.1: Measured alignment errors with 3D scanner in each DOF during the verification of the alignment trials. In chapter 4 a review is made of the impact on power output of angular deviations. If these deviations are acceptable from a structural point of view is dependent on the used joining method, but this is out of scope for this project.

blade sections could be aligned with one another. Colour plots of the second and third scan are also visible in appendix A.

2.4. Discussion of alignment results

In this chapter the tools and alignment method used in the Hyller project have been described. It was found during the alignment trials that with trained technicians the alignment of both sections could be done in about half an hour. However, this time can be reduced further if the operation of, in this case, the six-axis manipulator can be simplified. As was explained in section 2.1, all movement points were made such that none of the movement directions were over constrained. Unfortunately, this resulted in coupled motions for the designed tool. This did sometimes result in time being lost in figuring out in how the tool should be adjusted. With the 3D scans of the aligned parts it is verified that the achievable deviations are small. The second and third scan revealed that if it is required, the six-axis manipulator can be adjusted with a precision <2 mm. At the same time, making this adjustment took very little time. However, to determine how much the six-axis manipulator should be adjusted, one would need reference points on the tip section directly above the adjustment locations on the six-axis manipulator. Furthermore, one should also have the dimensions of these reference points. Unfortunately, the resources for doing this were not available during the Hyller project. Also, being able to align the parts in half an hour with the achieved precision was sufficient in the Hyller project.

The verification of the alignment with accurate 3D scanning did show that the alignment method with lasers does leave noticeable deviations. However, the alignment method with lasers can align the parts with a precision of $< \pm 3$ mm & $< \pm 0.15°$ if as accurate reference points are used as were used in the trial alignments. Whether these deviations are acceptable is reviewed partially in chapter 4. The alignment method that was reviewed in this chapter was with respect to a wind turbine blade with one split in the tip region. For which it is only required to align two parts with one another. Using this method for blades with a single split closer towards the root would also be possible, but a scaled-up version of the six-axis manipulator would be required due to the larger parts and higher masses involved. If the blade would be split in more than two sections, then the laser alignment method might not be the best choice. As in the used process each section is aligned with respect to the previous section, all misalignments are stacked on-top of one-another. So, for example, if the blade would be spilt in five sections and each section would have a 0.1° flapwise angular deviation, then the last section would be off by 0.5°. Depending on the blade length and split locations, this could potentially result in the blade hitting the tower during operation. Aligning the pieces of a wind turbine blade split in more than two sections would thus require another alignment method.

3

Mould marks as reference points

As was explained in the introduction, LM Wind Power uses mould marks to provide reference points on their wind turbine blades to correlate an in-mould position to an out of mould position. It would be possible to use another method to create reference points for the alignment process. However, to use as much as possible existing technologies, and as is stated in the objective, it is the idea to use mould marks as reference points and use these to determine the misalignments on-site. Only, as was also described in section 1.2.1, the positional accuracy which is required by the mould marks for the current application is not critical. Therefore, research question 1 was formulated as followed: *'What is the relative positional accuracy in x & z directions of mould marks on glass fibre polyester wind turbine blade laminates?'* An answer to this question will be given in this chapter. To do so, the hypothesised relation and test set-up are discussed in sections 3.1 and 3.2. This is followed by the test results in section 3.3. During the alignment of the first TA mould marks were used and a description of this is given in section 3.4. Finally, in section 3.5 all of this is combined in a conclusion to formulate an answer to research question 1.

3.1. Mould marks & geometrical variation of composite parts

Most moulds in the wind turbine industry are made from composites in a two-step process. The first step is usually milling/sanding a piece of foam accurately into the designed blade shape, usually called a plug. Then the second step, is using this plug as a mould on which the blade mould is produced. On the plug small bulges are left in the positions where the mould marks are supposed to be. These leave small imprints in the blade mould. Due to aerodynamic requirements, the height of a mould mark has to be 0.2 ±0.1 mm. This is achieved by drilling an eight mm wide hole with a depth of approximately 2 mm in the mould surface. This hole is filled completely flush with the mould surface with gel-coat. When the gel-coat cures, it shrinks which results in a small hole in the mould surface of 0.2 ±0.1 mm. Then in production, the fibres are placed in the mould and the resin is infused with a VARTM process. Apart from completely impregnating the fibres, the resin will also flow in the small holes in the mould surface. This leaves a small, but visible, bulge on the part surface which is referred to as a mould mark. In figure 3.1 a sketch is shown of a mould surface with mould marks and fibres. Due to shrinkage composite parts do not necessarily have the same geometry as the mould in which they are produced. As a result, the mould marks could have a relative movement relatively compared to one-another. According to Radford et al. [18] shrinkage in composites is caused by:

- Thermal anisotropy

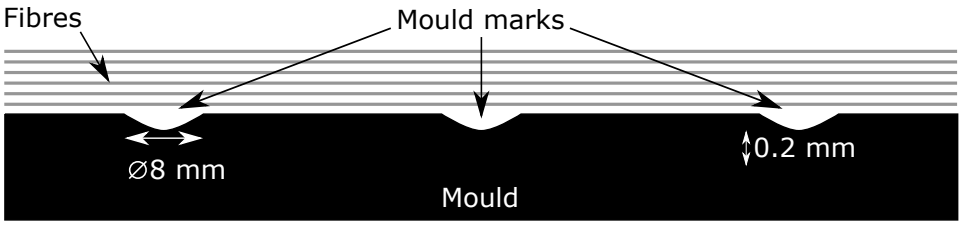

Figure 3.1: Sketch of mould with fibres and mould marks.

Most composites are made with resins that have an exothermic curing reaction or require consolidation at elevated temperatures. Once the part cools down, the mismatch in coefficients of thermal expansion (CTE) of the fibres and matrix results in residual stresses the in the laminate. As the by LM used polyester resin cures exothermically, the maximum temperature that is experienced by a laminate is depended upon the laminate thickness. Since more plies means more resin which results in more heat being generated, the shrinkage of thick laminates is higher than the shrinkage of thin laminates (In all directions for laminates with a similar lay-up).

- Chemical shrinkage
  The most commonly used resins in the wind turbine industry are epoxy, vinyl ester and polyester resins. All these resins have a volumetric shrinkage during their cure cycles, with polyester having the highest volumetric shrinkage during curing. Where the specific amount of resin shrinkage is also dependent on the degree of cure [39].

- Tool part interaction
  As the temperature of the laminate increases during the cure cycle, it results in the mould being heated as well. However, with the moulds of LM being made from the same material as the laminates and the maximum temperature during cure being below $100°C$, this contribution is limited for laminates being made at LM. The tool part interaction is much more of a concern for laminates being cured in metal tooling. Where the difference in CTE at elevated temperatures in for example ovens or heated moulds causes a change in geometry as the part and mould expand/retract at different rates.

- Gradients in material property
  The properties of a laminate are in part dependent on the ratio between resin and fibres. In the VARTM production process the resin is pulled through the fibres by a vacuum. As a result of varying vacuum levels, the ratio between resin and fibres can have small variations between different parts.

Next to these four influencing parameters, the fibre direction, and thus the fibre lay-up, also has an impact on how the laminates shrinkage. At LM three different fibre directions are used in the tip region of wind turbine blade laminates, these are 0° and ±45°. A 0° ply is usually referred to as unidirectional (UD) and this means that the fibres run in the lengthwise (z) direction of the blade. As is visualised in figure 3.2 a, the shrinkage in the fibre direction is small relative to the shrinkage in the direction perpendicular to the fibres. If ±45° fibre directions are used, with the same amount of fibres and resin, then the shrinkage in the x & z directions will be equal. Furthermore, the amount of shrinkage will be in between the shrinkage of the UD laminate in x & z directions, this is visualised in figure 3.2 b. The fibre lay-ups used by LM in the tip region consist out of fibres in the $0°\&\pm 45°$ directions, of which the shrinkage behaviour is visualised in figure 3.2 c. In the z direction the shrinkage will be in between the shrinkage of a & b, and this is also the case for the shrinkage in the x direction. Where the amount of shrinkage is dependent on the ratio between fibres in the x & z directions. With the help of classical lamination theory (CLT), the laminate strains can be calculated which are caused by the thermal anisotropy and chemical shrinkage experienced in the curing process [40–44]. The hypothesis is that the mould marks have a relative movement due to the laminate shrinkage. It is assumed that all mould marks are 0.2 ± 0.1 mm high and that they are not restricted by the mould in any way due to their low height. So, the resulting mould mark movement strains should be equal to the chemical & thermal laminate shrinkage strains. Furthermore, it is also hypothesised that the movement strains also vary from part to part due to production tolerances.

3.2. Methodology for measuring movement of mould marks

To find out how much the movement strains of mould marks are, measurements have been performed on laminates with four different lay-ups. In order to make a prediction of the movement strains, thin CLT was used to calculate the laminate shrinkage strains. The CTE and the coefficient of chemical shrinkage (CCS) in the 1 and 2 directions[1] of a laminate can be calculated with the following equations [40, 41]:

$$\alpha_1 = \frac{\alpha_f E_f V_f + \alpha_m E_m V_m}{E_f V_f + E_m V_m} \tag{3.1}$$

[1] The 1 & 2 directions indicate respectively the fibre and transverse fibre directions.

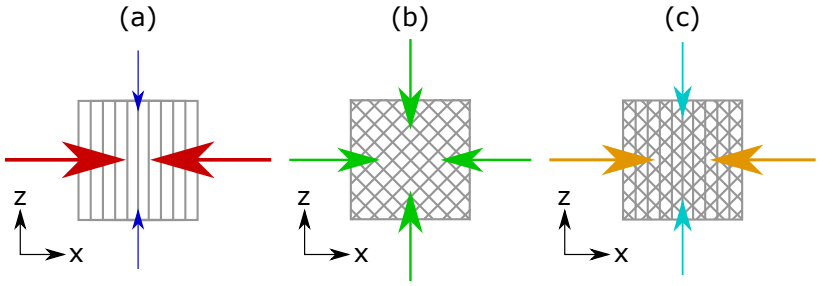

Figure 3.2: Visualisation of composite shrinkage for laminates with the same amount of fibres in different directions, inspired by [42]. Laminate (a) is a laminate with fibres only in the z direction, laminate (b) consists out of fibres in the ±45° directions and laminate (c) consists out of fibres in the 0° & ±45° directions.

$$\alpha_2 = \alpha_f V_f + \alpha_m V_m + \frac{\nu_f E_m - \nu_m E_f}{\frac{E_m}{V_f} + \frac{E_f}{V_m}} \tag{3.2}$$

$$\beta_1 = \frac{\beta_m E_m V_m}{E_f V_f + E_m V_m} \tag{3.3}$$

$$\beta_2 = \beta_m V_m + \frac{\nu_f E_m - \nu_m E_f}{\frac{E_m}{V_f} + \frac{E_f}{V_m}} \tag{3.4}$$

Where: α = CTE, E = Young's modulus, V = volume fraction, ν = poisson ratio, β = CCS and subscripts f & m indicate respectively the fibre or matrix. As only the in-plane strains have to be determined and the laminate thickness is much smaller than the other dimensions, thin CLT is used to calculate the strains due to chemical & thermal shrinkage. With this method, the specific position of each laminate ply is ignored and only the relative amounts of fibres in each direction are used [42, 43]. The properties of a single ply in the 1 and 2 directions are:

$$Q = \begin{bmatrix} \frac{E_1}{1-\nu_{12}\nu_{21}} & \frac{\nu_{21}E_2}{1-\nu_{12}\nu_{21}} & 0 \\ \frac{E_1}{1-\nu_{12}\nu_{21}} & \frac{\nu_{21}E_2}{1-\nu_{12}\nu_{21}} & 0 \\ 0 & 0 & G_{12} \end{bmatrix} \tag{3.5}$$

As the plies are laid up in different directions, the 1 & 2 directions are not always equal to the x & z directions of the laminate. By rotating the Q matrix, with the rotation matrix M, the material properties in the x & z directions can be determined:

$$M_\theta = \begin{bmatrix} \cos^2\theta & \sin^2\theta & 2\cos\theta\sin\theta \\ \sin^2\theta & \cos^2\theta & -2\cos\theta\sin\theta \\ -\cos\theta\sin\theta & \cos\theta\sin\theta & \cos^2\theta - \sin^2\theta \end{bmatrix} \tag{3.6}$$

$$C_\theta = M_\theta Q {M_\theta}^T \tag{3.7}$$

Then by summing the C matrices of all individual layers, the properties of the entire laminate can be determined. For example, one of the laminates on which the positions of mould marks are measured has a lay-up that consists out of 16% +45° fibres, 16% −45° fibres and 68% 0° fibres. The matrix properties of this laminate are thus as followed:

$$C = 0.16C_{45} + 0.16C_{-45} + 0.68C_0 \tag{3.8}$$

The loads applied to a laminate can be determined by multiplying the C matrix with the laminate strains. To calculate the strains that result from the internal stresses, one has to multiply the internal loads with the inverse of the C matrix. As a result, the strains of a laminate are:

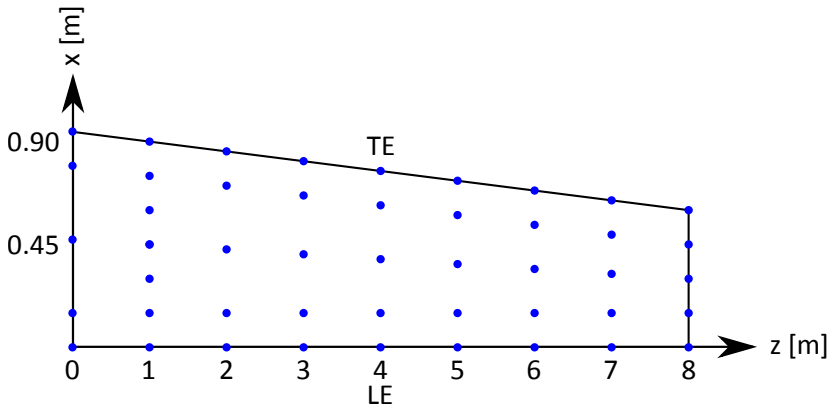

Figure 3.3: Schematic overview of all mould mark positions in the Hyller rout mould. Due to the reducing chord length, not all mould mark lines run parallel to the z axis. The middle and TE lines have an angle of respectively 1° and 2°.

$$\begin{pmatrix} \varepsilon_x \\ \varepsilon_z \\ \gamma_{xz} \end{pmatrix} = C^{-1}N \tag{3.9}$$

With N representing the load vector, in this case the loads created by chemical and thermal shrinkage. The CTE & CCS in the 1 and 2 directions can be calculated with equations 3.1 to 3.4. These need to be rotated and summed for all layers to find the internal load vector. So, the strains caused by chemical and thermal shrinkage can be calculated as followed [44]:

$$\boldsymbol{\alpha}_i = \begin{pmatrix} \alpha_x \\ \alpha_z \\ \alpha_{xz} \end{pmatrix} = M_i \begin{pmatrix} \alpha_1 \\ \alpha_2 \\ 0 \end{pmatrix} \tag{3.10}$$

$$\boldsymbol{\beta}_i = \begin{pmatrix} \beta_x \\ \beta_z \\ \beta_{xz} \end{pmatrix} = M_i \begin{pmatrix} \beta_1 \\ \beta_2 \\ 0 \end{pmatrix} \tag{3.11}$$

$$N = \sum_{i=1}^{k} R_i C_i \boldsymbol{\alpha}_i \Delta T + \sum_{i=1}^{k} R_i C_i \boldsymbol{\beta}_i \tag{3.12}$$

In these equations the k represents the number of layers, i represents the current layer, R represents the relative amount of the layer in the laminate. ΔT represents the temperature difference between the peak temperature during cure and the temperature at which the mould mark positions are measured. With MATLAB and typical values for LM laminates the shrinkage of laminates, and thus the movement of mould marks, can be predicted. In order to determine if this predicted movement is accurate with respect to reality, the mould mark positions were measured on different laminates. For these measurements, a measurement tape was taped on the mould or laminate surface going in a straight line next to the mould marks. As the mould marks are eight mm wide, the start & end point of each mark was measured, and the midpoint was taken as the mark location. In figure 3.3 a schematic overview is given of the mould marks made in the Hyller root mould. The LE & TE marks were made respectively 0.15 & 0.3 meters from the LE & TE. The middle line is in the middle of the mould and this marking pattern was repeated for eight z positions. However, due to the taper of the blade, the middle and TE mould mark lines have respectively a 1° and 2° angle with the z axis. As these angles are small, it is assumed that all mould mark lines are parallel in the z direction. The lay-up and sizes of the laminates on which the mould mark positions were measured are:

- *One layer UD laminate, made in Hyller root mould*
  Lay-up: one glass fibre layer of 1322 $gram/m^2$.
  z direction: measured three mould mark rows seven meters long.
  x direction: measured eight mould mark rows of maximally 0.75 meters long.
  ΔT not measured, assumed to be between $0°C$ to $-5°C$ as the laminate is only one layer thick.

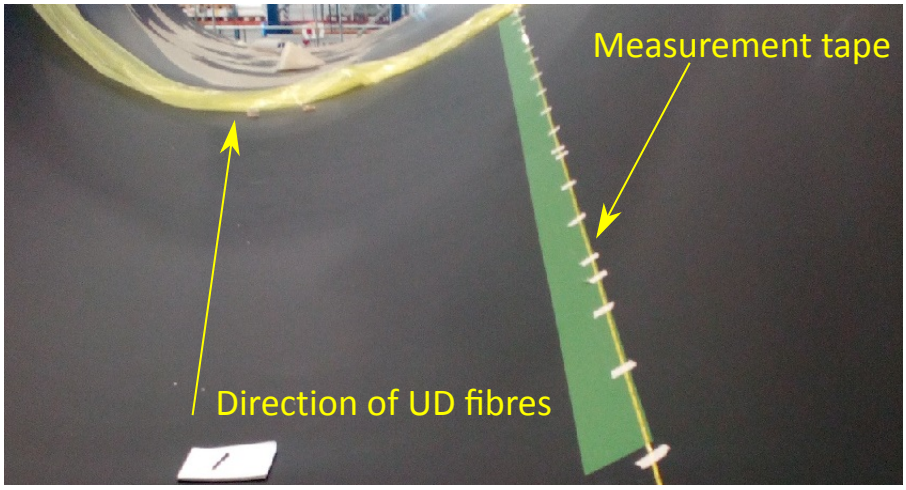

Figure 3.4: Picture from within LM88.4 UW root mould with a measurement tape taped alongside the T-spoiler mould marks, the UD fibre direction is also indicated.

- *LE glue flange mould laminate, made in Hyller root mould*
  Layup: balanced laminate with total fibre weight of 10210 $gram/m^2$.
  Fibre directions: 16% +45°, 16% −45° and 68% 0°.
  Two laminates with two rows of mould marks in the z direction can be measured.
  ΔT not measured, assumed to be between 0°C to −10°C based on experience from LM for the laminate thickness.

- *88.4 T-spoiler*[2] *marks, made in the LM88.4 UW mould:*
  As the Hyller reference blade is small compared to the current blade lengths, the laminate in the joint region is relatively thin compared to the laminate thicknesses one would have on an 80-meter-long blade split at 80% of the blade length. Therefore, the positions of the T-spoiler marks were measured on four different shells, as the laminate at the T-spoiler marks is much thicker than the laminate of the Hyller root. This should result in higher laminate shrinkage, and thus a higher mould mark movement. In figure 3.4 a picture of the T-spoiler marks is shown. As can be seen, the marks are not aligned with the direction of UD fibres. The angle with respect to the z axis is 7.5°.
  It is assumed that the balsa in the laminate does not have an influence on the shrinkage strains.
  Layup: balanced laminate with total fibre weight ranging from 27424 $gram/m^2$ to 17270 $gram/m^2$.
  Fibre directions range from 9% +45°, 9% −45° & 82% 0° to 12% +45°, 12% −45° & 76% 0°.
  ΔT not measured, assumed to be between −10°C to −20°C as the 88.4 root shell is produced with a two-step production process. First the shell is produced without the spar cap. As a result, the amount of heat being generated during the cure cycle of the laminate above the T-spoiler mould marks results in a difference smaller than 20°C. Once this is cured, the spar cap is lay-ed up and cured in a second process step. It is assumed that the high peak temperature of the second process step does not affect the shrinkage of the laminate above the T-spoiler marks.

All mould mark positions were measured with a measurement tape with mm marks, resulting in the measurement error being ±1 mm. However, all movements will be reviewed as strains in mm/m which results in the measurement error also being depended on the distance over which is measured. In all figures that show measurement results for mould mark movements, the measurement error is indicated as ±1 mm divided by the distance from first mould mark. In order to reduce the measurement error as much as possible, only the deviations over half the laminate length are reviewed. So, in x direction this results in the minimal measurement length being 0.4 meters and in z direction this is 4 meters.

During the project a total of three test articles were to be build. The mould mark pattern which is visible in figure 3.3 was made on both the UW and DW rout moulds. It is difficult to predict the mould mark movement as these marks cover the entire root section. This results in a great variability in lay-up as some marks are in

[2]A T-spoiler is an aerodynamic add-on that improves power output of wind turbine blades.

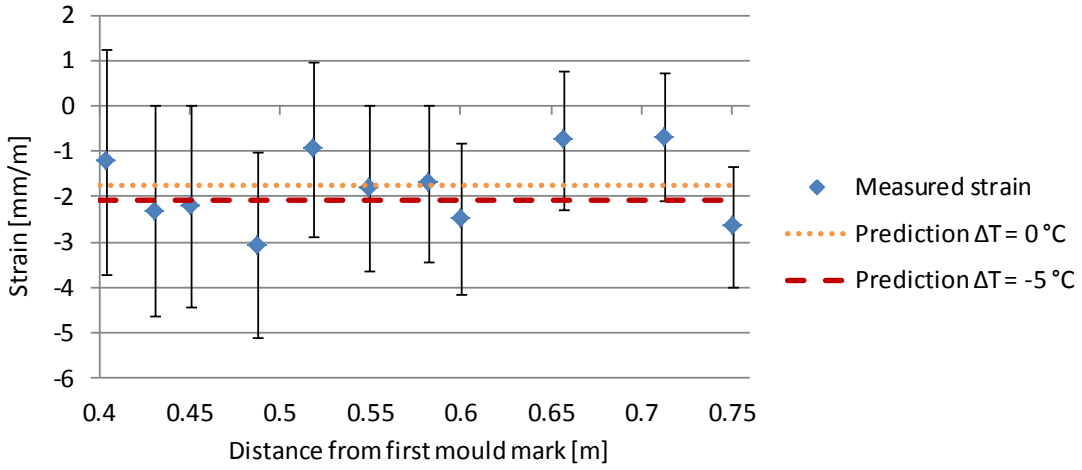

Figure 3.5: Measured mould mark strains on one-layer UD laminate in x direction, predicted strains for a ΔT of 0° and −5° also indicated.

the spar cap region, and others are in the balsa regions. Furthermore, there are also several ply-drops along the length of the blade (Also resulting in a varying ΔT). Therefore, the goal of the measurements on the Hyller TA root sections was to review the movement of mould marks in x & z directions relative to one-another up to eight meters from the joint. This would provide an indication of the movement of mould marks on an actual blade in the joint region, and how much the shrinkage varies from blade to blade. Unfortunately, only one TA root was produced and due to production difficulties most marks on this blade were lost as well. Therefore, the mould marks on the Hyller root are not reviewed in this report. This also reveals an issue with the usage of mould marks, they are easily lost. However, as the mould marks are used by LM in production, there are several different processes for recovering lost marks with other mould marks. Only the review of what the accuracy is of these processes is, is out of scope for this project.

3.3. Measurements of mould mark positional accuracy

In figure 3.5 the measured strains on the one-layer UD laminate in the x direction are visualised. As indicated before, the ΔT is assumed to be larger than $-5°C$. Thin CLT estimated a shrinkage of -1.75 mm/m for $\Delta T = 0°C$ and -2.08 mm/m for $\Delta T = -5°C$. With the average measured strain being -1.82 mm/m the observed strain correlates well with the predicted strain. However, the average measurement error is ±1.86 mm/m which means that the agreement between the prediction and reality could be a coincidence. In this case a more precise measurement method or larger measurement scale should be used to confirm that the mould marks move as much as is predicted with CLT. The movement was measured on a much longer scale in the z direction, of which the results are shown in figure 3.6. Since this is in the fibre direction of the laminate, the shrinkage is much lower. This results in the measurement error again roughly equal to the measured strains. Thin CLT estimated a shrinkage of -0.12 mm/m for $\Delta T = 0°C$ and -0.21 mm/m for $\Delta T = -5°C$. This again correlated well, as the average measured strain is -0.13 mm/m. Only with the measurement error being ±0.19 mm/m, it could again be a coincidence.

In figure 3.7 the mould mark movement observed on the LE glue flange mould laminate in the z direction is visualised. These measurements found an average strain of -0.16 mm/m with an average measurement error of ±0.17 mm/m. This correlates not as good with the prediction from thin CLT as in the two previously described measurements. For a $\Delta T = 0°C$ the predicted strain is -0.19 mm/m and for $\Delta T = -10°C$ a strain of -0.31 mm/m. Both predicted values are within the measurement error of the average strain. So, with the current data the hypothesis cannot be accepted nor be rejected, more accurate measurements are required to determine if the predictions are correct. These should also refine the predicted strain by measuring the maximum temperature during cure, as the current $\Delta T = 0°C$ to $-10°C$ gives a relatively wide range for the predicted strain. When all measured strains are compared to one-another, the pattern in measured strains is equal to the predicted strains visualised in figure 3.2. Namely the strains in x direction of a UD laminate being largest and the strains in the z direction of this laminate being smallest. Also, the strains on a triaxial laminate in the z direction being slightly larger than the strains in the z direction of a UD laminate.

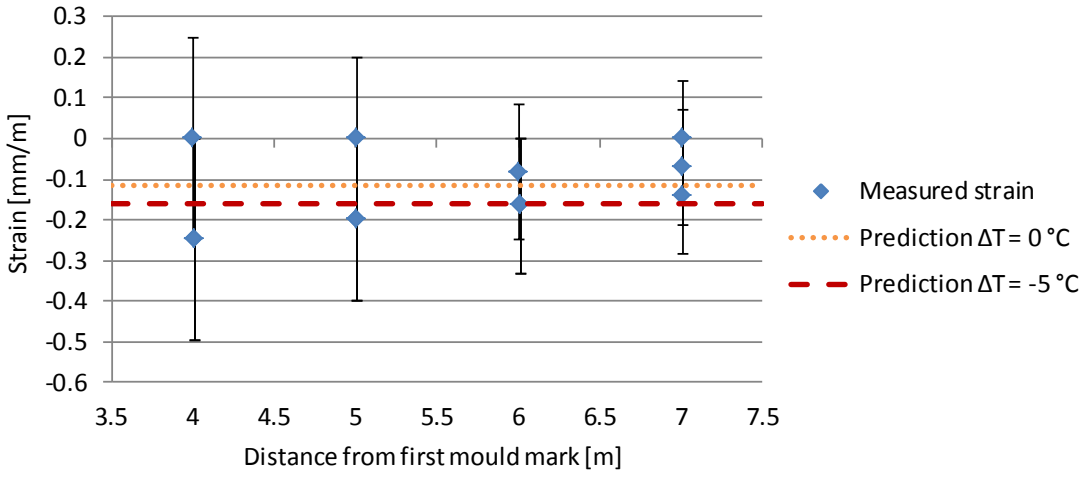

Figure 3.6: Measured mould mark strains on one-layer UD laminate in z direction, predicted strains for a ΔT of 0° and −5° also indicated.

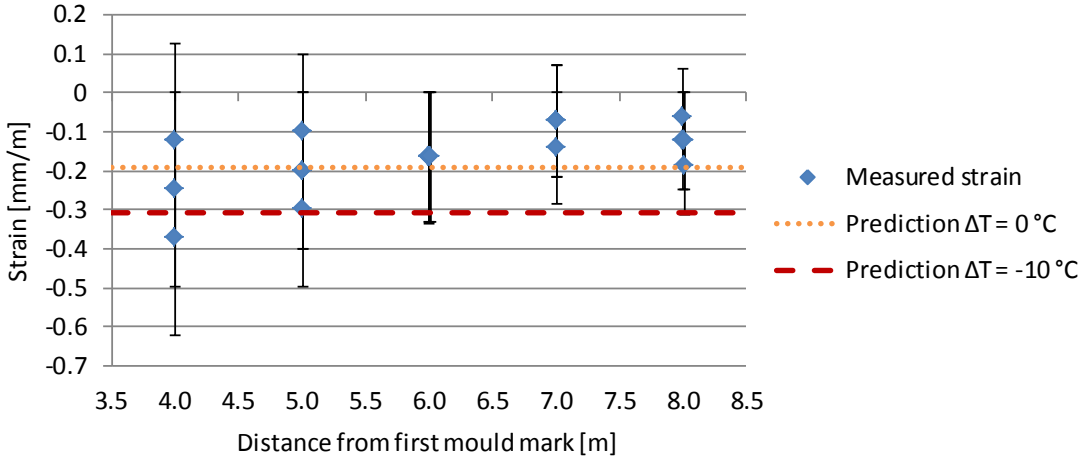

Figure 3.7: Measured mould mark strains on the LE glue flange mould laminate in the z direction, predicted strains for a ΔT of 0° and −10° also indicated.

With the measurements on four different LM88.4 root shells it is also possible to review the consistency of mould mark movements from one laminate to the next. The results of these measurements are shown in figure 3.8. It can be observed that the measured strains are varying (The average strains of shells 1 to 4 are respectively -0.27 mm/m, -0.23 mm/m, -0.16 mm/m and -0.16 mm/m). However, the values vary within the range of the measurement error (this is $\pm 0.17 mm/m$). So, based on this data it is not possible to conclude if there is a variation in mould mark movement from one laminate to the next. As there are play drops along the length of the root shell, the shrinkage strains were calculated for the laminate at the first mould mark and for the laminate of the last mould mark. The average of these two shrinkage strains is shown in figure 3.8 as the predicted strain. The average strain of all measurement mould marks on the four shells is -0.20 mm/m with an average error of 0.17 mm/m. For $\Delta T = -10°C$ the predicted strain is -0.29 mm/m, so the measured strain is lower but within the range of the measurement error. However, the predicted strain for $\Delta T = 0°C$ is 0.18 mm/m. So, it is possible that the assumed temperature differences of $-10°C$ to $-20°C$ are too high and that for a lower ΔT the measured and predicted strains do correlate well with one-another. However, considering that the total fibre weight is on average about 22 kg/m^2, it is not likely that the ΔT is only in the order of $2°C$.

During the alignment process reference points are required to determine the misalignments. In order to maximize the measurement distance, reference points on the LE and TE are desired as this is the furthest that the points can be apart. Maximizing this measurement distance is especially useful for the twist angle align-

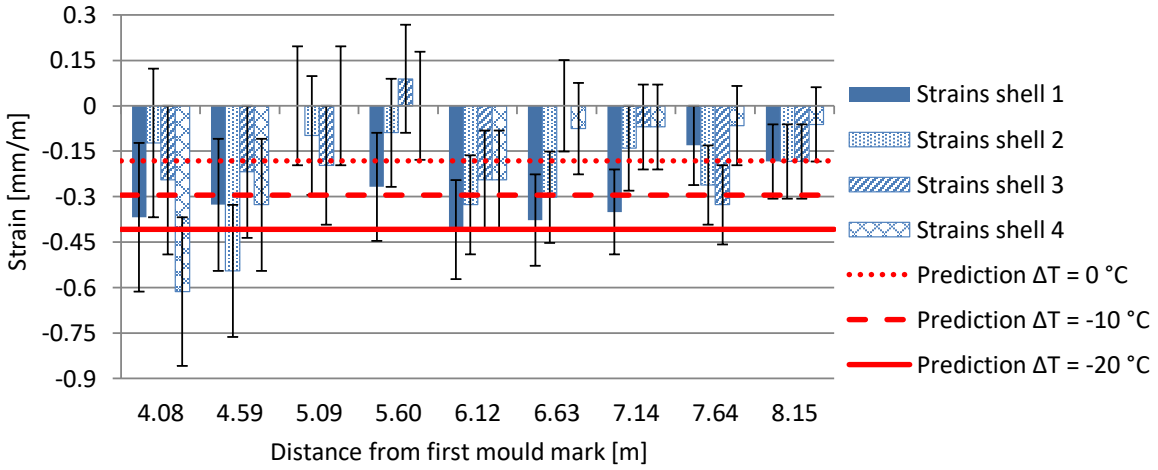

Figure 3.8: Measured mould mark strains of T-spoiler root mould marks on 88.4 root shells, at an angle of approximately 7.5° with the z axis. All four shells were built with the same design and production process.

ment. If the measurement error is ±1 mm at the reference points, then a larger distance in between the two points results in a smaller angular measurement error. With the TE being relatively thin, it is quite easy to determine the middle and use that as a reference point. But on the leading edge this is much more difficult due to the relatively high thickness. Next, the root of the blade is produced with a two-shell production process, which has the joint line of both shells on the LE. Manual angular grinders are used to restore the aerodynamic shape. Once this is restored, the joint line is over laminated by hand. As a result, it is not possible to have a mould mark on the LE. In order to mark the correct y position on the LE, two mould marks were used for the Hyller root. Both marks were placed at 150 mm from the LE on the same z position, one in the DW mould and one in the UW mould. The midpoint in between the two marks should give a good indication of the LE y position. From the scan of the Hyller TA, made with an accurate 3D scanner, it was determined that the y positioning was 0.4 mm off on both locations were this method was used. However, these two reference points could not be used in the alignment of the Hyller TA as they were positioned too far from the joining region. Initially there would have been reference points in the correct positions, but these were lost due to surface repairs made in the production of the root section.

3.4. Alignment of Hyller test article

In chapter 2 it was established that with good reference points the six-axis manipulator can be used to align the tip and root sections with a high accuracy. Also, as is shown in the previous sections, the movement of mould marks close to the joint is limited. So, the alignment method described in chapter 2 and mould marks were used in the alignment & joining process of the Hyller TA. Unfortunately, there were some problems in the production of the separate blade sections. This resulted in many of the mould marks being lost, as well as the LE glue-flange and the webs not being properly dimensioned. An overview with some pictures is visible in appendix B. Due to the wrong dimensioning of the components mentioned above, the tip section could not be manipulated to the desired position. Although it was possible to adjust the six-axis manipulator, the tip was lifted from its supports by the webs and LE glue flange, see figure 3.9.

In these non-ideal conditions, it was impossible to align the parts as good as in the alignment trials. Therefore, the six-axis manipulator with the tip was placed such that the alignment was as good as possible. After this the webs and UW shell were joined, next the blade was turned around, aligned and the DW shell was joined. To determine what the final alignment deviations were, the TA was placed LE down and then scanned, see figure 3.10. Then, the same method as used in section 2.3 was used to determine the misalignments. The found alignment deviations of the tip section relative to the root are visible in table 3.1. Also, in figure 3.11 the misalignments of the tip are visualised with cross-sections of the TA (in black), and the designed position of each cross-section (in red).

Figure 3.9: Picture of TA tip being pushed out of the supported position.

Figure 3.10: Picture of TA being scanned with LE down. Pallets only support the former root section, cranes to keep TE up. Tape was applied on the surface for the scanner to work properly

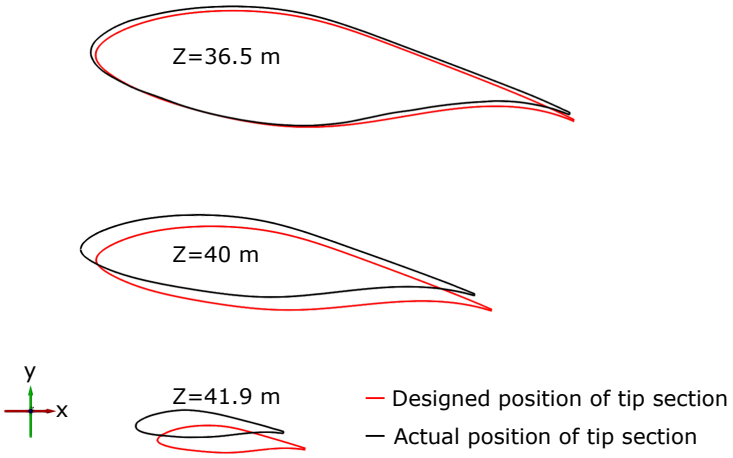

Figure 3.11: Deviations of three tip sections visualised. In red the designed positions of the tip section for three z positions, in black the actual positions of the tip section for the same three z positions.

	TA scan	Gravity corrected TA scan
Δx	4.0 mm	5.1 mm
Δy	6.7 mm	7.0 mm
Δz	25.1 mm	25.1 mm
$\Delta\alpha$	$0.53^{\circ}{}^{+0.07^{\circ}}_{-0.05^{\circ}}$	$0.47^{\circ}{}^{+0.03^{\circ}}_{-0.08^{\circ}}$
$\Delta\beta$	$0.18^{\circ}{}^{+0.07^{\circ}}_{-0.05^{\circ}}$	$0.18^{\circ}{}^{+0.07^{\circ}}_{-0.05^{\circ}}$
$\Delta\gamma$	$0.36^{\circ}{}^{+0.05^{\circ}}_{-0.02^{\circ}}$	$0.25^{\circ}{}^{+0.05^{\circ}}_{-0.03^{\circ}}$

Table 3.1: Measured alignment errors in each DOF for the Hyller TA, with the gravity corrected results in the second column.

During the scanning of the TA, the supports were placed on the blade root side before the joint. This resulted in a relatively large part of the TA hanging free. Due to the flexibility of wind turbine blades, the gravity will deform the blade a couple mm. To determine how much, a gravity load was applied to the TA finite element method (FEM) model, supported at same positions as in figure 3.10. Then it was calculated by how much the tip section would deform due to gravity. This showed that the tip would normally move by -14.3 mm in the x direction. This is 34% of the observed deviation in the x direction. Therefore, it was calculated that the alignment error for γ is 0.25° instead of 0.36°. Since the gravity causes a 0.11° difference in γ with these supports. However, this still does not explain all the misalignments. So, an overview of the causes for the misalignments is given below:

- Deviation in length (z)
  In order to create a taper in the shells of the root section, inlays were placed into the mould. Unfortunately, one of the inlays was too close to the root bolts which resulted in a shorter shell. To keep the end point of the webs as designed relative to the end point of the shell, the webs were placed closer to the root bolts. This resulted in a shorter root section. To keep the bond line thickness of the webs within the specified range, the tip section placement had to be compensated for the shorter root section. This resulted in the TA being shorter as designed. According to measurements with lasers and a measuring tape, the TA was 25 mm too short. The 3D scanning revealed that the TA was 25.1 mm too short, showing that the method used with the measuring tape and lasers is also accurate. This is also visualised in figure 3.12.

- Deviations in x
  For the alignment in the x direction the wrongly dimensioned LE glue-flange prevented a proper alignment (see figures B.4 & B.5 in appendix B). The lasers showed that the tip was off by 9 mm and the 3D scan showed that the tip was off by 5 mm. The difference could be caused by measurement errors or possible deformations of the tip section due it being pushed off from its supports by the LE glue-flange, see figure 3.9.

- Deviation in α
  Due to repairs on the blade sections, the reference points used for the twist angle alignment were lost. To recreate the reference points hand cut contour moulds were used. During the alignment process of the TA the lasers showed that the twist angle was aligned properly, only the 3D scan of the TA disproves this. If it is assumed that the TE was in the right position, then the LE would be off by -7 mm in the y direction. Furthermore, the 3D scan was used to determine the positional accuracy of the LE reference point on the root section, what showed that it was of by -3.1 mm in the y direction. Also, the TE of the root section was 5 mm too thick which probably resulted in the reference point being off by 1-2 mm in the y direction. So, compared to the inaccurate reference points, the twist angle is off by -2 to -3 mm or approximately 0.15°. This is roughly similar to the observed twist angle deviations in chapter 2. This makes it likely that the largest part of the twist alignment error in is caused by inaccurate reference points.

- Deviations in y, β & γ
  As can be seen in table 3.1, the deviations of y, β & γ were also larger compared to the trial alignments. As the exact same method was used for aligning, it is unlikely that this is solely due to misalignment errors and incorrect reference points (0.18° deviation for β means that the tip reference point is 24.7

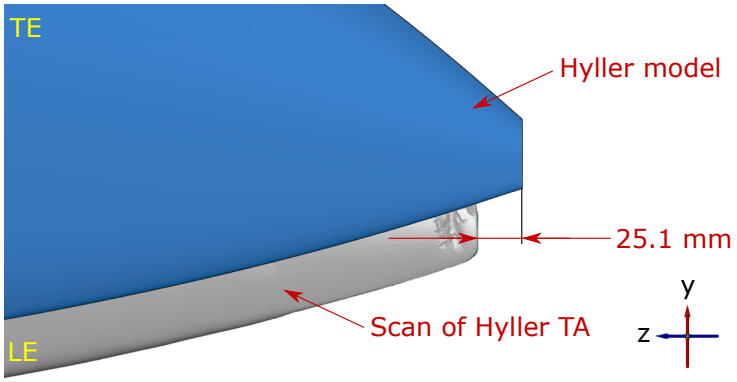

Figure 3.12: Deviations of tip section at absolute blade tip (in grey) relative to model (in blue).

mm off, see figure 3.11). With the tip being pushed from the LE support, see figure 3.9, and the tip being strapped to these supports, it is likely that the blade section could be slightly deformed due to the manipulations of the six-axis manipulator. When the blade was moved off the six-axis manipulator it could spring back, causing the tip to be in another position as when the alignment was finished.

The wrong dimensioning of the LE glue-flange, see pictures in appendix B, was related to most of the misalignments of the tip section. During the production of the TA this was already expected, however the tight schedule did not allow for making a properly dimensioned LE glue flange. Therefore, the TA production was continued while the alignment of the blade sections is considerably worse compared to the trial alignments.

3.5. Conclusions

The used measurements of mould marks can be used to answer the first research question. This question is formulated as followed:

What is the relative positional accuracy in x & z directions of mould marks on glass fibre polyester wind turbine blade laminates?

The relative positional accuracy in x & z directions of mould marks on glass fibre polyester wind turbine blade laminates is dependent on the laminate lay-up. The measured relative movement strains on wind turbine blade laminates ranged from -0.13 mm/m to -0.16 mm/m in the z direction. Unfortunately, only on one laminate the strains could be measured in the x direction, which indicated a movement of -1.82 mm/m. It was hypothesised that the mould mark positions vary due to chemical and thermal shrinkage. With thin CLT the shrinkage strains were predicted for each laminate. For a thin UD laminate the measured movement strains were in the range of the predicted strains in both the x & z directions, but on the lower side. On the LE glue flange mould laminate and the LM88.4 T-spoiler marks the measured movement strains were lower than the predicted strains. However, all predicted strains were within the measurement error of the measured strains. This was mainly due to the measurement error being relatively large. Therefore, it is not possible to draw strong conclusions from the presented data. However, the presented data does suggest that the positions of mould marks can be predicted with thin CLT, only it will predict a too large variation. For the predicted strains, typical LM Wind Power laminate values were used, and the peak curing temperatures were unknown. It could be that with more accurate data of the laminate properties the predictions will be more accurate. Another possibility is that the movement strains of mould marks are lower than the chemical and thermal shrinkage combined. This could be caused by the edge of the mould mark hole providing additional constraints that result in a restricted mould mark movement. So, when the laminate above the mark starts to shrink during gelation, the edge of the mould mark reduced the movement compared to the fibres above the mark. More research is required to determine if the mould marks do have a lower movement then CLT predicts, as was suggested by the measurement data.

By measuring the T-spoiler marks on different shells it could be reviewed if the movements vary from blade to blade. As only four root shells were produced the sample size is limited. The measurements revealed a variation from one laminate to the next, only this variation was within the measurement error. Therefore,

it is not possible to conclude that the movement strains are varying. Due to all deviations being smaller than the measurement errors, the current data suggests that the movements are consistent. More accurate measurements are required to determine if the movements are indeed consistent. Mould marks were also used on two locations on the TA root section to mark the y position of the LE point. An 3D scan revealed that both marks were only 0.4 mm off. Combining all these results it is possible to conclude that using mould marks as reference points on tip split wind turbine blades is possible. The movements strains are relatively high in the x/width direction. However, wind turbine blade sections are not very wide in the tip region. For example, the Hyller blade had a width of 0.9 meters and for an 80-meter-long conceptual tip-split blade the width is only 1.2 meters at the split. So, based on the one measurement in the x direction, the marks deviate maximally two mm from the designed position. In the length wise direction, the marks show a smaller movement strain as this is the main fibre direction. If one chooses the split line as a reference line, the marks will not deviate more than two mm for the first four meters when also accounting for higher shrinkage rates due to the higher peak temperature (Based on the predicted movements of the LM88.4 T-spoiler marks for $\Delta T = -20°C$). Compared to the blade root, which is much further away, the shrinkage will be much higher. This could be corrected by measuring the blade length and adjusting the z position of the tip accordingly.

Also, an attempt was made to align the Hyller TA with the same precision as was achieved in the trial alignments (See chapter 2) while using mould marks as reference points. Unfortunately, there were some problems in the production of the Hyller TA. As surface repairs were necessary on the TA blade sections, the most important reference points were lost. This immediately reveals a shortcoming of mould marks, they are quite easily lost. Furthermore, the alignment of the TA was also complicated by components of the separate sections being improperly dimensioned. All of which complicated the alignment process. In table 3.1 the alignment deviations as were determined with an 3D scan are shown. However, it was also noticed that the scan of the TA was influenced by gravity and with FEM some deviations could be partially explained. However, the alignment deviations are still considerably larger than the deviations found in the trail alignments (see table 2.1). Whether these deviations are acceptable is partially reviewed in chapter 4. As the blade has also finished structural testing[3] with only minor damages observed on a repair of a production defect, the deviations did not cause structural failure and are thus acceptable from a structural point of view for the current design.

[3]The entire blade life was structurally tested according to the same blade certification standards as the LM42.1, the Hyller reference blade. The test article passed these, and additional fatigue tests, without structural damage to the interested areas.

4

Influence of angular misalignments on power output

In section 1.2.2 the research questions related to the aerodynamics were presented. In this chapter the answers to these research questions are given. In order to do this, simulations were made with lifting line simulation software. A description of how this works is given in section 4.1. In section 1.2.2 it was also stated that the twist angle is most likely the critical alignment angle and this statement is tested in section 4.2. With the alignment trails (Chapter 2) it was shown that it is possible to align the twist angle with an accuracy of $< \pm 0.1°$ in the right conditions. However, the twist alignment error on the TA was considerably worse, being about 0.5° off. This is in the same range as the manufactured twist deviations. With the achieved twist misalignments being the same order of magnitude as the allowable manufactured twist deviations, both will be considered in a more in-depth review of the relation between the twist angle deviations and the power output. The hypothesised relation, test set-up and results can be found in section 4.3. Furthermore, it is also reviewed in section 4.4 what the relation is between the average twist error of the tip section and the variance in power output. In section 4.5 all of this is combined and answers to the aerodynamic research questions are formulated.

4.1. Lifting line simulation software

In order to determine the effects of angular deviation between the tip and root, several simulations of a tip split blade over 70 meters in length with varying angular deviations were made. Although the reference blade for the Hyller project is a 42.1-meter blade, it is an old blade. Furthermore, with the average onshore wind turbine having a blade length of about 50 meters, it is likely that for tip split blades to be economically viable, the blade length will have to be longer than the currently used 50 meters [45]. So, to make the resulting data more equal to likely first applications the simulations were performed on a 70+ meter long blade, split at 82% of its length. For the simulations themselves, a lifting line program build by the LM aero department was used. This is an accurate simulation method at a low computational cost [46].

The lifting line simulation software works by dividing the wind turbine blade in several sections. For each section the lift and drag due to the 3D flow are calculated, as well as the aerodynamic effects of each section on the other sections. By summing all these effects; the power, thrust and flapwise root bending moment (FRBM) of the wind turbine can be calculated [46]. In order to limit the scope for all the simulations made in this chapter the following assumptions have been made:

- 70+ meter long blade, designed by LM Wind Power
- Split location at 82% of blade length from root
- Blade is operated at rated speed
- Blade joint has no impact on power output
- Blade root is connected to hub without any twist deviation
- Blade pitch is constant

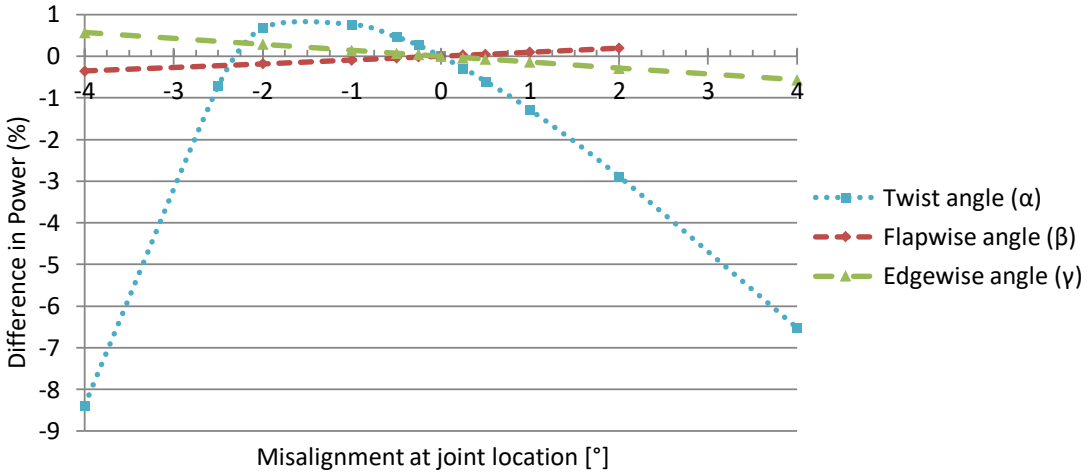

Figure 4.1: Result of lifting line analysis for tip split blade with several misalignments at the joint location.

%ΔPower	Deviation $\pm 1°$	Deviation $\pm 0.5°$	Deviation $\pm 0.25°$	Deviation $\pm 0.10°$
Twist angle ($\Delta\alpha$)	$+0.77/-1.29$	$+0.46/-0.60$	$+0.26/-0.28$	$+0.11/-0.12$
Flapwise angle ($\Delta\beta$)	$+0.10/-0.09$	± 0.05	± 0.02	Not simulated
Edgewise angle($\Delta\gamma$)	± 0.14	± 0.07	$+0.04/-0.03$	Not simulated

Table 4.1: Different twist tolerance levels based on different alignment strategies.

4.2. Differences in power output due to deviations in α, β & γ of tip section

To compare the differences in power output due to deviations in α, β & γ, several blade geometries were made with angular deviations of the tip section in α, β & γ directions. Then the relative differences in power output relative to a blade without angular deviations were determined with the lifting line simulation program. In figure 4.1 and table 4.1 the results from the lifting line simulations are visualised. As can be seen, twist angle deviations have by far the biggest impact on power output, as was also the expectation (see section 1.2.2). Based on figure 4.1 the difference in power output seems to be related linearly to the angular deviations in flapwise & edgewise directions in the range from $-4°$ to $4°$, which is not true for the twist angle deviations.

Furthermore, based on the data visible in table 4.1 a twist angle deviation in the order of $\pm 0.1°$ is roughly equal to a flapwise angular deviation in the order of $\pm 1°$, and assuming a linear relation for the edgewise angular deviations between $\pm 0.5°$ & $\pm 1°$, a $\pm 0.71°$ flapwise angular deviation. So if it is assumed that the trailing edge at the root of the tip section is in the correct position, then the LE at the root of the tip section has to be placed with an accuracy of ± 1.6 mm whereas the tip of the tip section has to be placed with an accuracy of ± 86 mm or ± 122 mm for the deviations in edgewise or flapwise directions respectively, in order to have the same effect on power output as a twist angle deviation of $0.1°$.

When the results of the trial alignments and the Hyller TA alignment, see tables 2.1 & 3.1, are reviewed with table 4.1 in mind. The achieved alignment accuracy of the tip section in the flapwise & edgewise directions is sufficient in all measured alignments, as the differences in power are always be lower than $\pm 0.05\%$ according to the results from the lifting line simulations. For the twist angle deviations achieved in the alignment trials, the deviations are probably sufficient since the effects on power output are around $\pm 0.1\%$. However, the twist misalignment of the TA tip section will cause roughly a 0.6% difference in power according to the lifting line simulations. This is a power loss that can probably be noticed on the AEP of a wind turbine. Only with this alignment error being similar to the allowed manufactured twist angle deviations, it is necessary to include these while studying the relation between the twist angle and the power output. This study is described in the next section.

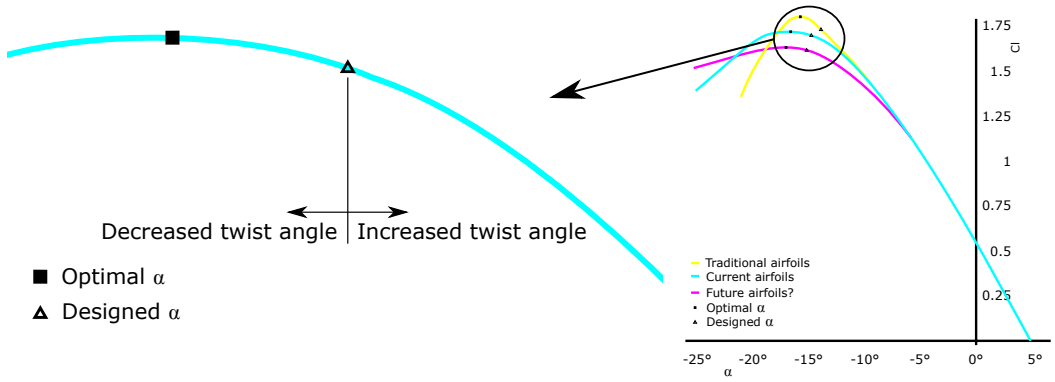

Figure 4.2: Left the hypothesised shape of the power curve due to twist angle deviations with the relation to the $C_l - \alpha$ on the right.

4.3. Twist angle & tip split wind turbine blades

In order to find an answer to research question 2.1, the relation between the twist angle at the tip and the variation in power output must be determined for tip-split blades with manufactured and alignment twist errors. The hypothesised relation between the these two is a power curve that is similar in shape as a $C_l - \alpha$ curve around the designed α, illustrated in figure 4.2. It is known for wind turbines that power $\propto \alpha$ [47]. Thus, for a decreased twist angle the power output will increase, but not by much, and a plateau will be formed. For an increased twist angle the power output will reduce with an increasing rate. To determine if this hypothesis is correct, simulations have been made. The set-up of these simulations is described in section 4.3.1 and the results are described in section 4.3.2.

4.3.1. Test set-up

As both the twist alignment deviations and the manufactured twist deviations are reviewed, both deviations have to be added to the nominal blade. For the manufactured twist deviations, LM Wind Power does not have publishable data. The two papers from Petrone et al. [30] and Campobasso et al. [31] which reviewed the effect of manufactured twist deviations, used manufactured twist tolerances that were not based on published manufacturing deviations. Both state that the used values are 'typical manufacturing tolerances'. So, in order to have a measured reference for the manufactured twist deviations the scan of the Hyller TA from section 3.4 was reviewed. In the data from this scan, manufactured twist deviations can be found. Along the length of the TA the twist angle was reviewed at six points and the manufactured twist deviations at these points is visible in table 4.2. This shows that the twist angle deviation varies along the length of the blade, with a variation that is somewhat like a sinusoidal relationship.

To mimic this, it was assumed that the manufactured twist deviation varies linearly or sinusoidal with different periods. In table 4.2 it is visible that the maximum rate of change observed on the TA is 0.24° per meter. Different sinusoidal twist deviation distributions were used as manufactured twist deviations. The maximum rate of change in these manufactured twist angle deviations is equal to the observed maximum rate of change of 0.24° per meter. This means that there are six different sinusoidal distributions. Of all these manufactured twist error distributions, the maximum twist deviation is limited to the accepted manufactured twist tolerance values of LM Wind Power. Although the data in table 4.2 did not show it, one linearly varying manufactured twist deviation was added, bringing the total manufactured twist deviation distributions to seven. A couple of these twist distributions are visualised in figure 4.3. In order to have a complete and balanced set, there were also seven negative distributions added. These are reversed in sign relative to the seven previously mentioned manufactured twist distributions. This results in a set of fourteen different manufactured twist distributions. The twist alignment error was added on top of each distribution. For this, eleven misalignment values ranging from −3° to +3° were used. These deviations where applied to the entire tip section which causes a step change in the twist distribution and this is visualised in figure 4.4. As a result, the total number of blades which where simulated is 154 (14x11).

Z-position	Manufactured twist angle deviation	Rate of change
29 m	0.08°	$0.02°m^{-1}$
30 m	0.32°	$0.24°m^{-1}$
32.5 m	0.08°	$-0.10°m^{-1}$
36.5 m	−0.09°	$-0.04°m^{-1}$
40 m	0.08°	$0.05°m^{-1}$
41.9 m	0.36°	$0.15°m^{-1}$

Table 4.2: Twist angle deviations measured on the Hyller TA. As can be seen, the manufactured twist deviation varies non-linearly along the length of the TA. The rate at which the twist angle changes in-between the measurements is also shown.

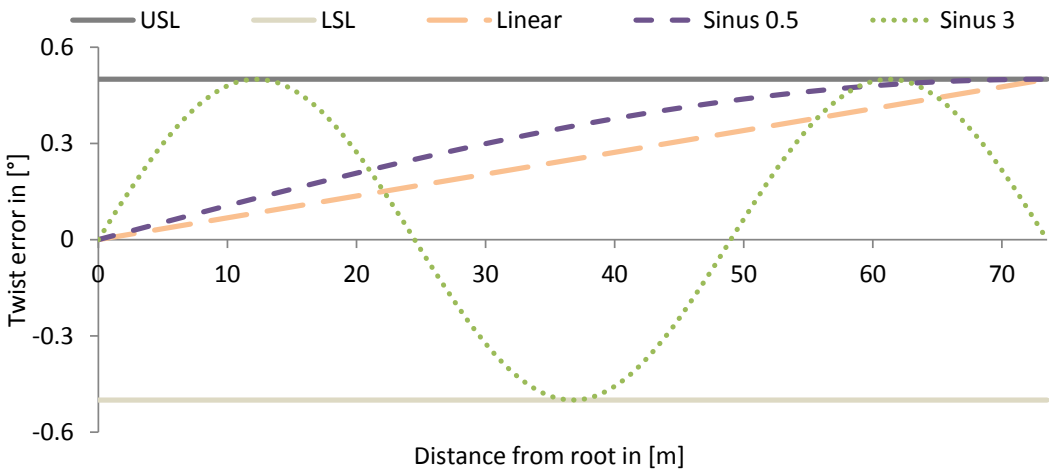

Figure 4.3: Overview of the assumed positive manufactured twist deviation distributions. The number in the name means the number of half periods along the length of the blade.

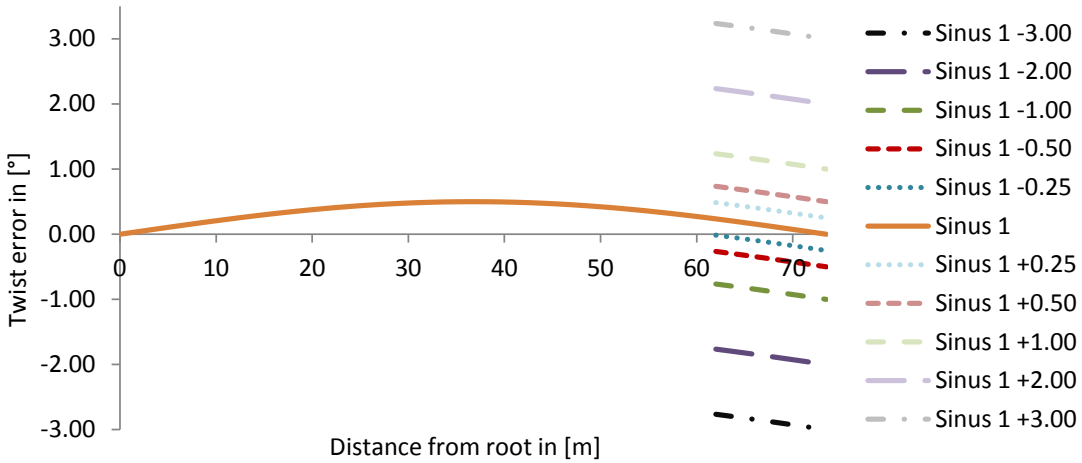

Figure 4.4: Overview of the assumed positive manufactured twist deviation distributions with alignment deviations at the joint. The specific twist misalignment at the joint is indicated by the second number in the name of the twist error distribution.

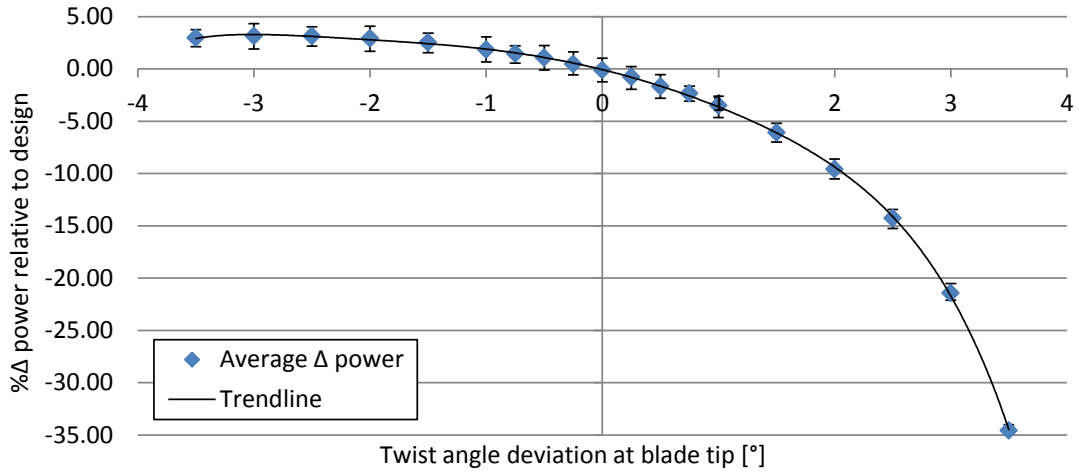

Figure 4.5: Power differences for wind turbine blades containing manufactured and alignment twist deviations. Differences in power are sorted on twist angle deviations at absolute blade tip for blades containing twist defects due to manufacturing and misalignments.

4.3.2. Outcome

The differences in power output due to the twist angle deviations, determined with lifting line simulations, are visible in figure 4.5. It can be seen in this figure that a negative twist angle will result in a marginally larger power output and a plateau is formed. For a positive twist angle deviation, the blade will produce less power compared to the designed blade. Also, this power loss is non-linearly related to the twist angle deviation. Comparing the shape from figure 4.5 with the predicted shape which is visualised in figure 4.2, it seems that the shape has a flatter plateau region and a faster decline in power output. This could be because the power of a wind turbine is the lift of a blade section multiplied with the distance of this section to the blade root. Since the twist angles of the tip section have a relatively long distance to the blade root, all differences in lift are magnified for the differences in power. However, the exact cause for this cannot be determined from the available data. However, going back to the work of Ahmed [24], the shape of the curve has more similarities with the $C_L - \alpha$ curve of the future aerofoils, see the purple line in figure 1.4. Considering that the used blade for the simulations, was designed after 2016, and the paper from Ahmed is from 2012. The, in his paper, mentioned future aerofoils might be in use already. Further research would be required to determine how the precise shape of the $C_L - \alpha$ curve influences the precise relationship between the power output and the twist angle deviation at the tip. This is not done within this project as it is out of scope and is left as a recommendation (see chapter 7).

4.4. Relation average twist error tip section & variance in power output

With the relation between tip angle and power output, shown in figure 4.5, it is clear that the twist angle at the blade tip, and thus the twist angle of the tip section, has a direct influence on the power output of the entire wind turbine. As was stated in section 1.2.2, it might be possible to use the additional freedom of a split in the tip region to reduce the variance in power output compared to single piece wind turbine blades. The pitch controller on a wind turbine blade is balancing the torque of the three blades on a wind turbine. As a result, the entire turbine produces as much energy as the worst blade on the turbine. By reducing the variance in power output, the worst blade of three randomly selected blades is more likely to have a larger power output due to a reduced spread in power output values. This should then result in a larger power output for the wind turbine, which could lead to lower cost wind energy.

So, the relation between the variance in power output, due to twist errors, and the absolute average twist error of the tip section after joining has to be reviewed. This would also provide an answer to research question 2.2. With figure 4.5 in mind, it is hypothesised that a larger average twist error of the tip section will result in a larger variance in power output and a smaller average twist error of the tip section will result in a smaller variance in power output. Furthermore, it is also hypothesised that the relation is non-linear with a more exponential relation rather than a logarithmic. This is based on the shape of the line in figure 4.5 around 0° twist angle deviation at the blade tip. An enlargement of this is visible in figure 4.6. If the twist angle devia-

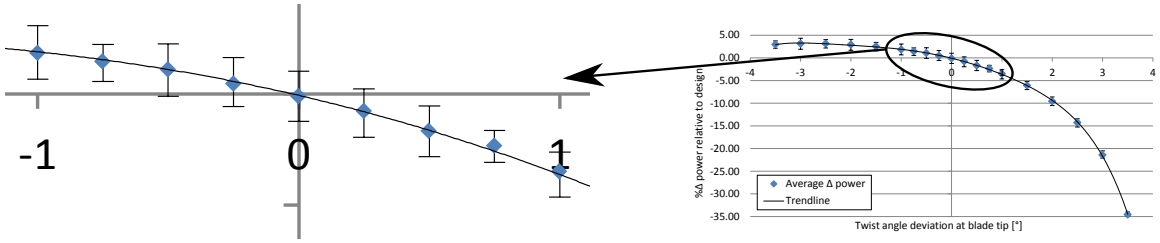

Figure 4.6: Enlarged view of the twist angle deviation at the blade tip and the resulting difference in power relative to a nominal blade.

tion at the blade tip is small, then the difference in power is small. However, once the twist angle deviation increases, the difference in power becomes non-linearly larger. To determine if these hypotheses are correct, additional blade geometries with twist angle deviations were simulated. The set-up of these simulations is described in section 4.4.1 and the results of these simulations are described in section 4.4.2. Furthermore, the relation between the variance in power output and the absolute average twist error of the tip section can be used in a practical application. Namely how twist alignment tolerances for tip-split wind turbine blades could be defined in order to have a similar or reduced variance in power output as compared to single piece wind turbine blades. This is described in section 4.4.3.

4.4.1. Test set-up

To test this hypothesis additional lifting line analyses were performed. In these analyses the same assumptions are made as were made in section 4.3.1, with the additional assumption that all twist alignment deviations are normally distributed, like what Petrone et al. and Campobasso et al. [30, 31] did. The total number of unique blade geometries used to test the hypothesis is 280. These geometries are made by combining the below parameters as followed:

- 14 different base shapes, same as were used in section 4.3.1
  - Linear, Sinus 0.5, Sinus 1, Sinus 1.5, Sinus 2, Sinus 2.5, Sinus 3
  - Negative of above distributions
- 2 different maxima and minima for manufactured twist deviations, see figure 4.7
  - Up to upper & lower specified limits (USL & LSL) for manufactured twist deviations from LM
  - Up to half of the USL & LSL for manufactured twist deviations from LM, indicated by the number 2 after distribution name (For example sinus2 2.5, see figure 4.7)
- 5 different twist misalignments at the blade split location
  - $0.5°, 0.25°, 0°, 0.25°, 0.5°$
- 2 different tip alignment strategies, see figure 4.7
  - Use tip as is, perfect alignment would have no step change in twist angle at split location (A)
  - Perfect alignment would have an average twist deviations of 0° on tip section (B)

In order to compare the average twist error of a tip section with the variance in power output the blade geometries were grouped into different blade sets. Where groups are based on two different alignment strategies with different normally distributed alignment tolerances. This resulted in a total of thirteen blade sets which are defined as followed:

- Single piece
  This is all blade geometries with tip A and an alignment deviation of 0°. As a result, this should resemble single piece wind turbine blades with manufactured twist deviations. In order to make this group, and the other groups, more normally distributed. The blades with manufactured twist deviations up to half the specified limits were added twice to each blade set.[1]

- Joint A (2 blade sets)
  The blades in these sets are the blades with a normal tip section. The first joint A set has the twist angle alignment deviations going up to ±0.5°, and the second joint A set has the twist angle alignment deviations going up to ±0.25°. To make the twist angle alignment deviations also more normally distributed

[1] So the blades with manufactured twist deviations ranging between ±0.5° are once in each set, while the blades with manufactured twist deviations ranging between ±0.25° are present twice in each set (One original and one copy). This is also the case in all other blade sets.

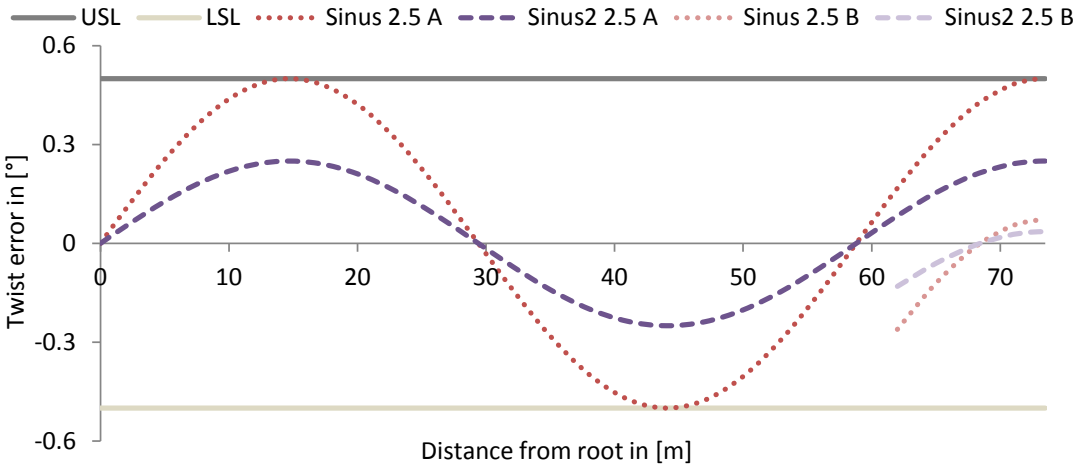

Figure 4.7: Visualisation of four sinus 2.5 blades twist error distributions. Where the sinus3 & sinus4 distributions have an optimized tip placement.

the set of joint A also has blade geometries with twist alignment errors of ±0.25° and 0° added two and three times respectively.

- Joint B (2 blade sets)
  The blades in these sets are the blades with a twist optimized tip section. The first joint B set has the twist angle alignment deviations going up to ±0.5°, and the second joint B set has the twist angle alignment deviations going up to ±0.25°. The same method as used for the joint A sets of making the twist alignment errors more normally distributed was applied.

- Tip A (4 blade sets)
  The blades in these sets are sorted on the twist angle error at the absolute blade tip. The tip A sets have the normal tip sections. The twist angle deviations in each of the four groups are in the following ranges; the first: ±1°, the second: ±0.75°, the third: ±0.5° and the fourth: ±0.25°.

- Tip B (4 blade sets)
  The blades in these sets are sorted on the twist angle error at the absolute blade tip. The tip B sets have the optimized tip sections. The twist angle deviations in each of the four groups are in the following ranges; the first: ±0.875°, the second: ±0.625°, the third: ±0.375° and the fourth: ±0.125°.

4.4.2. Outcome

In figure 4.8 the absolute average twist deviation of the tip section and the relative variance in power output of each blade set is shown. The absolute average twist error has to be reviewed because the twist deviations of every blade set are symmetrical around zero. So, the average twist error on each tip section is 0 for all blade sets. When a trend line is fitted through the data, it shows an exponential relationship between the two, as was hypothesised. With an F test it was tested if the variance in power of each set is significantly different compared to single piece blades with manufactured twist errors. This showed that 1 blade set has a statistically significant lower variance and 3 sets have a statistically significant higher variance.

Reducing the variance in power output is desirable as the power performance of each blade should be more consistent. However, if it would increase the structural loads, reducing the twist error on the tip section might not be desirable. The lifting line simulation program also provides the relative differences in thrust and flapwise root bending moment (FRBM). These can be used to indicate if the structural load increase or decrease. The thrust of a wind turbine blade is essentially the total lift that the blade produces. The FRBM is the resulting bending moment in flapwise direction due to the thrust. However, these might not have similar relations because the total thrust could decrease while the FRBM increases. This can happen if the centre of thrust moves towards the tip, resulting in a longer moment arm and an increase in FRBM while the thrust decreases.

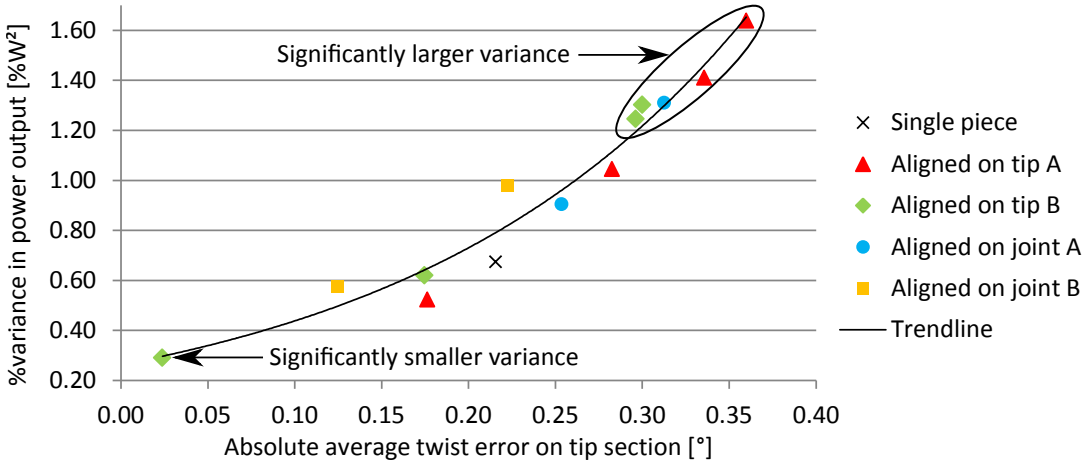

Figure 4.8: Variance in power output versus the absolute average twist error on tip section for various blade sets.

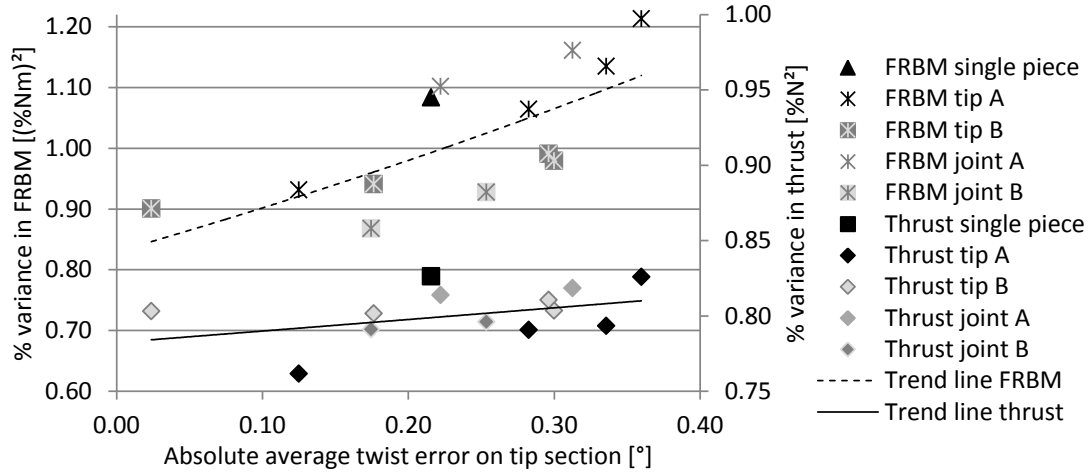

Figure 4.9: Variance in flapwise root bending moment (FRBM) & thrust versus the absolute average twist error on tip section for all blade sets.

In figure 4.9 the absolute average twist error on the tip section is plotted against the variance in FRBM (left axis) and thrust (right axis) for all blade sets. The thrust variance reduces marginally for a reduction in twist error on the tip section. For the blade set with the lowest variance, it reduced with 7.8%. F-tests were also made and revealed that there are no significant differences compared to the variance in thrust of single piece blades. The variance in FRBM reduces stronger with a reducing twist error on the tip section, in the best case with 20%. However, F-tests showed that none of the blade sets have a statistically significant lower variance in FRBM compared with single piece blades. It is logical for the variance in FRBM to decrease faster than the variance in thrust. This because the FRBM is the sum of the thrust of each section multiplied with the distance of that section to the root. Since the difference in thrust variance is caused by a reduction of twist angle deviations in the tip region, the multiplication with the length from the tip to the root results in a magnification of the differences in variance. All results from these simulations are shown more detailed in Appendix C.

4.4.3. Practical application of test results

For the Hyller project LM would like to have alignment tolerances, grouped as minimal, recommended and extensive. If one wishes to do this as good as possible, the differences in AEP due to different tolerances should be determined. This is out of scope for this project. So, it is only possible to make estimates of the allowable tolerances based on the results of the last lifting line analysis. However, the simulations are only performed at rated speed for one blade design, with one split location and the assumption that the joint does not influence the power output. Therefore, the estimated tolerances based on these simulations might be

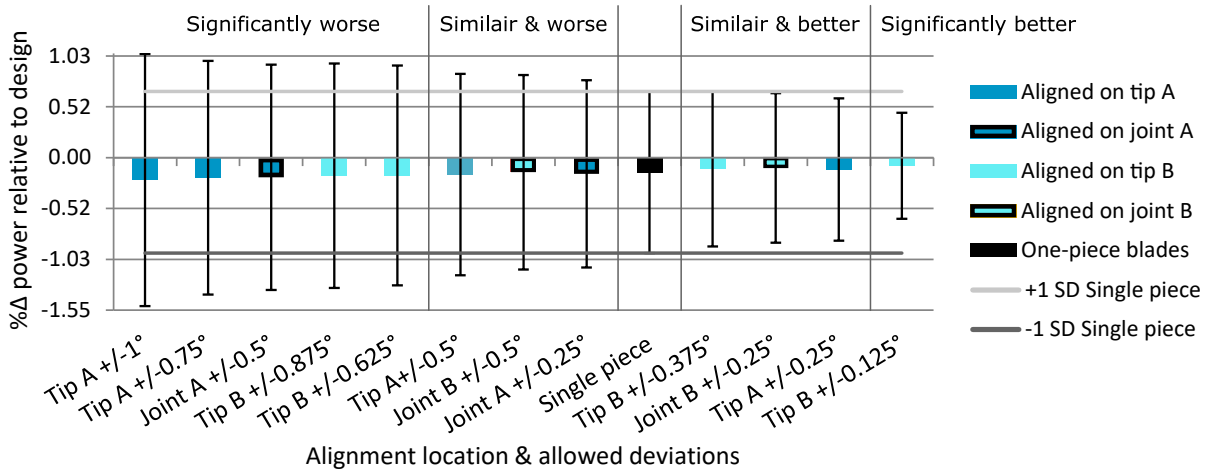

Figure 4.10: Average difference, with standard deviations, in power output for several twist alignment tolerances & alignment strategies

	Use tip as is (A)		Optimized tip (B)	
Twist tolerance	Joint	Tip	Joint	Tip
Extensive				+/-0.125°
Recommended		+/-0.25°	+/-0.25°	+/-0.375°
Minimal	+/-0.25°	+/-0.5°	+/-0.5°	

Table 4.3: Different twist tolerance levels based on different alignment strategies.

conservative or progressive when used on real wind turbine blades, which one is not possible to determine with the available data. Nevertheless, the knowledge of what tolerances should be used for a wind turbine operating in these hypothetical conditions does provide some insight into what order of magnitude the real-life tolerances could be. So, one can determine if these tolerances are achievable and economically viable. The same simulation data as is visible in figure 4.8 is presented differently in figure 4.10.

In the most optimal case the mean power output can increase by 0.066% and the standard deviation reduces by 34.4%. To achieve this, the twist manufacturing deviations of the tip part are averaged, and it is aligned on the absolute blade tip with a tolerance of ±0.125°. Based on the results of the verification of the alignment trials, see table 2.1, this could be achievable. However, this might only be possible if the accuracy of the used reference points is similar to the accuracy of the reference points used in the trial alignments. Furthermore, all components in the blade sections should also be accurately dimensioned and positioned. Otherwise this is not achievable, as was observed in the alignment of the Hyller TA. The tolerance groups are defined as followed:

- Minimal → Similar & higher variance in power output.
- Recommended → Similar & lower variance in power output.
- Extensive → Significantly lower variance in power output.

An overview of the proposed minimal, recommended and extensive tolerances presented in table 4.3. Based on the Hyller TA alignment and the alignment trials, most of the minimal tolerances should be achievable. It is likely that with improvements to the components the recommended tolerances are achievable. And as was also described above, in similar conditions as the trial alignments the extensive tolerances should be achievable. Which tolerances are economically viable is something LM should decide for themselves. Also, for the best alignment strategy LM should determine if averaging the twist errors on each tip section and adding an additional process step is worthwhile.

4.5. Conclusion

In this chapter the data has been presented which is used to answer research questions 2, 2.1 and 2.2. The answers to the research questions will also be presented in this order.

Research question 2:

How do the differences in power output of twist angle deviations compare to the differences in power output due to flapwise and edgewise angular deviations?

The differences in power output due to twist angle deviations are much larger compared to the differences in power output due to flapwise and edgewise angular deviations, see also figure 4.1. As was also stated in section 4.2, a twist angle deviation in the order of ±0.1° is roughly equal to a flapwise angular deviation in the order of ±1°, and assuming a linear relation for the edgewise angular deviations between ±0.5° & ±1°, a ±0.71° flapwise angular deviation, see table 4.1. This confirms the assumption made in section 1.2.2 that the twist angle is most critical of the three possible angular deviations. Especially when it is also considered that the twist angle is coupled with the chord length and the other two angles are coupled with the length of the tip section. This means that a mutual alignment difference for the reference points on the chord of 1.56 mm has a similar impact on the power output as a mutual difference of 122 mm for the flapwise reference points and an 86.7 mm difference for the edgewise reference points. Therefore, the required alignment precision in the twist angle is most critical.

Furthermore, the simulation results show an 0.57% increase in power output for a negative edgewise angle of −4°. This is in line with what is described in literature. Only with the current manufacturing techniques producing a single piece blade with an edgewise angle results in additional manufacturing challenges. By purposely joining the blades with a negative edgewise angle one can increase the power output of a turbine blade without these challenges, if one manages to join both sections with a negative edgewise angle. Considering that a 0.57% increase in power output will result in an increased AEP, aligning the parts as such could improve the business case of a split blade which should lower the cost of wind energy.

Research question 2.1:

What is the relation between the twist angle at the tip and the resulting variation in power output on a tip-split blade containing small twist errors due to manufacturing and misalignments?

The relation between the twist angle at the tip and the resulting variation in power output is a non-linear relation for a tip-split wind turbine blade that contains small twist deviations due to manufacturing and misalignments. As was hypothesised in figure 4.2, a negative twist angle deviation of the blade tip will result in a marginally higher power output, and a plateau is formed. A positive twist angle error of the tip section will result in a non-linearly increasing loss of power. This hypothesis was confirmed with the results visible in figure 4.5. However, considering the effects on power output, the twist angle will probably not be allowed to deviate as much as was reviewed in these simulations. Only if one evaluates the effects of twist angle deviations for a smaller range, then the manufactured twist deviations have to be taken into consideration as well. As the manufactured twist deviations can be compensated completely by the twist alignment deviations. To review this, research question 2.2 was defined:

Research question 2.2:

What is the relation between the variance in power output, due to twist errors, and the absolute average twist error of the tip section after joining?

The relation between the variance in power output, due to twist errors, and the absolute average twist error of the tip section after joining is exponential. Compared to single piece wind turbine blades that contain manufactured twist deviations, the variance in power output improves with a decreasing rate for reduced absolute average twist errors of the tip section. Whereas the variance in power output increases with an increasing rate for an increasing absolute average twist error on the tip section. By combining all these simulation results, an estimate can be made for the twist alignment tolerances that result in a similar and smaller variance in power output. For a turbine operating in the same conditions as were used in the simulations,

a ±0.25° tolerance for the twist angle of the blade tip will result in a slightly smaller variance in power output. However, the additional freedom of the tip can also be used to set the average manufactured twist angle to zero before starting the alignment process. If such a tip section is aligned with a twist angle tolerance of ±0.125° on the blade tip, then one will get a significantly lower variance in power output. During the alignment trials is was shown that it is possible to align the tip section with such a precision. Therefore, if the assumed manufactured twist tolerances are an accurate representation of reality. Then this could to possibly lead to a reduction in the cost of wind energy.

5

Profile thickness & two shell production process

For a split blade to be successful, it needs to be joined with a sufficiently strong joint. As was explained in section 1.2.3, calculating if a joint is sufficiently strong is possible once the geometry and material strengths are known. From the design the general geometry is known and from material strength tests the design values of the used materials are known. Only due to manufacturing tolerances and misalignments the geometry of the joint will be varying slightly. In the previous chapters the range in which these misalignments will be is described. However, the specific geometrical variations due to the manufacturing processes are unknown. With the flapwise direction being critical from a structural point of view, the profile thickness variation on LM42.1 blades, produced with a two-shell production process, was reviewed. This review is added in appendix D. This review shows that there is a variation of the profile thickness, whether this is acceptable or not is out of scope for this project. Only within the scope of this project it is reviewed how the component thickness and position influence the profile thickness. In section 5.1 the hypothesised effect of these deviations and the made assumptions are described. The test set-up to test this hypothesis is described in section 5.2, followed by a description of the tests results in section 5.3. Also, to better control the placement of the webs, a tool was developed which should improve the positioning. The design build and usage of this tool is described in section 5.4. All of this is then combined in a conclusion (section 5.5) in which an answer to research question three is formulated. This question was formulated as followed: *'What is the influence of component thickness & position on the local profile thickness in the web region for a two-shell wind turbine blade production process?'*

5.1. Hypothesis & set-up of profile thickness deviations measurements

When reviewing the entire two-shell blade production process there are many parameters that might have an influence on the profile thickness. In order to simplify this review, only the local variations in profile thickness are reviewed and several assumptions are made:

- Profile thickness only dependent on component position/thickness
  In this review the only components which are thought to be of influence on the profile thickness are: web position, bondline thickness and shell thickness. All these components are visualised in figure 5.1.

- Mould does not deform
  In this analysis it is assumed that the mould does not deform during the closure process. In reality, some small deformations of the mould are allowed during the closure process. As it is possible to make the moulds very stiff, but this does increase mould cost. So, the mould deformation is a trade-off between stiffness and tool cost. Since the profile thickness in the near vicinity of the joint is only of influence of the joint strength, it is possible to locally reinforce the mould to reduce/eliminate the mould deviations.

- Web height does not vary due to mould type
  With the webs being made in a female mould, it is not possible for the webs to have a larger height as is designed. It is of course possible for the webs to have a shorter height. However, with the web mainly

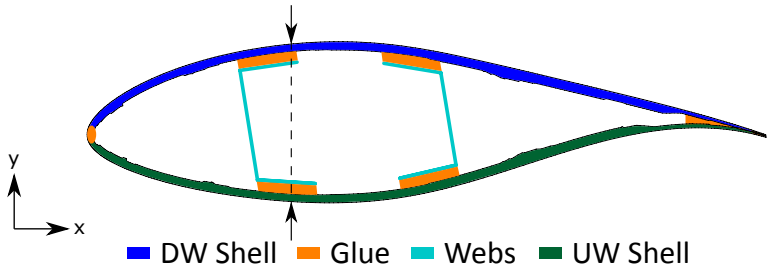

Figure 5.1: Wind turbine blade profile in joint region with all important components visualised. The dashed line with arrows indicates the measurement position of profile thickness.

being a piece of foam, it is assumed that the dimensional stability of the used foam will result negligible variation in web height, wherefore a variation in web height is neglected from this review.

- Bondline thickness deviation equal on top & bottom of webs
  In production trial closures are performed with pieces of clay instead of glue to determine the gap in-between the shells and the webs. With spacers on the underside of the webs, the gaps between the shells and the webs are equalized on both sides. Therefore, it is assumed that the deviations in bondline thickness are equal above and below the webs.

- Webs cannot move individually or rotate
  In order to reduce process time in the two-shell production process, both webs are connected to one another every couple of meters to allow placement of both webs at once. As a result, it is not possible for one web to move to the LE, and for the other web to move to the TE. Furthermore, it is assumed that the spacers in between the webs and the shells prevent the webs from rotating, which might influence the profile thickness.

- Shell thickness can deviate only by [0,+2] mm (y direction)
  Due to a fixed number of plies and a maximum vacuum level, the thickness on the shell cannot become thinner as the designed value. Due to lower vacuum levels it is possible for the shell thickness to increase. So also based on the observed deviations found in appendix D, it is assumed that the shell thickness will deviate maximally by 2 mm.

- Bondline thickness can deviate by [0,+9] mm (y direction)
  In this analysis it is assumed that the bondline thickness cannot become thinner as the designed value, due to the usage of spacers. The maximum positive deviation in bondline thickness is assumed to be nine mm, as this will result in a much ticker profile thickness as compared to the maximum allowable profile thickness, see appendix D.

- Web position can deviate by [-9,+9] mm (x direction)
  For this analysis it is assumed that the webs can deviate nine mm from their designed position in both directions. Where a movement towards the LE is negative and a movement towards the TE is positive. In the current two-shell production process the webs can potentially have larger deviations. However, because the webs from both sections have to be joined to one-another, a special tool is designed and used to locally limit the movement of the webs (This is described in section 5.4). The assumed maximum deviations of ±9 mm are larger than is allowable for the web joint.

So, it is hypothesised, with these assumptions, that the order in which the profile thickness is influenced is bondline thickness > web position > shell thickness. The reasons for this hypothesis are as followed:

1. Bondline thickness, can have relatively large deviations on both sides of the webs. As a result, a deviation of one mm will cause a two mm increase in profile thickness.

2. Web position, can have relatively large deviations in position. A deviation of one mm will result in an increase of less than one mm in profile thickness. Exact deviation dependent on used aerofoil.

3. Shell thickness, can only have a two mm deviation in thickness and has an increase in profile thickness equal to the deviation.

5.2. Used methodology for measuring deviations in profile thickness

In order to test the hypothesis of the previous section, it was considered to build a couple of blade sections with a two-shell production process and apply deviations to the components. Then by measuring the profile thickness one could determine what the relation is between the component thickness/position and the profile thickness. However, the costs associated with doing this are quite high. As one would have to build many blade sections, while also accurately controlling the applied deviations. Therefore, as a low-cost test method, deviations were applied to 2D drawings on a one to one scale, where all other parameters are kept constant. Doing the measurements in this way does require an additional assumption about what happens at the LE & TE of the blade. Since a thicker blade in the web region also influences the size of the gap/bondline thickness at the LE & TE. In section 1.2.3, it is explained that the profile thickness is reviewed as the loads in this direction are critical for the structural design. Furthermore, considering that these loads are created due to bending moments, the DW shell is loaded in compression and the UW shell is loaded in tension. However, as is visible in figure 5.1, the LE & TE are in the middle of the blade or the neutral line. As a result, the stresses created by the bending moments are low due to the short distance from the neutral line. Therefore, the geometry of the LE & TE is not critical for the strength calculations in the flapwise directions, so the effects that component deviations have in the LE & TE region are neglected. It is assumed that the bond-line will become thicker or that the shell will deform locally and that this does not have an influence on profile thickness. As a result, the measurements were done as followed:

- Review performed on LM42.1 wind turbine blade at z = 35 meters
  For this review a 2D drawing a blade section of the LM42.1 was used, as this is the reference blade in the Hyller project. The profile thickness is reviewed at z = 35 meters as this is the split location.

- Profile thickness measured perpendicular to the chord
  The goal of these measurements is to determine the possible step height in the spar caps (see figure 1.5), so the profile thickness is measured perpendicular to the chord which in the same direction as the step.

- Profile thickness measured at 30% of chord length
  In production at LM, the profile thickness is also measured perpendicular to the chord and by coincidence also at z = 35 meters (see appendix D). Therefore, to be able to directly compare the results from these measurements with the measurements from production, the profile thickness is also measured at 30% of the chord length. This position is also visualised in figure 5.1 by the dashed line.

- Applying deviations to shell thickness & bondline thickness
  The deviations in shell thickness and bondline thickness are applied in the y direction that is indicated in figure 5.1. As this is also the direction in which the profile thickness is measured, an applied deviation of one mm to the DW/UW shell results in a one mm increase in profile thickness. For the bondline thickness, an applied deviation of one mm will result in a two mmm increase. This because of the assumption that the bondline thicknesses on both sides of the webs are equal, see section 5.1.

- Applying deviations to web position
  The deviations to the web position are applied in the x direction. This will result in a thinner or thicker bondline thickness due to the curvature of the used aerofoil. Therefore, the shell position is adjusted such that all bondline thicknesses around the webs remain equal. To achieve this, the DW & UW shell y positions were changed such that the bondline thicknesses on the left-hand side of the LE web is as designed (see figure 5.1). Then, the DW & UW shells were rotated such that the bondline thicknesses at the LE web remain equal and the bondline thicknesses at the right-hand side of the TE web are also as designed. After this is done, the profile thickness can be measured.

5.3. Measured profile thickness deviations

The measured profile thicknesses are visible in figure 5.2. As can be seen, the hypothesis is incorrect. Although the bondline thickness had by far the biggest influence (as was expected), the movement of webs does almost have no influence on the profile thickness. Although a nine mm movement of the webs to the TE does cause a 1.5 mm reduction in profile thickness, it is still smaller than the two mm increase in profile thickness one would get from a two mm thicker shell. In figure 5.2 only one line is shown for applied deviations to the DW or UW shell thickness. This is because increasing the shell thickness of the DW shell has the same

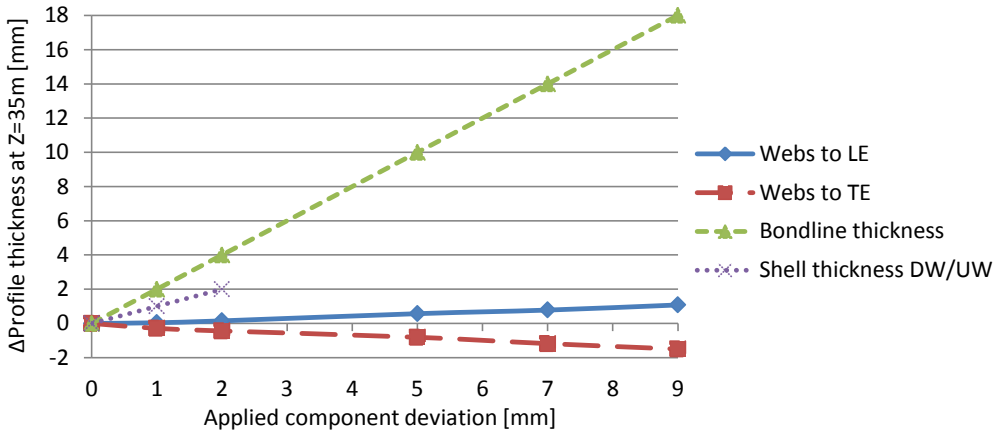

Figure 5.2: Profile thickness due to deviations of components.

impact on the profile thickness as increasing the shell thickness of the UW shell. Therefore, the deviation in profile thickness due to both shells can be +4/0 mm, whereas the possible deviation in profile thickness due to the position of the webs is +1.1/-1.5 mm. It is of course debatable if the webs only deviate ±9 mm from the designed position in production. However, measuring the web position at around 80% of the blade length on actual blades is difficult or possibly impossible without cutting the blade in sections. However, for tip split wind turbine blades it is possible to more accurately control the web position in the joint region, since tip end of the root section is 'open'. In section 5.4 it is described how this was done on the Hyller TA root.

In the measurement results it can be observed that moving the webs towards the TE results in a thinner profile thickness. Whereas one could expect an increase in profile thickness when placing the webs towards the TE due to the decreasing thickness of the aerofoil, see figure 5.1. On the drawings with such deviations applied to the web position, this was also observed when the profile thickness at the designed position of the TE web was reviewed. However, the results in figure 5.2 show the profile thickness measured at 30% of the chord length, this is at the dashed line in figure 5.1. So, if the LE web moves towards the TE, then the profile thickness will decrease at the measurement position because the distance between the shells increases due to the shape of the aerofoil. This shows that the deviations in profile thickness are also dependent on the measurement position.

5.4. Placement of webs on Hyller TA root

In the analysis that is described in the previous sections, it is assumed that the webs can only deviate ±9 mm from the designed position. It was also mentioned that it is questionable if the webs do not have larger deviations in their position in a normal production environment. If the deviations in web position are much larger than the ±9 assumed here, then it can be expected that the profile thickness will deviate more than was observed in the performed measurements. To produce the Hyller test article, it is required to control the web placement to limit the bondline thickness of the web joint to acceptable levels. This makes it a valid assumption that the web position, and the profile thickness, do not deviate more than in the above analysis. To reduce the possibility for the webs to move, a tool was designed and build that would limit the movement of the webs to less than < ±9 mm. The web holder that was constructed is visible in figure 5.3, where it is placed in the TA DW root mould prior to a test closure. The design of this tool is as followed:

- Tool has to be removable after blade closure
  As seen from the root, both webs are converging relative to one another. So, the tool that is designed to hold the web ends in place should be dismountable, such that it can be removed once the root production is finished. If one would simply try to remove the tool without dismounting it, then the converging webs would prevent the tool from being pulled out from in between the webs.

- Tool should work in moulds of single piece blades
  The tool should fit inside a closed mould without making any modifications to the mould. As this does

allow for using the same mould as is used in the production of the same blade as a single piece variant.

- Four blade cross-sections and three beams used for x & y positioning of webs
  For the Hyller TA the webs stopped at z = 35.24 meter. This cross-section was cut from wood for the correct x & y positioning of the web holder in the mould (Number 1 in figure 5.3). For more stability of the tool in the mould, the cross-section of z = 35.5 meters was also cut from wood (Number 2 in figure 5.3). To hold the webs in the correct position, the cross-sections of z = 34.7, the position on which the shells end, and z = 34.6 were also cut from wood (Numbers 3 & 4 in figure 5.3). However, as these had to fit inside the blade and around the webs, only the region around the webs was cut from wood. Then, to connect all these wooden cross-sections, three slots were designed in all cross-sections at the same x & y position. Such that wooden beams could be slit through all the cross-sections to make one tool (Number 5 in figure 5.3). The webs can then be put in the tool which holds them in the right x & y position relative to one-another in the mould.

- Tapered slot at web ends
  To make the web joint, both web ends are tapered down. So, to hold the web ends in the correct z position relative to one another, a tapered slot was made at the web ends (Number 5 in figure 5.3).

- Z position of tool in mould
  The last unconstrained web positioning variable is the z position of the tool in the mould. On the mould the z position is marked every meter. To have the webs in the correct position, a laser was used that to show the z = 35-meter position (from the distance marks on the mould) onto the web holder tool. The previously mentioned tapered slots start at z = 35 meters. So, by lining up the start of these slots with the laser line, the web tool can be positioned in the correct z position.

Although the tool that was used in the production of the Hyller TA is not a fully industrialized tool, it did fulfil its purpose of limiting the movement of webs such that they could be joined with one another. Only after the structural testing of the TA was finished and it was cut-up, the bondline thicknesses of the web joint could be measured. In figure 5.4 a picture is shown of one of the two web joints cut along its length. On this piece of the TA the bondline thickness of the web joint could be measured. This revealed that the bondline thickness deviated ±2 mm from the designed thickness. The cause of this deviation could not only originate from misplacing the webs on the root section, but also from a misplacement of the webs on the tip section and alignment errors. Therefore, more tests are required to determine the possible deviations in web position with this web holder tool.

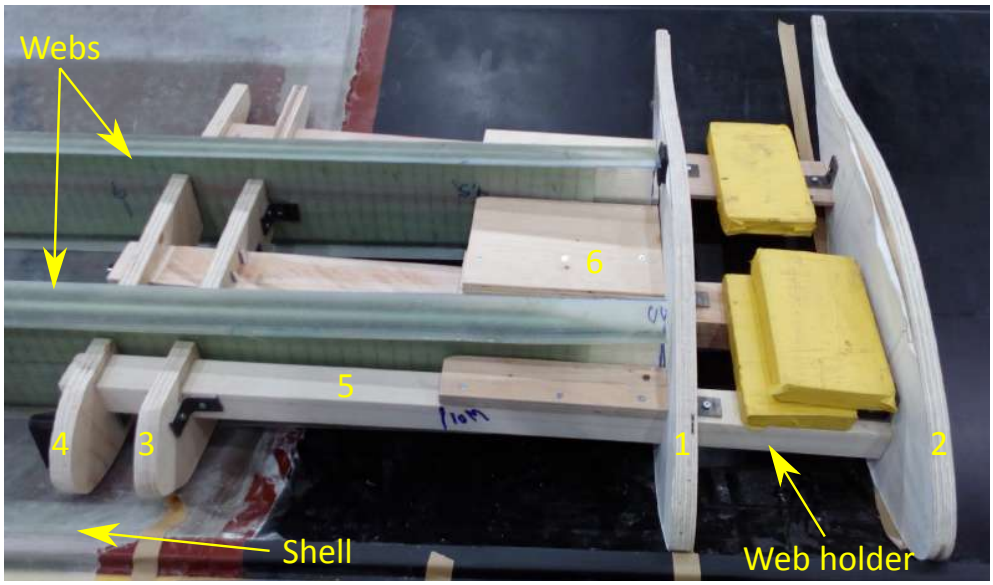

Figure 5.3: Picture of web holder with webs laying on DW shell/mould of TA root section prior to test closure.

Figure 5.4: Picture of cut web joint, designed bondline thickness was 6 mm and achieved bondline thickness was 5-8 mm.

5.5. Conclusion

In this chapter the influence of component thickness and position on the local profile thickness was reviewed for the two-shell blade production process. In order to do this, several assumptions were made (See section 5.1). With the results from measurements on 2D drawings with a one on one scale an answer to research question three can be formulated, which is only valid under the assumed conditions. This research question was formulated as followed:

What is the influence of component thickness & position on the local profile thickness in the web region for a two-shell wind turbine blade production process?

In a two-shell wind turbine blade production process the component thickness & position influences the local profile thickness in the web region linearly in the reviewed range of applied component deviations. It was hypothesised that the bondline thickness deviations would have the largest influence on the profile thickness, followed by deviations in the web position and lastly by deviations in shell thickness. As is visible in figure 5.2, this is not correct. The bondline thickness does have the biggest impact on profile thickness, but the shells have the second biggest impact on the profile thickness. And the web position only has a minor impact on the profile thickness for deviations up to ±9 mm. This is because the deviations in web position are in the x direction and the deviations in bondline or shell thickness are in the y direction. So, the impact on the profile thickness will always be the same as was observed in this chapter, no matter how the local geometry of the blade is. For web movement along the x axis, the shells are pushed further apart, or they can move closer together. How much the shells move due to a movement of the webs is dependent on the local geometry. If both shells would be flat, then moving the webs along the x axis would not cause any deviations in the profile thickness, because the distance in between the shells is equal everywhere. As the curvature of the shells is relatively low at the designed web positions (see figure 5.1), applying small deviations to the web position does result in small deviations of the profile thickness.

However, as can also be seen in figure 5.1, the curvature of the shells increases strongly close to the LE and the TE of the blade. Therefore, it is expected that the relation between the blade profile thickness and the deviation in web position is not linear for larger deviations in web position then is reviewed in this chapter. So, it is not unlikely that, if in the current production process the web position can deviate more than is assumed here, the web position could cause large deviations in profile thickness. Only to make the web joint, the web position is allowed to deviate by less than the here reviewed applied deviations. Furthermore, in this review the deviations were measured on the cross section of the LM42.1 at z = 35 meters. If this would be reviewed for different cross-sections, then the deviation in profile thickness due to applied deviations in web position are likely to be different. For lower shell curvature around the designed web position, the impact on profile thickness should be lower and for higher shell curvatures the impact of web positioning deviations should be larger. Therefore, the observed relation due to web movement should be the same for split blades on which the webs are adhesively joined and with a similar local geometry to that of the Hyller blade.

As was also noted in section 5.3, the effect of web position on profile thickness is also dependent on the position where the profile thickness is reviewed. However, with the web position being limited by a web holder to join the webs, the possible deviations in web position and profile thickness are restricted or possibly eliminated. Therefore, it would be best to first review by how much the web position can deviate when they are placed with a tool, like the web holder that was used in this project. Then, one should not measure the deviations in profile thickness at 30% of the chord length, as this does not reveal how the profile thickness varies for the entire spar cap region. In order to get an understanding how geometry of the blade varies in the spar cap region, one should measure the deviations at least at both edges of the spar cap region and if possible at more points on the spar caps. This would show how the local differences in geometry vary for the entire spar cap region; this can then be used to design a proper joint.

6

Profile thickness & one-shot infusion and cure production process

The mass of a split wind turbine blade will be higher as compared to a single piece blade due to the presence of a joint. Therefore, LM Wind Power uses a one-shot infusion and production process to reduce the mass of the tip section. Ideally the weight saved in the tip section is greater than the added weight of the joint. As this could lead to additional weight savings on the blade root and turbine which could lead to additional cost reductions. In the one-shot production process blades are produced as followed: all fibres are placed in one mould half of a matched-die mould, then the mould is closed, and all fibres are infused at once. As a result, the assembly process step required in the two-shell production process is not necessary. Furthermore, the usage of a matched-die mould with soft components is expected to reduce the geometrical variation in the tip section as compared to the two-shell production process. Only this is a new process for LM Wind Power, making it unknown if this is a correct assumption. Therefore, the profile thickness was measured in the web region on five tips which were produced during the Hyller project. These measurements are described in section 6.1. These measurements showed a larger variation in the profile thickness as was expected. In order to determine if this difference can be explained by a variation in the mould geometry due to the mould closure process, tests were held, and the results are described in section 6.2. Another possible cause for the observed variation could be the position, angle and height of the webs. A review about this can be found in section 6.3. With all these results the last remaining research questions can be answered, which is done in the conclusion (section 6.4).

6.1. Measurements of profile thickness variations

Like in the two-shell production process, matched die moulds are used in the one-shot production process. Only in the two-shell production process all components are already infused and cured once the mould is closed. As a result, high forces are required to close the mould to force the components to comply to the mould geometry. In the one-shot production process all fibres are still dry and flexible when the mould is closed, which should lead to the mould closure forces being much lower. Therefore, it is assumed that the mould geometry is not varying in the one-shot infusion production process. As a result, the only possible variation in profile thickness could come from shrinkage. By splitting the blade section into its individual components, it is possible to make an estimate of this variation. In figure 6.1 a schematic overview of a blade section is visualised. In the tip region, the blade consists of a thin laminate (the shells) and webs. With thin CLT, see section 3.2, the shrinkage of the blade section can be estimated. For this the following parameters were used:

- Web shrinkage in y direction (height)
  Lay-up: Balanced sandwich laminate with fibres in ±45° in the y-z plane.
  ΔT: Assumed to be $-10°C$ due to thin laminate thickness.
  Web height: Maximally 160 mm on tip region.
  For simplicity assumed that foam core does not influence laminate shrinkage, it contracts freely with the laminate.

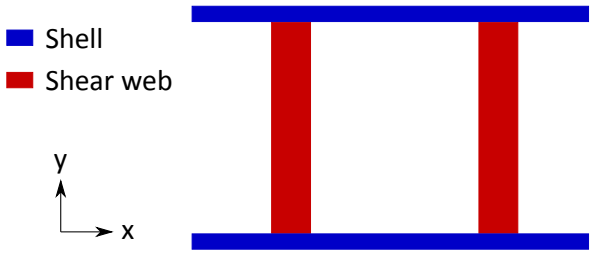

Figure 6.1: Schematic overview of web region on wind turbine blade section.

- Shell shrinkage in y direction (out of plane)
  Lay-up: As this is perpendicular to the fibre direction, the shrinkage is equal to the shrinkage in the transverse fibre direction of a UD laminate with the same thickness, regardless of the in-plane lay-up.
  Thickness: 10 mm for one shell.
  ΔT: Assumed to be $-20°C$ due to relatively thin spar cap in the tip region.

With thin CLT the shrinkage strain of the webs is found to be -1.01 mm/m and -3.06 mm/m for the shells. This results in the webs shrinking maximally 0.16 mm and one shell shrinking 0.03 mm. Therefore, the resulting deviation in profile thickness is estimated to be 0.22 mm. This leads to a hypothesis that the profile thickness measurements will only reveal deviations due to measurement error, as this is much larger than the deviation due to shrinkage. The set-up of these measurements is described in section 6.1.1 and the results of the measurements are visualised in section 6.1.2.

6.1.1. Measurement set-up & estimate of measurement error

Ideally the blade profile thickness of the tip section would have been measured at the split location (z=35 m), as this is the position where the possible step heights in the spar caps need to be found. Unfortunately, this was not possible due to the method used to join the blade sections. Also, the surface of the tip section did not have any mould marks. Therefore, all the measurements points had to be manually marked on each blade. For this, the z positions distance marks on the mould were used to mark the z position on each blade before demoulding. The first z distance mark on the mould past the area affected by the joint is at z=37 m, 2 meters from the root of the tip section. To gather more data about the profile thickness deviations, the profile thickness was also measured at z=38 m, the second closest marked position to the root of the tip section. With these two distance marks on the mould, the z measurement points on the DW shell were marked before the tip section was removed from the mould. After this the blade was cut into pieces and these were put in the UW side of the mould. Then the distance marks of the UW mould were used to mark the z position on the UW side of the blade. It was observed that the 37- and 38-meter marks on UW and DW mould halves where on slightly different z positions. In figure 6.2 a picture is shown that was taken during the measurement process; on which the different z position markings are visualised. There are two potential causes for the different z position markings. The first are the distance marks on the mould, a tolerance of ±5 mm was allowed on the z positioning of these marks. The second is the placement accuracy of the cut blade pieces in the UW mould. Due to cutting up the blade, the width of the saw resulted in a small loss of material. So, when the cut pieces were placed in the UW mould, the width of the saw had to be recreated which allowed for some variation in the z position. This leads to a variation in the z position for each measurement, but the z position deviated less than ten mm on all tip sections. With the z positions marked, the x positions had to be marked as well. This was done by placing a measurement tape over the marked z positions and every 50 mm a mark was made from 200 to 500 mm. This covers the spar cap region, for which the possible step heights are sought.

To get an estimate of the measurement error due to marking the x & z position incorrectly, the 3D CAD model was used. In this model the profile thickness was measured for each (x,z) position and these positions ±10 mm for z. For each (x,z) position the standard deviation was calculated which ranged from 0.74 mm to 0.96 mm, depending on the location. As a measurement tape with mm marks was used to mark the x positions, each x position could vary with ±1 mm. To get an estimate of the differences in profile thickness due to this variation, the profile thickness was also measured for each (x,z) position in the CAD model with a ±1 mm variation in x position. Again, the standard deviation of all possible measurements at each position (x,z) was calculated. This deviation in profile thickness varied from 0.11 to 0.34 mm depending on the position.

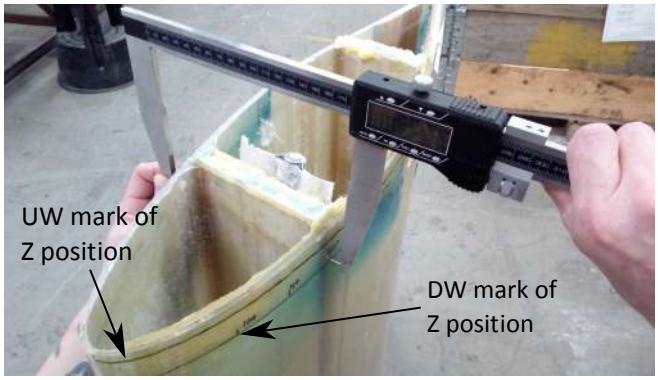

Figure 6.2: Picture taken during profile thickness measurements on tip section produced with one-shot production process, with UW and DW positions marked on blade surface.

The standard deviations due to z & x positional errors were added to one another and were used as the measurement error for each (x,z) position. As a result, the measurement error is depended on the measurement location and ranges from ±0.88 to ±1.3 mm.

During the Hyller project only four tips were produced on which these measurements could be performed, so the amount of data is limited compared to the analysis in appendix D. Furthermore, as this were the first tip sections produced with this new production process, there were a lot of changes to the entire process set-up from one part to the next. However, all these changes were made to resolve production defects at other locations. Only it is not ruled out that these changes also effected the profile thickness at the measurement positions. So once the production process is 'stable' it could be wise to redo the profile thickness measurements.

6.1.2. Results of tip variation measurements

The results of all measurements relative to the CAD model at each (x,z) position are visualised in figures 6.3 & 6.4. The observed profile thickness variations are larger than the expected variation. At z = 37 m the variation in profile thickness is found to be within +1 to -7 mm and at z = 38 m figure it is found to be within -1 to -8 mm. Furthermore, close to the mid-point (x = 350 mm) the variation in profile thickness is smaller, -1 to -5 mm for z = 37 m and -2.7 to -7.7 mm for z = 38 m. This is mostly due to tip 3, which is much thicker compared to the other tip sections. There are also differences when comparing the deviations in profile thickness between the different z locations. At z = 37 m the deviations in profile thickness reduce somewhat when viewed from LE to TE. Whereas the deviations are more constant on the profile at z = 38 m. Based on these measurements, tip sections produced with a one-shot infusion and cure production process have a variation in profile thickness smaller than +1 to -8 mm.

As is mentioned before, the measurement error is relatively large. In the data of the 3D TA scan it is also possible to see the deviations of the tip section relative to the 3D model. Unfortunately, the TA had a surface repair that covered the area on which the variation in profile thickness was measured. This made it not possible to compare the 3D scan of the TA with the measurements described above. However, in the data of this scan it is possible to review the difference in profile thickness around z = 40 m. This showed a profile thickness deviation in the order of -4 mm in the web region, indicating that the results above might be influenced by measurement error. When comparing these results to the found deviations in profile thickness of blades produced with the two-shell production process (see appendix D), then the deviations of one-shot produced tips are notably smaller. In the next sections possible causes for the observed deviations in profile thickness are reviewed.

6.2. Measurements of mould closure variations

One of the possible causes for the deviations observed in the previous section could come from closing the matched-die mould. The space in between the two mould halves governs the final part geometry. So, if the position of the top mould half can vary, then this will cause a variation in the part geometry. To determine if there is a closure variation in the Hyller tip mould, a test was set-up and this is described in section 6.2.1. In

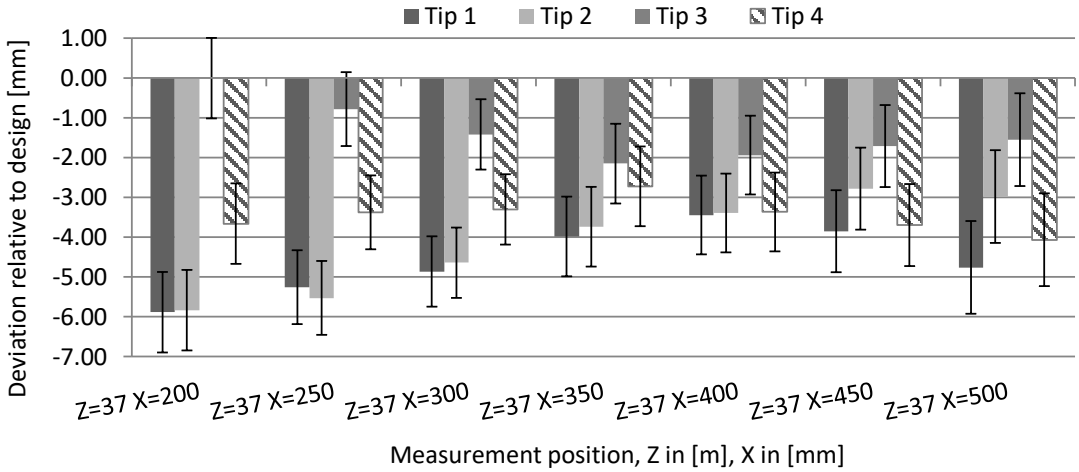

Figure 6.3: Deviations in profile thickness relative to CAD model in web region at z = 37 meters.

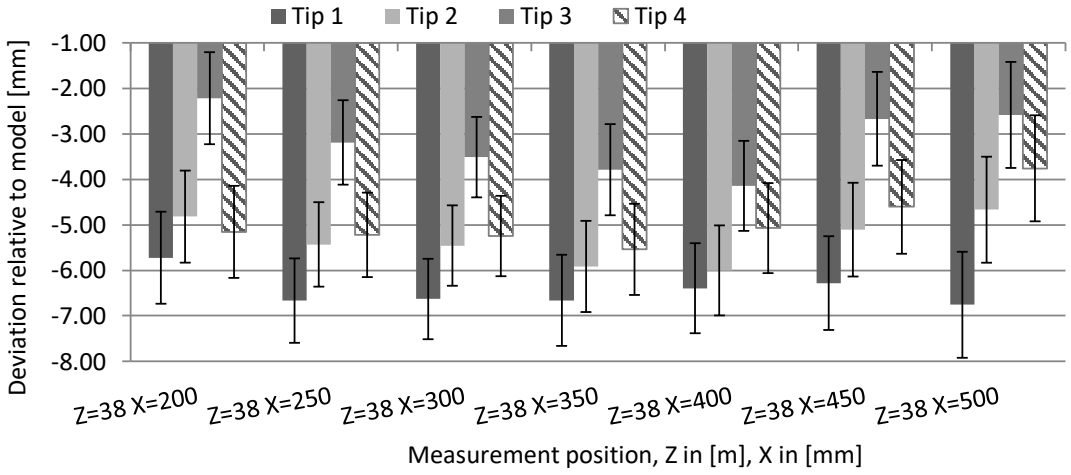

Figure 6.4: Deviations in profile thickness relative to CAD model in web region at z = 38 meters.

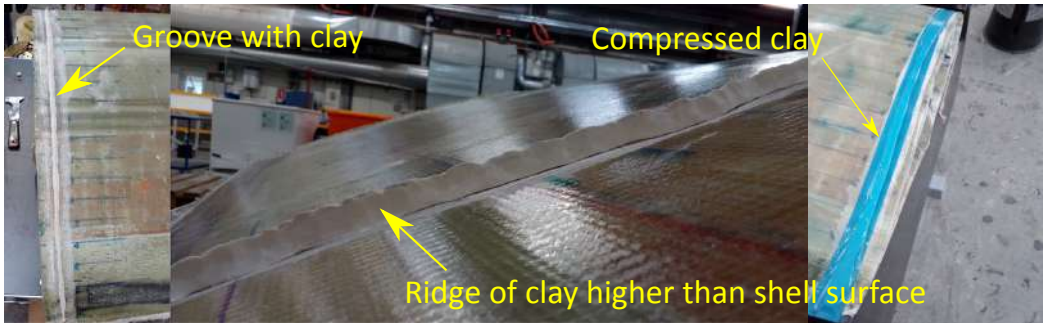

Figure 6.5: Pictures of mould closure test section with clay applied, prior to closure in left and middle pictures and after closure in right picture.

section 6.2.2 the results of these measurements are described.

6.2.1. Set-up to measure mould closure variation

To determine how much the variation in profile thickness is due to the mould closure process, closure tests were performed with the root piece of a one-shot tip, clay and a calliper. Two grooves were grinded into a blade section of a previously produced tip section all around the aerofoil at approximately z=35.05 & z=36 meters. These positions were chosen as they are close to the edges of the used tip piece. A small amount of clay was placed in the grooves to make a ridge higher than the surrounding material, see left and middle pictures in figure 6.5. The clay was then covered loosely by tape to prevent it from sticking to the mould. Next, the section was placed into the DW mould halve and the mould was closed. This deforms the clay such that it would take the same shape as the mould, see left picture in figure 6.5. Then the mould was opened and with a calliper the blade thickness would be measured at several points, similar as in the previous section. Only the possible measurement errors are different. Since the same blade section was used in every test, and the measurement points were marked permanently on the surface, misplacing the calliper was not possible. However, with this test set-up there are two other possible causes for measurement errors:

1. Placement accuracy of the tip section into the DW mould halve.
   As the section with clay must be paced in the mould prior to each closure trial, it is possible that there are small placement variations which would result in a different impression into the clay. Therefore, the root piece of a tip section was used for the mould closure tests. As it could be placed visually in the same position for every closure relative to the root of the mould.

2. Measurement accuracy with calliper touching clay.
   To measure the profile thickness with a calliper, one must touch the clay on both sides of the profile. As the clay is soft and a large calliper had to be used to measure the profile thickness, it is difficult to only let the calliper touch the clay without making an indentation. This results in a difference in profile thickness compared to the non-indented clay produced by the mould closure process.

To get an estimate of how much the clay is accidentally indented during the measurements, two mould closure tests were measured twice. Then by reviewing the difference in profile thickness of the first and second measurements, one gets an idea of the difference in profile thickness due to accidental indentations by the calliper. The standard deviation of these differences is assumed to be the measurement error for the mould closure tests which was found to be 0.96 mm. As this is relatively large compared to the found variation in profile thickness (See 6.1.2), two other measurement methods were considered that should have a lower measurement error (unfortunately both turned out to be infeasible):

1. Make 3D scan of tip piece after mould closure test.
   The main problem is touching the clay without making an indentation. This can be mitigated by using a measurement method that does not physically touch the clay. The same 3D scanner as was used in chapters 2 & 3 could be used for doing this. Unfortunately, using such a 3D scanner is costly so it was not done.

2. Use glue instead of clay.
   By replacing the soft clay which remains soft with for example glue, one could also resolve the issue of

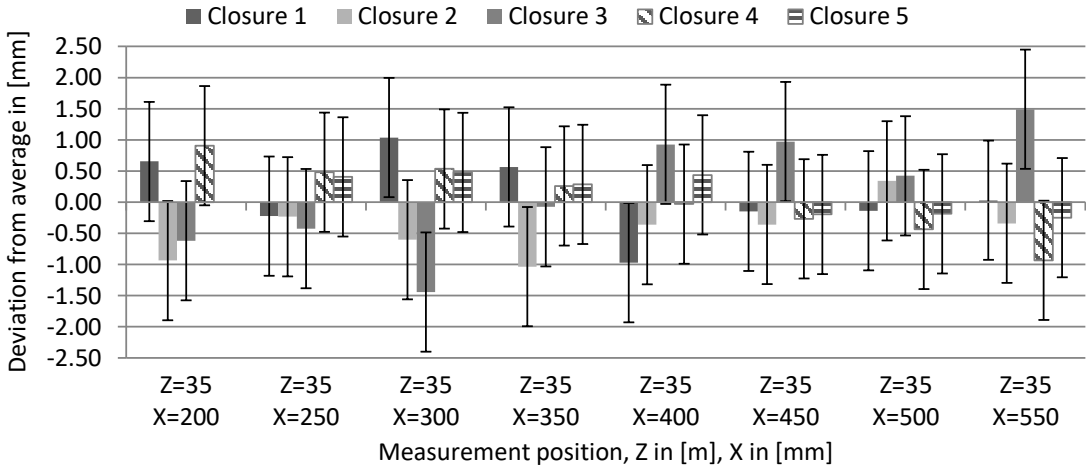

Figure 6.6: Mould closure deviations relative to average profile thickness in mm.

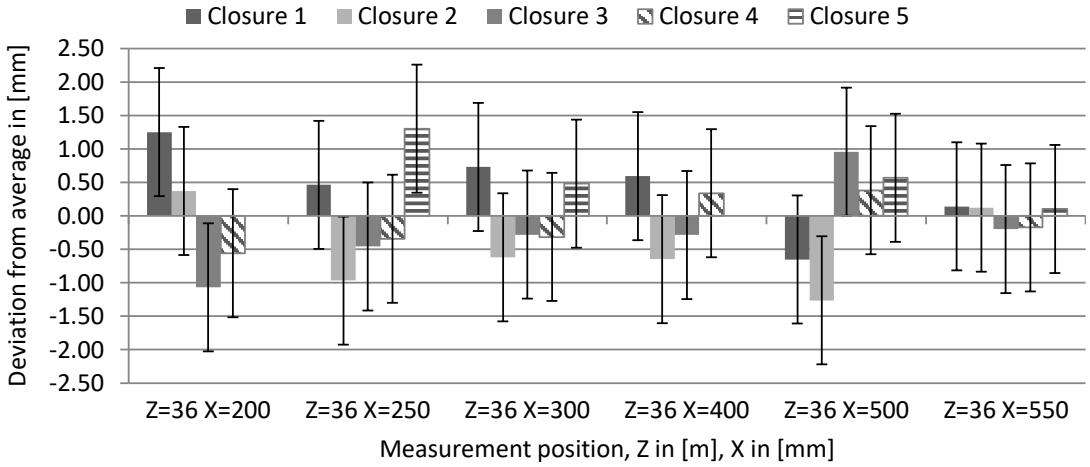

Figure 6.7: Mould closure deviations relative to average profile thickness in mm.

clay indentation. In this case the process would work completely similar as with clay. Only when the mould is closed, the glue cures before the mould is opened again. So, when one measures the profile thickness, it is not possible to make an indentation. This would introduce the glue shrinkage as a new measurement error which would require additional tests to determine its size. However, this method does also require a lot of in mould time to let the glue cure which was not available as the moulds were in use to produce tip sections.

6.2.2. Measured thickness variation due to closure

In total five closure tests have been performed and the results of these tests are visible in figures 6.6 & 6.7. These figures show that the measured deviation in profile thickness relative to the average is smaller than ±2 mm. However, for five values the measurement error of ±0.96 mm indicates a possibly larger or smaller deviation. Since the measurement error of the used test set-up is roughly ±1 mm, it is not possible to determine the exact variation in profile thickness due to the mould closure process. Also, according to the test results, it is incorrect to assume that the variation in mould geometry, due to the mould closure process, is negligible. However, more accurate tests are required to precisely determine the variation in profile thickness due to the mould closure process. These tests could potentially be done by one of the two methods described above.

6.3. Influence of webs on profile thickness

The measurements described in section 6.1.2 indicate that the variation in profile thickness with the one-shot infusion and cure production process is smaller than +1 to -8 mm relative to the model. This variation can be explained in part by the mould closure process. As is described in the previous section, this process causes a variation smaller than ±2 mm. So, there are other causes as well for the variation in profile thickness. In chapter 5, it was found that the web position has an influence on the profile thickness in the two-shell production process. However, as a matched-die mould is used in this production process, and all materials are still flexible when the mould is closed. It was assumed that these materials would deform or move during the mould closure process due to the mould stiffness, eliminating it as a variable. To determine if this assumption is correct, it is reviewed in this section if the web position, height and angle also have an influence on the profile thickness in the one-shot infusion and cure production process. In section 6.3.1 the possible variables and test set-up are described, and the results of this test are described in section 6.3.2.

6.3.1. Possible variables & test set-up

Due to the webs being connected to one-another in the two-shell production process and the presence of distance plugs, both webs act as one big part. In the one-shot infusion and cure production process the webs are not connected to one-another. As a result, they can move individually towards the LE or TE and they can also rotate along the z-axis. This already generates a total of eight possible deviations[1]. Since there were only four tip sections on which the variation in profile thickness could be measured, it was quite difficult to determine which variables have caused the variation in profile thickness. However, reviewing the produced tip sections, it was observed that the webs only had a clockwise rotation[2]. Only as this production process was also in an experimental phase, the web height was also varied to have the correct compression on the glass in the UW & DW shells. So, the total amount of possible variables remains eight.

To determine the effect of each variable individually, the same method of modifying a 2D drawing on a one to one scale as was used in section 5.2 was also used to determine the effect of each variable on the profile thickness. In these measurements, the same assumptions are made as in section 5.2 about the effects in the LE & TE region. The measurements were done as followed:

- Review performed on LM42.1 wind turbine blade at z = 35 meters
  For this review a 2D drawing a blade section of the LM42.1 was used, as this is the reference blade in the Hyller project. The profile thickness is reviewed at z = 35 meters as this is the split location.
- Profile thickness measured perpendicular to the chord
  The goal of these measurements is to determine the possible step height in the spar caps (see figure 1.5), so the profile thickness is measured perpendicular to the chord which in the same direction as the step.
- Profile thickness measured at five points in web region
  To compare the results from the measurements on 2D drawings with the results from section 6.1.2, it is required to measure the profile thickness on the same locations. As this was difficult, the profile thickness was measured at five points in the web region. From these points the average deviation in profile thickness was calculated. By also calculating the average deviation in profile thickness found in section 6.1.2 the results can be compared.
- Web positions assumed to deviate ±12 mm
  The web position measurements (described below bulled list) indicated deviations of 35 mm in web position at z = 37 and 22 mm at z = 38 mm. Therefore, it was chosen to assume that the webs can deviate ±12 mm in position.
- Web height assumed to deviate 0 to -3 mm
  In production the web height was varied by cutting the web in halve along its length and then gluing it back together. It was done in this way because all materials used for making webs had already been ordered. Therefore, the web height varied in production by 0, 1 or 2 cuts. As the height of a cut is approximately 1 mm, it is assumed that the web height varies with 0 to -3 mm.

[1] LE web: to LE, to TE, (counter-) clockwise rotation; idem for TE web
[2] Viewed from the blade tip while the blade is in the mould with UW up.

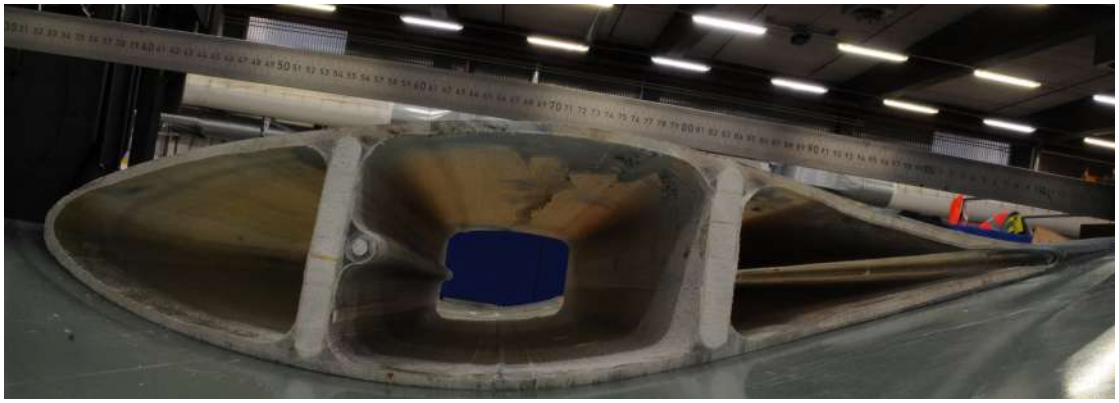

Figure 6.8: Picture of tip section produced with one-shot infusion and cure production process laying in the mould. From this picture the position and angle of each web can be determined.

- Web angle assumed to deviate 0 to +10 °
  The web position measurements (described below bulled list) indicated deviations up to +8°in web angle. So, it was chosen to assume that the webs can deviate 0 to +10°.

- Applying deviations a component
  When a deviation is applied to one of the webs, the shell position and angle need to be changed as well. Otherwise the shell thickness and gap between webs & shells size would not be constant. When this is done, the profile thickness can be measured.

For the comparison between the 2D measurements and the measurements from section 6.1.2, it is also necessary to know what the web position, angle and height was on each of the four measured tip sections. From production documentation the used web heights are known. To determine the web position and angle, a camera with manual zoom and a remote shutter was placed in the mould. Then each cut blade section was placed in the correct mould position as good as possible. By putting a ruler on top of the blade section it is possible to correlate the in-picture length with the real length in mm. With Inkscape the position of each web was determined relative to the LE and with an angle measurement tool the web angle could be measured. One picture of a tip section laying in the mould that was used for this is visible in figure 6.8.

6.3.2. Results of measurements

The results of the measurements on 2D drawings are shown in figure 6.9. These show that for each parameter the TE web has a stronger influence on the profile thickness compared to the LE web. Furthermore, the web position seems to be linearly related to the profile thickness for deviations up to ±12 mm. This also seems to be the case for the influence of the web height for deviations up to -3 mm and the web angle does not have a linear relation with the profile thickness for deviations up to +10°. These measurement results were also compared with the measured profile thickness deviations which are described in section 6.1.2. This to review if a trend, like the ones shown in 6.9, can be spotted. No similar trends could be observed, except for the TE web position. In figure 6.10 these trends are visualized. However, as these trend lines are based on only four data points for each z position, the result might be a coincidence.

As the aerofoils for z = 35, 37 & 38 meters are similar, a similar variation in profile thickness would be expected. The trend line based on the TE web position at z = 38 meters differs +3.85% in gradient from the gradient found in the 2D drawing for z = 35 meters. The trend line based on the measurements at z = 37 meters has a -19.2% difference in gradient. However, if the measurements of the fourth tip are excluded from this review, then the gradient of the trend line is only -0.096% different. This tip was reviewed more closely to determine if this measurement point can be marked as an outlier. This showed that for the webs of this tip section were made from a different and more flexible foam, leading to an additional variable. This could be a reason to exclude the fourth tip section from this review. However, this would also change the gradient of the trend line for the TE web at z = 38 meters, resulting in a +15% difference. As the TE web at z = 37 meters was further from the LE, it could be that it is compressed more due the usage of more flexible foam. Whereas the TE web at z = 38 meters was closer to the LE, which could mean that the compressional forces are smaller,

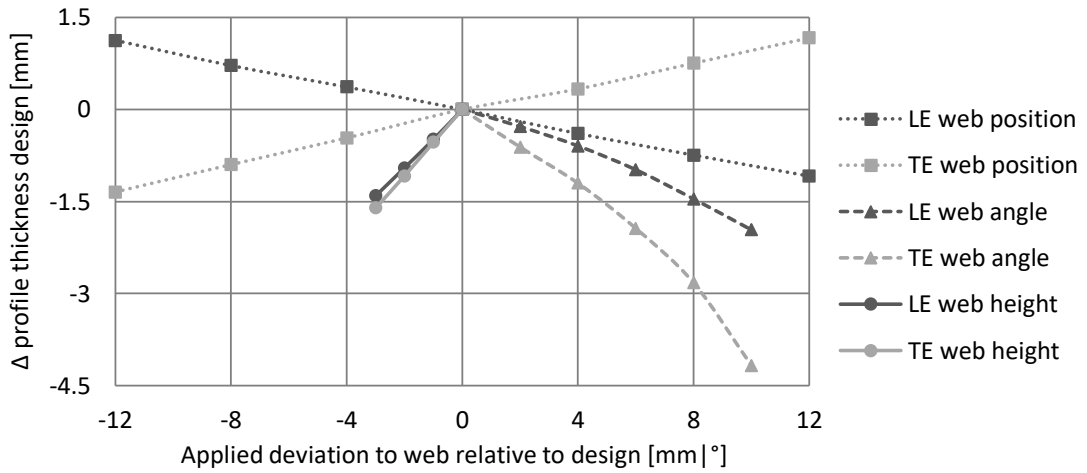

Figure 6.9: Deviations in profile thickness for differences in web position, location and height for z = 35 meters based on measurements on modified 2D drawings.

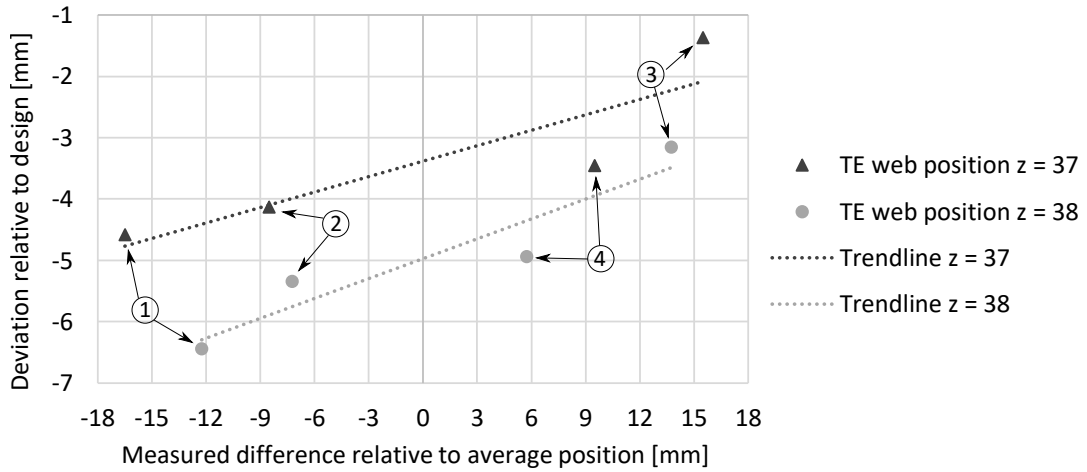

Figure 6.10: Influence of TE web position on profile thickness in web region. Deviations in profile thickness are relative to the design or the average of the measured web position. The encircled number shows which tip is related to which data points, the numbers are equal to the tip numbers in section 6.1.2.

and therefore the observed differences in profile thickness are smaller. To accurately determine the relation between the TE web position and the profile thickness more tip sections will have to be produced, measured and compared. In appendix E the other figures are shown which were used to determine if there are similar trend lines in the data from section 6.1.2 and figure 6.9.

6.4. Conclusion

In this chapter the blade to blade variation in profile thickness was reviewed. It was observed that this variation was larger as can be expected from shrinkage and measurement errors alone. Therefore, additional reviews were made to determine if the possible causes for this larger than expected variation could be found. With all these reviews the remaining research questions can be answered, of which the first one, research question 4, was defined as followed:

What is the blade to blade profile thickness consistency in the web region of wind turbine blade tip sections produced with a one-shot infusion and cure production process?

The blade to blade consistency in profile thickness in the web region of wind turbine blade tip sections, produced with a one-shot infusion and cure production process, is a variation in profile thickness smaller than +1 to -8 mm relative to the model. This is found in the measurements at 56 points, spread over two z

positions on four different tip sections. The variation in profile thickness relative to the model was expected to only come from shrinkage. With CLT it was calculated that this would result in a reduction of maximally of 0.22 mm. As the shrinkage should be similar on each blade, the blade to blade variation in profile thickness was expected to be even smaller. However, the used measurement process has a measurement error in the order of ±1 mm. So, the expected results of these measurements was a variation on the order of ±1 mm. As this was not the case, the initial assumptions could be incorrect. Therefore, questions 4.1 and 4.2 where was defined as followed:

What is the blade to blade profile thickness consistency in the web region due to closing the matched-die Hyller mould in the one-shot production process?

The blade to blade consistency in profile thickness in the web region due to closing the matched-die Hyller mould, in the one-shot production process, is a variation smaller than ±2 mm in profile thickness. It is not possible with the current test results to determine more precisely what the variation is, as the measurement error was in the order of ±1 mm. Since the total variation in profile thickness was found to be smaller than +1 to -8 mm relative to the model, the mould closure process and the shrinkage cannot be the only cause for the observed variation. So, it was also reviewed if this variation could be caused by variations in the web position, angle or height. With this review, an answer can be formulated for research question 4.2, defined as followed:

What is the influence of web location, -angle and -height on the profile thickness of wind turbine blade tip sections produced with a one-shot production process?

The web location, -angle and -height influence the profile thickness in the web region of wind turbine blade sections produced with a one-shot production process. For the web location, a linear relation between the deviation in web position and the deviation in profile thickness in the range ±12 mm was observed. This is similar for the web height for deviations up to -3 mm. And the web angle has a non-linear relation with the profile thickness for deviations up to +10°. Furthermore, in all cases the TE web had a bigger influence on the profile thickness than the LE web. This is most probably due to the lower curvature of the shells around the LE web as compared to the shell curvature around the TE web. When the observed deviations in the web parameters from the produced tip sections were also reviewed in relation to the deviations in profile thickness. The trend of the TE web position on the produced tip sections is similar to the trend observed on measurements of 2D drawings. A similar trend could not be spotted for the other variables.

The influence of the TE web position on the profile thickness was reviewed at the 2D drawing of the blade 35 meters from the root. And the profile thickness was measured at 37 and 38 meters from the blade root. Therefore, the influence of the TE web position might be different due to the different aerofoils. Only, due to the relatively small distance in between the measurement locations, the aerofoils have a similar geometry which should lead to a similar influence and trendline. When the TE web is placed closer to the TE of the blade, it slightly deforms the mould during the closure process, resulting in a thicker profile. Combining this with the results from the mould closure trials, it is might be possible to explain all the deviations in profile thickness as compared to the 3D CAD model. With the mould closure variation being smaller then ±2 mm relative to the average during the measurements and the TE web position causing maximally a 3 mm deviation (On the measured tip sections), the total deviation could be 7 mm. This is in the order of the measured variation in profile thickness. So, the mould closure process and the variation in TE web position could be the major causes for the observed profile thickness deviation. However, this is not a profound conclusion as only four tip sections were measured, and the measurement errors were relatively large. More tests are required to accurately measure the profile thickness variations and to determine the causes for the variations in profile thickness. These tests could for example be done with an 3D scanner. Furthermore, the observed trend on the influence of the TE web position has to be reviewed, as the found correlation could be a coincidence due to the combination of all variables. Only, it could also be that the variation in profile thickness is caused by deviations in mould geometry and that the shrinkage predicted with CLT is incorrect.

7

Conclusion & Recommendations

This thesis describes part of the Hyller project of LM Wind Power in which a tip split wind turbine blade was build and structurally tested. Developing wind turbine blades with split tips instead of single-piece blades should ultimately lead to a cost reduction for wind energy. These cost reductions are the result of: less expensive transportation, allowing for higher power yields because of increased blade lengths in sites with limited accessibility and possibly site-specific optimization of tip sections. Considering The Paris Agreement on carbon-dioxide reduction, wind energy is of increasing importance, since it could replace fossil fuels associated with high carbon-dioxide emissions. Innovation that makes wind energy more accessible and more affordable, will speed-up the energy transition to low carbon-dioxide energy sources. This research, therefore, aimed to contribute to wind turbine innovation by investigating if wind turbine blade sections of a tip split blade, can be aligned and joined on-site to yield a similar power output at rated speed as single-piece wind turbine blades. This was done by reviewing the following three subjects:

1. On-site alignment of wind turbine blades sections.
   As the transportation cost of wind turbine blades is dependent on the blade length, the cost of wind energy could be reduced if the length that needs to be transported at once can be reduced. Only this does require that the blade is aligned and joined on-site. Therefore, alignment tooling was built, and trial alignments were held to determine with what precision both sections can be aligned with one-another while using low cost alignment tooling. To be able to accurately align both parts, one should be able to accurately determine on-site the position and orientation of each blade section. A method currently used by LM Wind Power to determine positions on the blade after demoulding are mould marks. These are mostly used as reference points to position aerodynamic add-ons, only these do not require a high positional placement accuracy. Therefore, a review was made to determine the relative positional accuracy of mould marks. The conclusions and recommendations related to these subjects are described in section 7.1.

2. Aerodynamic impact of alignment deviations on tip-split blades.
   To achieve a similar power output for a tip-split blade as is achieved with a single piece blade (Operating in the same conditions and with the same blade length). One should know what alignment deviations are aerodynamically acceptable for a similar power output. Therefore, the impact of angular alignment deviations on the aerodynamic performance was reviewed by simulations. The aerodynamic effects of positional deviations were not reviewed as it was assumed that these only have a local effect on power output. The conclusions and recommendations that followed from these reviews are described in section 7.2.

3. Structural joining considerations.
   By splitting the blade, it is required to make a joint which lasts the lifetime of the blade. The joining technique and determining what alignment tolerances are required is out of scope for this project. However, to produce the blade sections in the Hyller project different production processes were used. This can result in blade geometry variations which could affect the structural strength of the joint. With the flapwise loads being critical on wind turbine blades, the blade to blade variation in profile thickness

was reviewed for blade sections in the joint region for the different production processes. The conclusions and recommendations related to the variation in profile thickness due to the used manufacturing processes are described in section 7.3.

7.1. Alignment tooling, process and mould mark reference points

A low-cost alignment tool, named the six-axis manipulator, was build. This tool was used with lasers to align actual size parts. With some training the alignment of both sections could be done in about half an hour. This time can be reduced further by optimizing the tools for simpler operation. Therefore, it is recommended to make production equipment electrically controlled to allow for fast and easy operation for the operators. When the used lasers in the alignment process indicated that the parts were aligned to within a mm from their designed position, a verification of the alignment with a 3D scanner was made. These scans showed that the tip section was aligned with a precision of $< \pm 3$ mm & $< \pm 0.15°$. (See section 7.2 for the effect of angular deviations on the power output)

This alignment accuracy was achieved with accurate reference points. An actual size tip piece was used in these alignment trials, that was cut into two pieces to get a tip and root section. The used reference points were scratches in the surface made before the blade section was cut into two pieces. As these scratches formed one continues line before the blade section was cut in two, they showed accurately whether both sections were aligned properly during the alignment process. To determine if mould marks can provide good reference points, their positional accuracy was reviewed. It was expected that the position of mould marks could vary due to chemical and thermal shrinkage. With thin classical lamination theory (CLT) an estimate was made of the shrinkage strains for different laminates. In most cases the measured movement strains of mould marks were comparable and slightly lower than the strains estimated with thin CLT. However, the measurement error was relatively large compared to the measured movement strains. Therefore, it is recommended to do more accurate experiments to determine if the predictions made with thin CLT always overestimate the movement strains. If that is the case, then it could be that the edge of the mark in the mould provides additional constrains that restrict the mould mark movement. More accurate tests can for example be done by using a 3D scanner to measure the movement strains on the laminates. While also measuring the peak curing temperature to make a more accurate prediction of the shrinkage with thin CLT.

As another trial, mould marks were used on the Hyller test article (TA) root to mark the y position of the LE point at two locations. A 3D scan revealed that both marks were only 0.4 mm off compared to the actual y position of the LE point. This showed that for short distances mould marks can be used as accurate reference points. Another weakness of using mould marks as reference points is that they are easily lost due to surface repairs, as was experienced during the production of the Hyller TA. Therefore, it is recommended to review if low cost 3D scanners could be used to determine the misalignments of the blade sections, eliminating the need for reference points. The alignment of the TA was further complicated by components of the separate blade sections being improperly dimensioned. A 3D scan revealed that the tip section deviated $< \pm 5$ mm & $< \pm 0.5°$. However, these misalignments were also caused in part by the gravity load. To correct for this, a gravity correction factor was determined with FEM to compensate the found deviations for the gravity load. Using such a gravity correction factor is standard practise at LM Wind Power when processing 3D scans of full blades. In the meantime, the structural testing of the TA has been finished and it passed all structural certification tests with only minor damages (at one of the production defect repairs outside the joint region). This proves that the achieved alignment accuracy was acceptable from a structural perspective. Only with the TA alignment being not as good as the alignment achieved during the during the alignment trials, it is recommended to build another tip section with properly dimensioned components and the same alignment process. This to determine if the precision achieved in the alignment trials can also be achieved in the production of separately produced (test) blades.

7.2. Effect of angular deviations on power output

The simulations of angular alignment deviations showed that a twist angle deviation in the order of $\pm 0.1°$ is roughly equal to a flapwise angular deviation in the order of $\pm 1°$ in terms of Δ power output, and $\pm 0.71°$ edgewise angular deviation[1]. This was also expected based on literature, only no literature was found that quan-

[1] Due to limited simulation data, a linear relation is assumed for the edgewise angular deviations between $\pm 0.5°$ & $\pm 1°$ to estimate a similar Δ power output

tified the angular deviations relative to one-another. Additional simulations were preformed to determine the relation of twist angle deviation on power output on wind turbine blades that also contain manufactured twist deviations. These simulations showed that the twist angle at the blade tip has a non-linear relation with the variation in power output for tip split wind turbine blades. A negative twist angle deviation of the blade tip will result in a marginally higher power output, and a plateau is formed. A positive twist angle error of the tip section will result in a non-linearly increasing loss of power. This was also expected based on how the lift of an aerofoil section changes when the angle relative to the local airspeed is varied. As this is what happens when twist angle deviations are applied.

For the twist angle deviations in the range of ±1°, the variation due to the manufactured twist deviations is of the same order of magnitude as the effect of twist alignment deviations. This results in the twist alignment deviations either reducing or increasing the variation in power output of a tip-split blade compared to a single-piece blade. Therefore, the relation between the variance in power output, due to twist errors, and the absolute average twist error of the tip section after joining was reviewed. This revealed an exponential relationship between the two. With the made assumptions about the manufactured twist deviations, single piece wind turbine blades were approximately in the middle of the reviewed range of absolute average twist errors of the tip section. As a result, the variance in power output can be reduced significantly, only this requires a large reduction in the absolute average twist error. Simultaneously, the variance in power output can become significantly worse, for which only a small increase in the absolute average twist error is required due to the exponential relationship.

Based on these results it was reviewed what twist alignment tolerances could lead to a similar or smaller variance in power output, for a turbine operating in the same conditions as were used during the simulations. This showed that a smaller and similar variance in power output is achieved with a twist alignment tolerance of ±0.25°. Furthermore, by first averaging the manufactured twist deviations and then aligning the twist angle with a tolerance of ±0.125° the variance in power output can be reduced significantly. From the alignment trials it is known that these twist alignment deviations are achievable with low cost alignment tooling. For the alignment tolerances of flapwise and edgewise angles, the angular alignment deviations were in the trails and on the TA smaller then ±0.5°. Based on simulation that compared the three angular deviations, the difference in power output due to a twist angle deviation of ±0.1° already causes a larger difference than a flapwise or edgewise angular deviation of ±0.5°. Therefore, it is recommended to set the tolerances for the flapwise and edgewise angular deviations to ±0.5° as it is achievable and has a small impact on the power output. However, when using these values as tolerances, it is recommended to review if this deviation is allowed with respect to the tower clearance for the flapwise deviation. It is also recommended to align the tip section with a negative edgewise angular deviation as this increases the power output. However, all these simulations have been performed on one wind turbine blade design operating at rated speed. Therefore, the following recommendations are made to review the impact of twist angle deviations on power output and the variance in power output:

- Review impact on power for other blade designs (length, split location, aerofoils).
- Review impact on power at other wind speeds.
- Review if the assumed manufactured twist angle deviations are an accurate representation of reality.
- Review with more twist misalignments at the blade split location.
- Review with other twist error reduction strategies on the tip section to reduce the variance in power output.
- Review how the pitch controller affects the power output on wind turbines, having three different blades with varying manufactured and alignment twist deviations.
- Review if the significantly reduced variance in power output results in an increase in AEP.
- Review if tip-split wind turbine blades can be designed and joined with a negative edgewise angle to increase the power output.

7.3. Variation in profile thickness due to production processes

The third subject which was reviewed was the variation in profile thickness in the web region for the two different production processes used in the Hyller project. This revealed that for a two-shell wind turbine blade production process, the shell & bondline thickness and web position influence the local profile thickness linearly in the web region. Furthermore, the bondline thickness has the biggest impact on profile thickness; the shells have the second biggest impact and the web position only has a minor impact for the reviewed placement deviations. In the current two-shell production process the web position could have much larger deviations. However, the open end at the tip of the root section allows for the usage of additional tooling that limits the positional deviations of the webs. Such a tool was also made as part of this thesis and the webs were approximately in the correct position on the TA. Only due to a shortage of time, the possible deviations in web position with this tool could not be reviewed. So, it is recommended to review how much the web position can deviate while using a web holder tool, similar in design as was used in this project. Furthermore, as the bondline thickness is controlled using distance plugs, it is recommended to limit the allowable distance plug heights, as this has the largest influence on the profile thickness in the two-shell production process. These results are based on measurements on 2D drawings, therefore, it is recommended to verify these findings with measurements on actual parts.

The blade to blade consistency in profile thickness in the web region of wind turbine blade tip sections, produced with a one-shot infusion and cure production process, is a variation in profile thickness of +1 to -8 mm relative to the model. This is caused in part by a variation in mould geometry due to the mould closure process. It was found that this causes a variation smaller than ±2 mm in profile thickness. Furthermore, it was reviewed if this variation in profile thickness could also be caused by the web location, -angle and -height. Based on measurements on 2D drawings, the web location has a linear relation between the deviation in web position and the deviation in profile thickness in the range ±12 mm. This is similar for the web height for deviations up to -3 mm. The web angle has a non-linear relation with the profile thickness for deviations up to +10°. Furthermore, in all cases the TE web had a bigger influence on the profile thickness then the LE web.

The results of these measurements on 2D drawings were compared to measured deviations of four produced tip sections. This only revealed a similar trend for the TE web position and the profile thickness. With the influence of the TE web position being reviewed on 2D drawings 35 meters from the blade root and measurements on the produced blade sections being done at 37 & 38 meters from the blade root, it is not a direct comparison. However, the observed trends are all similar. A possible explanation could be that the TE web is indeed the cause for the observed deviations in profile thickness. When the TE web is placed closer to the TE of the blade, it slightly deforms the mould during the closure process. This could possibly allow for relating the TE web position to all profile thickness differences. However, more research is required and therefore the following recommendations are made related to the one-shot infusion and cure production process:

- Review the variation in profile thickness on more blade sections with a more accurate measurement method. For example, with 3D scanners.
- Review the variation in profile thickness due to the mould closure process with a more accurate measurement method.
- Review in production if the position of the TE web does indeed have a direct relatable influence on the profile thickness.
- Review if both webs can be linked to one another, like is done in the two-shell production process. This would eliminate the ability for the webs to move independently and rotate.
- Review placement accuracy of webs and if it can be improved by using a placement tool.

Bibliography

[1] C. Hall, *Energy Return on investment*, ser. Lecture Notes in Energy. Springer International Publishing, December 2016, vol. 36.

[2] U. N. F. C. on Climate Change, "The paris agreement," http://unfccc.int/paris_agreement/items/9485.php Accessed 11/05/2017, November 2016.

[3] Y. Kumar *et al.*, "Wind energy: Trends and enabling technologies," *Renewable and Sustainable Energy Reviews*, vol. 53, pp. 209–224, 2016.

[4] S. Pfeifer, "Subsidy-free renewable projects on 'cusp of breakthrough'," https://www.ft.com/content/1960c6fe-2dea-11e8-a34a-7e7563b0b0f4 Accessed 30/04/2018, March 2018.

[5] J. Deign, "Subsidy-free renewable projects on 'cusp of breakthrough'," https://www.greentechmedia.com/articles/read/what-it-takes-to-get-subsidy-free-offshore-wind#gs.0iZzc8g Accessed 30/04/2018, April 2018.

[6] M. Peeters, G. Santo, J. Degroote, and W. V. Paepegem, "The concept of segmented wind turbine blades: A review," *Energies*, vol. 10, no. 8, p. 1112, 2017.

[7] J. Osborne, "As wind turbines grow, so does transportation challenge," https://www.houstonchronicle.com/business/energy/article/As-wind-turbines-grow-larger-so-does-the-6840315.php Accessed 22/08/2018, February 2016.

[8] A. Wagner, "Record-breaking transport of wind turbine blade," http://www.mammoet.com/en/news/record-breaking-transport-of-wind-turbine-blade/ Accessed 31/05/2017, August 2016.

[9] M. Froese, "Ge presents haliade-x, the world's most powerful offshore wind turbine," https://www.windpowerengineering.com/business-news-projects/ge-presents-haliade-x-worlds-powerful-offshore-wind-turbine/ Accessed 30/04/2018, March 2018.

[10] A. Dutton, T. Geiger, C. W. Kensche, M. Olesen, J. Korsgaard, and D. Van Delft, "Design concepts for sectional wind turbine blades," in *EWEC-CONFERENCE-*, 1999.

[11] A. Dutton, C. Kildegaard, T. Dobbe, R. Bensoussan, C. Kensche, F. Hahn, D. Van Delft, and G. De Winkel, "Design, structural testing, and cost effectiveness of sectional wind turbine blades," 2000.

[12] F. Hahn, C. Kensche, R. Paynter, A. Dutton, C. Kildegaard, and J. Kosgaard, "Design, fatigue test and nde of a sectional wind turbine rotor blade," *Journal of Thermoplastic Composite Materials*, vol. 15, no. 3, pp. 267–277, 2002.

[13] A. Dutton, C. Kildegaard, D. van Delft, G. de Winkel, C. Kensche, T. Dobbe, and R. Bensoussan, "Pg4. 19 the potential of sectional wind turbine blades," in *EWEC-CONFERENCE-*, 2001, pp. 310–313.

[14] Z. Qin, L. Zhang, K. Yang, J. Wang, C. Liao, and J. Xu, "Determining division location for sectional wind turbine blades," *Energies*, vol. 10, no. 9, p. 1404, 2017.

[15] S. B. Nielsen, "Analysis and prognosis of the energy market," in *Presentation at All Engineering Day of LM Windpower*. MAKE consultants, November 2017.

[16] S. Shafii, H. Obermaier, R. Linn, E. Koo, M. Hlawitschka, C. Garth, B. Hamann, and K. I. Joy, "Visualization and analysis of vortex-turbine intersections in wind farms," *IEEE transactions on visualization and computer graphics*, vol. 19, no. 9, pp. 1579–1591, 2013.

[17] P. J. Schubel and R. J. Crossley, "Wind turbine blade design," *Energies*, vol. 5, no. 9, pp. 3425–3449, 2012.

[18] D. Radford and T. Rennick, "Separating sources of manufacturing distortion in laminated composites," *Journal of Reinforced Plastics and Composites*, vol. 19, no. 8, pp. 621–641, 2000.

[19] J. C. Lin, "Review of research on low-profile vortex generators to control boundary-layer separation," *Progress in Aerospace Sciences*, vol. 38, no. 4-5, pp. 389–420, 2002.

[20] L. Gao, H. Zhang, Y. Liu, and S. Han, "Effects of vortex generators on a blunt trailing-edge airfoil for wind turbines," *Renewable Energy*, vol. 76, pp. 303–311, 2015.

[21] T. Burton, N. Jenkins, D. Sharpe, and E. Bossanyi, *Wind energy handbook*. John Wiley & Sons, 2011.

[22] J. D. Anderson, *Fundamentals of Aerodynamics*, 5th ed. Mc Graw Hill, 2011.

[23] C. Thumthae and T. Chitsomboon, "Optimal angle of attack for untwisted blade wind turbine," *Renewable energy*, vol. 34, no. 5, pp. 1279–1284, 2009.

[24] M. R. Ahmed, "Blade sections for wind turbine and tidal current turbine applications–current status and future challenges," *International Journal of Energy Research*, vol. 36, no. 7, pp. 829–844, 2012.

[25] Y. Bazilevs, M.-C. Hsu, J. Kiendl, and D. Benson, "A computational procedure for prebending of wind turbine blades," *International Journal for Numerical Methods in Engineering*, vol. 89, no. 3, pp. 323–336, 2012.

[26] T. Ashwill, G. Kanaby, K. Jackson, and M. Zuteck, "Development of the sweep-twist adaptive rotor (star) blade," in *48th AIAA Aerospace Sciences Meeting Including the New Horizons Forum and Aerospace Exposition*, 2010, p. 1582.

[27] S. Larwood, C. Van Dam, and D. Schow, "Design studies of swept wind turbine blades," *Renewable Energy*, vol. 71, pp. 563–571, 2014.

[28] R. Lanzafame and M. Messina, "Optimal wind turbine design to maximize energy production," *Proceedings of the Institution of Mechanical Engineers, Part A: Journal of Power and Energy*, vol. 223, no. 2, pp. 93–101, 2009.

[29] T. Dhert, T. Ashuri, and J. R. Martins, "Aerodynamic shape optimization of wind turbine blades using a reynolds-averaged navier–stokes model and an adjoint method," *Wind Energy*, vol. 20, no. 5, pp. 909–926, 2017.

[30] G. Petrone, C. de Nicola, D. Quagliarella, J. Witteveen, and G. Iaccarino, "Wind turbine performance analysis under uncertainty," in *49th AIAA Aerospace Sciences Meeting including the New Horizons Forum and Aerospace Exposition*, 2011, p. 544.

[31] M. S. Campobasso, E. Minisci, and M. Caboni, "Aerodynamic design optimization of wind turbine rotors under geometric uncertainty," *Wind Energy*, vol. 19, no. 1, pp. 51–65, 2016.

[32] H. Bendemra, P. Compston, and P. J. Crothers, "Optimisation study of tapered scarf and stepped-lap joints in composite repair patches," *Composite Structures*, vol. 130, pp. 1–8, 2015.

[33] L. Bloom, J. Wang, and K. Potter, "Damage progression and defect sensitivity: An experimental study of representative wrinkles in tension," *Composites Part B: Engineering*, vol. 45, no. 1, pp. 449–458, 2013.

[34] S. Mukhopadhyay, O. J. Nixon-Pearson, and S. R. Hallett, "An experimental and numerical study on fatigue damage development in laminates containing embedded wrinkle defects," *International Journal of Fatigue*, vol. 107, pp. 1–12, 2018.

[35] A. Reinarz, T. Dodwell, T. Fletcher, L. Seelinger, R. Butler, and R. Scheichl, "Dune-composites–a new framework for high-performance finite element modelling of laminates," *Composite Structures*, vol. 184, pp. 269–278, 2018.

[36] B. Yenilmez, M. Senan, and E. M. Sozer, "Variation of part thickness and compaction pressure in vacuum infusion process," *Composites Science and Technology*, vol. 69, no. 11-12, pp. 1710–1719, 2009.

[37] F. Acernese, M. Agathos, K. Agatsuma, D. Aisa, N. Allemandou, A. Allocca, J. Amarni, P. Astone, G. Balestri, G. Ballardin *et al.*, "Advanced virgo: a second-generation interferometric gravitational wave detector," *Classical and Quantum Gravity*, vol. 32, no. 2, p. 024001, 2014.

[38] GOM, "Gom acceptance test: Acceptance/reverification according to vdi/vde 2634, part 3," Recieved by email from Zebicon, December 2017.

[39] Y. Nawab, S. Shahid, N. Boyard, and F. Jacquemin, "Chemical shrinkage characterization techniques for thermoset resins and associated composites," *Journal of Materials Science*, vol. 48, no. 16, pp. 5387–5409, 2013.

[40] M. Shokrieh, S. Akbari, and A. Daneshvar, "A comparison between the slitting method and the classical lamination theory in determination of macro-residual stresses in laminated composites," *Composite Structures*, vol. 96, pp. 708–715, 2013.

[41] Y. Min, "Prediction of coefficients of thermal expansion and chemical shrinkage of laminate," LM Windpower internal document, 2017.

[42] C. Kassapoglou and S. Koussios, "Ae4asm109 - design and analysis of composite structures 1," TU Delft Master course Q3 2016-2017.

[43] D. Gay and S. V. Hoa, *Composite materials: design and applications*. CRC press, 2007.

[44] C. Dong, "Modeling the dimensional variations of composites using effective coefficients of thermal expansion," *Journal of composite materials*, vol. 43, no. 22, pp. 2639–2652, 2009.

[45] EWEA, "Wind energy's frequently asked questions (faq)," http://www.ewea.org/wind-energy-basics/faq// Accessed 28/08/2018.

[46] W. Phillips and D. Snyder, "Modern adaptation of prandtl's classic lifting-line theory," *Journal of Aircraft*, vol. 37, no. 4, pp. 662–670, 2000.

[47] M. J. Hossain, H. R. Pota, V. A. Ugrinovskii, and R. A. Ramos, "Simultaneous statcom and pitch angle control for improved lvrt capability of fixed-speed wind turbines," *IEEE Transactions on sustainable energy*, vol. 1, no. 3, pp. 142–151, 2010.

A

Scan data of trial alignments

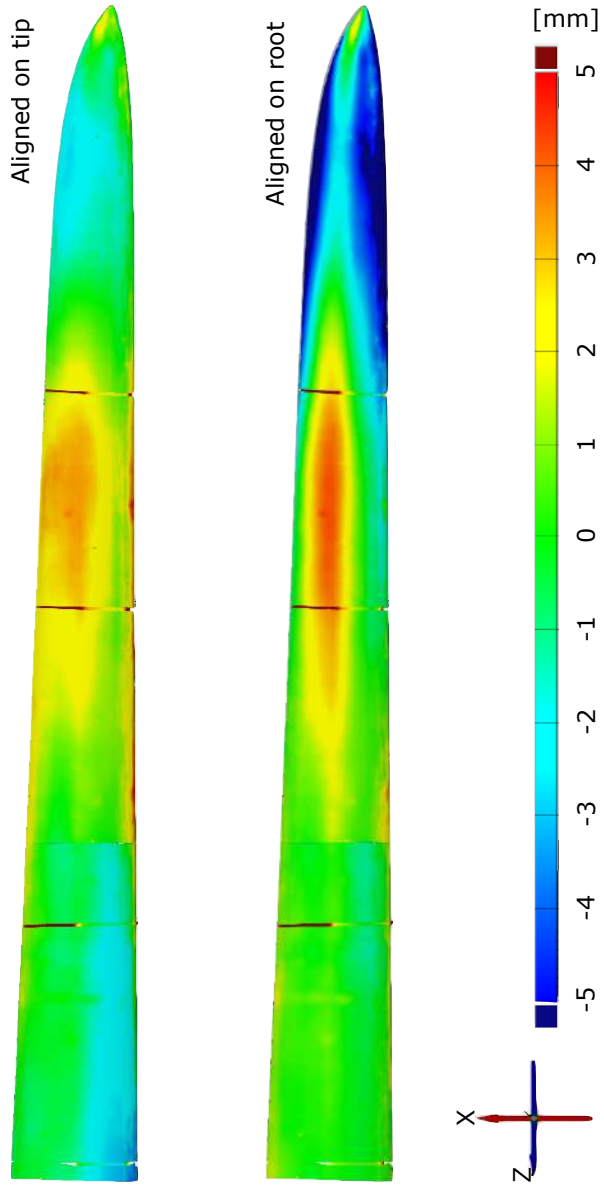

Figure A.1: Colour plot of deviations from first scanned alignment. Made by Zebicon with GOM scanner.

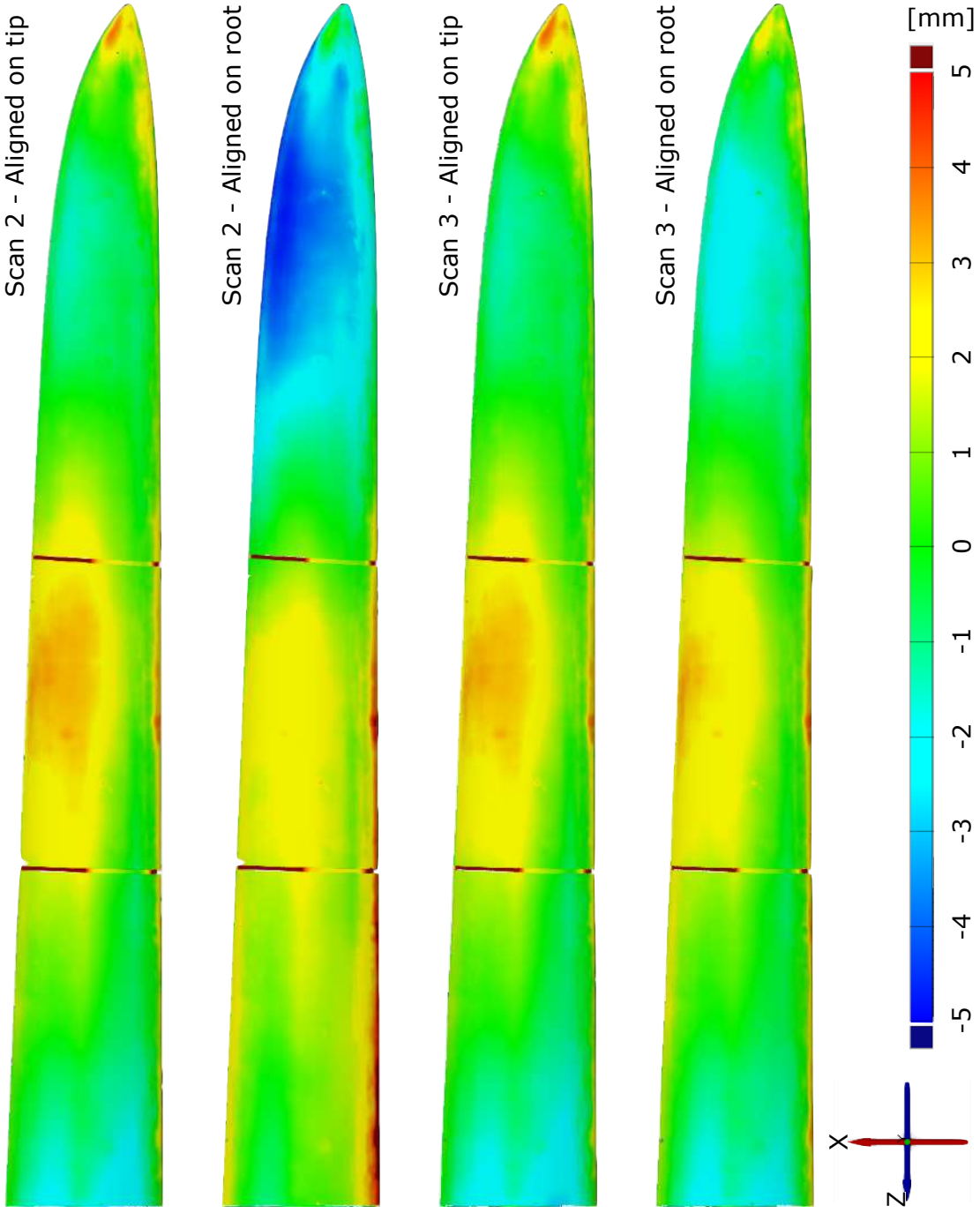

Figure A.2: Colour plot on tip of deviations from second and third scanned alignments. Made by Zebicon with GOM scanner.

B

Pictures of test article at the joint

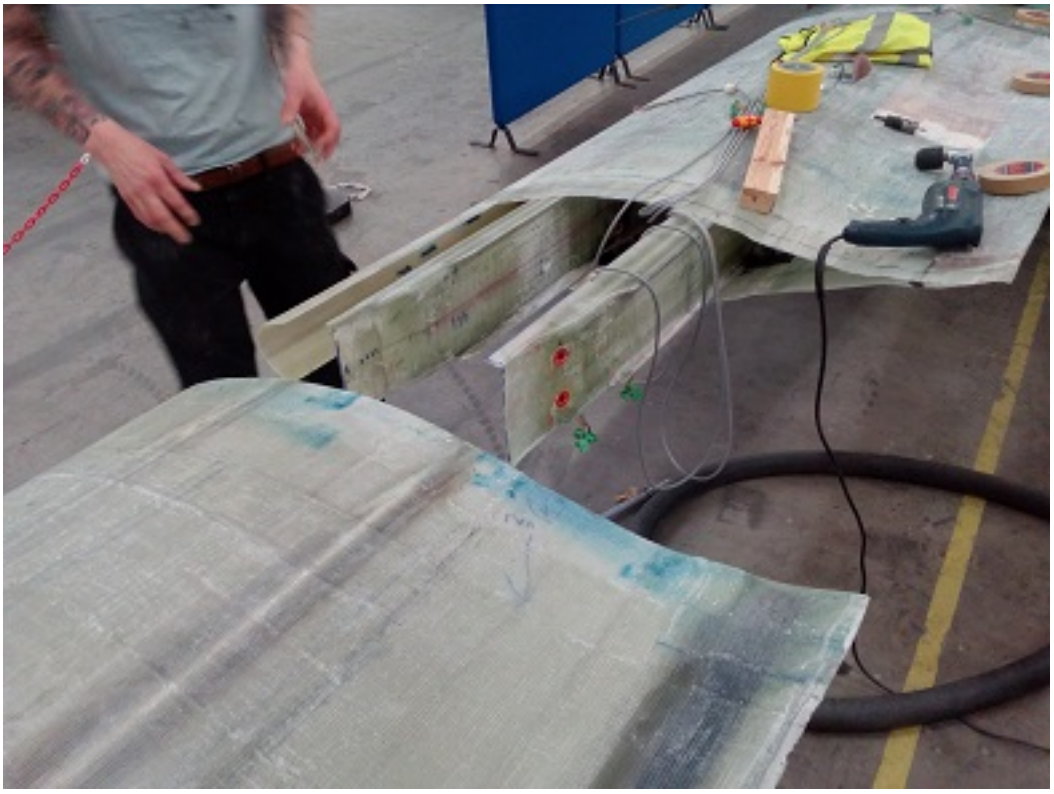

Figure B.1: View with the tip of root section and root of tip section prior to alignment.

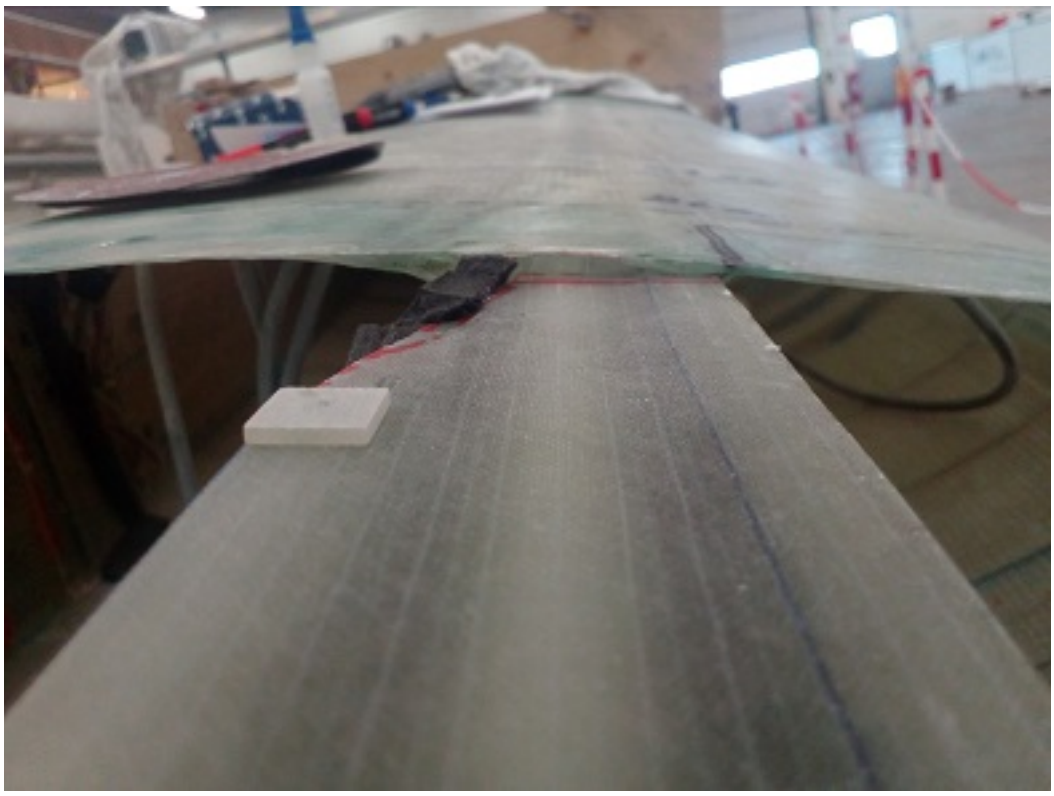

Figure B.2: Picture of tip shell almost resting on LE web. For a good alignment, the tip had to be moved down further.

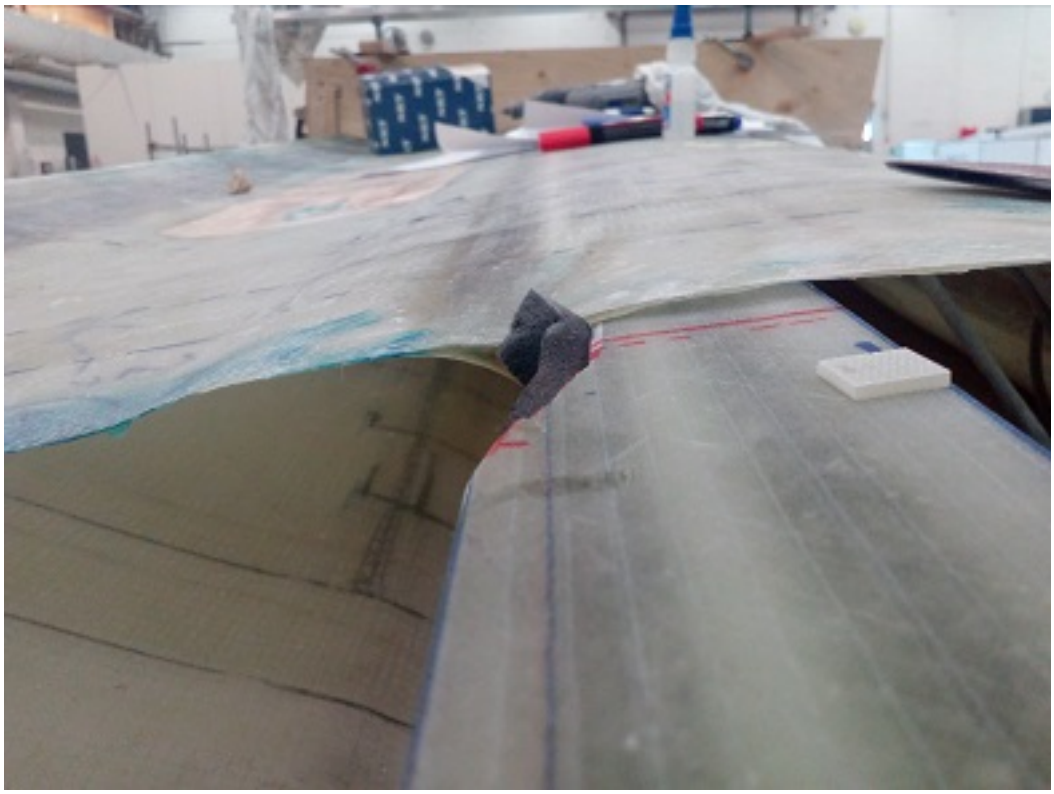

Figure B.3: Picture of tip shell resting on TE web. For a good alignment, the tip had to be moved down further.

Figure B.4: Picture of not-fitting LE glue flange, this prevented adjusting the tip to the correct position

Figure B.5: Picture of not-fitting LE glue flange, the cavity in-between the shell and flange was 32 mm, whereas the design was a constant cavity of 3 mm.

C

Twist simulation data

	Single piece	Tip A			Tip B			Joint A		Joint B	
		+/-1°	+/-0.75°	+/-0.5°	+/-0.25°	+/-0.875°	+/-0.625°	+/-0.375°	+/-0.125°	+/-0.5°	+/-0.25°	+/-0.5°	+/-0.25°
Total number of blades	42	210	202	178	118	210	206	126	42	378	168	378	168
Number of unique blades	28	140	132	116	76	140	136	84	28	140	84	140	84
ABS AVG tip error	0.360	0.336	0.313	0.300	0.296	0.283	0.222	0.254	0.216	0.175	0.125	0.176	0.024
Average power [%]	-0.15	-0.23	-0.20	-0.17	-0.12	-0.18	-0.18	-0.12	-0.08	-0.20	-0.16	-0.15	-0.11
Standard deviation	0.82	1.28	1.19	1.02	0.72	1.14	1.12	0.79	0.54	1.14	0.95	0.99	0.76
Variance	0.67	1.64	1.41	1.04	0.52	1.30	1.25	0.62	0.29	1.31	0.90	0.98	0.58
F-Test	1.00	0.00	0.01	0.10	0.30	0.01	0.02	0.71	0.01	0.01	0.27	0.14	0.49
Average thrust [%]	-0.09	-0.08	-0.08	-0.07	-0.07	-0.07	-0.05	-0.06	-0.06	-0.04	-0.04	-0.05	-0.03
Standard deviation	0.91	0.89	0.90	0.90	0.90	0.89	0.89	0.90	0.91	0.90	0.89	0.87	0.90
Variance	0.83	0.79	0.82	0.80	0.81	0.79	0.80	0.81	0.83	0.80	0.79	0.76	0.80
F-Test	0.96	0.83	0.92	0.87	0.89	0.82	0.82	0.48	1.00	0.87	0.82	0.72	0.93
Average FRBM [%]	-0.08	-0.07	-0.07	-0.06	-0.06	-0.06	-0.05	-0.06	-0.05	-0.04	-0.03	-0.04	-0.03
Standard deviation	1.10	1.07	1.08	0.99	1.00	1.03	0.96	1.05	1.04	0.97	0.93	0.97	0.95
Variance	1.21	1.13	1.16	0.98	0.99	1.06	0.93	1.10	1.08	0.94	0.87	0.93	0.90
F-Test	0.68	0.89	0.82	0.63	0.67	0.90	0.46	0.07	1.00	0.55	0.33	0.53	0.56

Table C.1: Overview of data used to from lifting line simulations for section 4.4.

D

LM42.1 blade to blade variations

The Hyller root is produced with the traditional two shell LM production method. Because this two shell production method is already in use for many years, it is possible to review the blade to blade variations. As a start, the production data of three plants in North-America from January till April 2017 were studied. In this time frame a total of 311 LM42.1 blades where produced in three different factories. On all the blades in this set the production tolerances stated in table D.1 where applicable. Note that only for the profile thickness a maximum value is defined. As an example all measured blade profile thicknesses at 35 meters from the root have been plotted in figure D.1. As is visible in this figure, no data points are outside the specified limits. A statistical analysis was performed to review the tolerance confidence intervals. To do this Matlab was used to make a non-parametric fit through the data, as it gave the best data fit.

D.1. Analysis results

For all different measurement points, except for the vacuum level, the mean, 90%, 95% and 99.7% confidence intervals were found and shown in table D.2 and D.3. Respectively compared with the mean or target value. For example, 90% of the produced blades will have a blade profile thickness at 35 meters of 224 mm +5.9 or -3.5 mm, where the set tolerances are ±7 mm. The results from these tables could thus be used to determine what the currently achieved tolerances are for 90%, 95% and 99.7% of the produced blades. A grey cell in these tables means that, statistically speaking, an out of specification value is expected. Therefore these cells are greyed out because this would require corrective action before the blade is released from the factory.[1]

From these tables it is clear that most blades are produced within a tighter then required tolerance band. Because the Hyller project is aiming for a split in the tip region, the measurements near the tip are reviewed per factory and mould per mould. So it can be determined if there are important differences. In figure D.2 the results are shown for the main laminate thickness with a 90% confidence interval.[2] The colours in this figure

[1] UW = Up Wind aerofoil side, DW = Down Wind aerofoil side. Or when compared to aeroplane wings respectively bottom and top side.
[2] Note that there is no value defined for the maximum main laminate thickness, see also table D.1.

Table D.1: Target value per category and allowable deviations for LM42.1 wind turbine blade

	Min	Target	Max	Tolerance	Unit
Main Laminate Thickness UW at 15000 mm from root	26.24	29.44	-	-3.2	mm
Main Laminate Thickness UW at 20000 mm from root	26.5	29.44	-	-2.94	mm
Main Laminate Thickness UW at 25000 mm from root	22.86	25.53	-	-2.67	mm
Vacuum level at infusion start upwind	80	85	-	-5	%
Main Laminate Thickness DW at 15000 mm from root	26.24	29.44	-	-3.2	mm
Main Laminate Thickness DW at 20000 mm from root	26.5	29.44	-	-2.94	mm
Main Laminate Thickness DW at 25000 mm from root	22.86	25.53	-	-2.67	mm
Blade profile thickness at 20.0 m from root	461	472	483	±11	mm
Blade profile thickness at 35.0 m from root	217	224	231	±7	mm

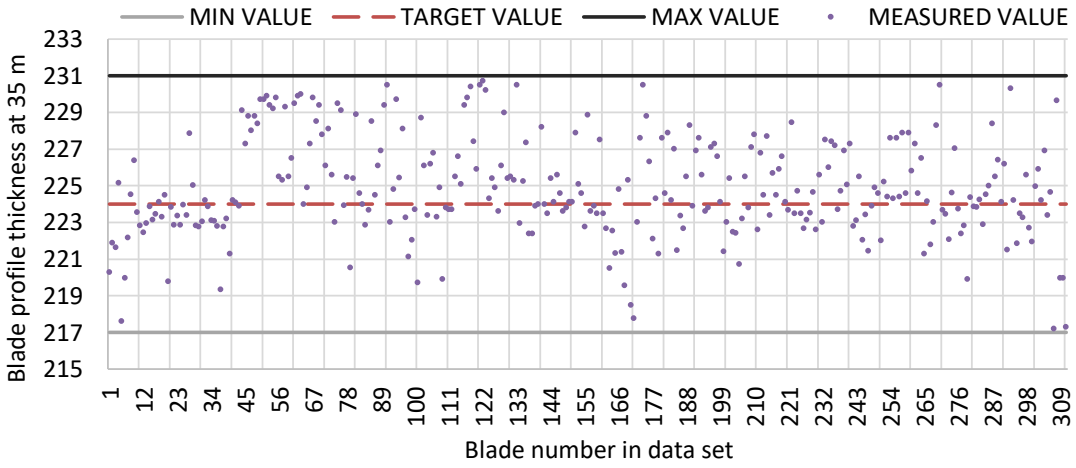

Figure D.1: Measured blade profile thickness at 35 meters from root for all 311 blades

[mm]			Mean	90%		95%		99.70%		100.00%	
Total	Blade profile thickness	20 m	472.7	5.8	-10.3	7.5	-11.2			10.3	-11.7
		35 m	224.6	5.3	-4.1	5.8	-5.3			6.4	-7.6
	Main laminate thickness UW	15 m	27.5	1.24	-0.89	1.62	-1.03	4.74			-1.3
		20 m	27.13	1.22		1.72		4.37			-0.6
		25 m	23.61	1.38		2.57		5.04			-0.8
	Main laminate thickness DW	15 m	28.12	1.42	-1.20	1.78		3.78			-1.9
		20 m	27.8	1.36	-1.00	1.71	-1.15	4.06			-1.3
		25 m	24.17	1.45	-1.02	2.6	-1.16	4.51			-1.3

Table D.2: Currently achieved tolerance confidence intervals on 42.1 blades produced in North-America with respect to mean

[mm]			Target	90%		95%		99.70%		100.00%	
Total	Blade profile thickness	20 m	472	6.5	-9.6	8.2	-10.5			11	-11
		35 m	224	5.9	-3.5	6.4	-4.7			7.0	-7.0
	Main laminate thickness UW	15 m	29.44	-0.7	-2.83	-0.3	-2.97	2.8			-3.2
		20 m	29.44	-1.1		-0.6		2.06			-2.9
		25 m	25.53	-0.5		0.65		3.12			-2.7
	Main laminate thickness DW	15 m	29.44	0.1	-2.52	0.46		2.46			-3.2
		20 m	29.44	-0.3	-2.64	0.07	-2.79	2.42			-2.9
		25 m	25.53	0.09	-2.38	1.24	-2.52	3.15			-2.7

Table D.3: Currently achieved tolerance confidence intervals on 42.1 blades produced in North-America with respect to target

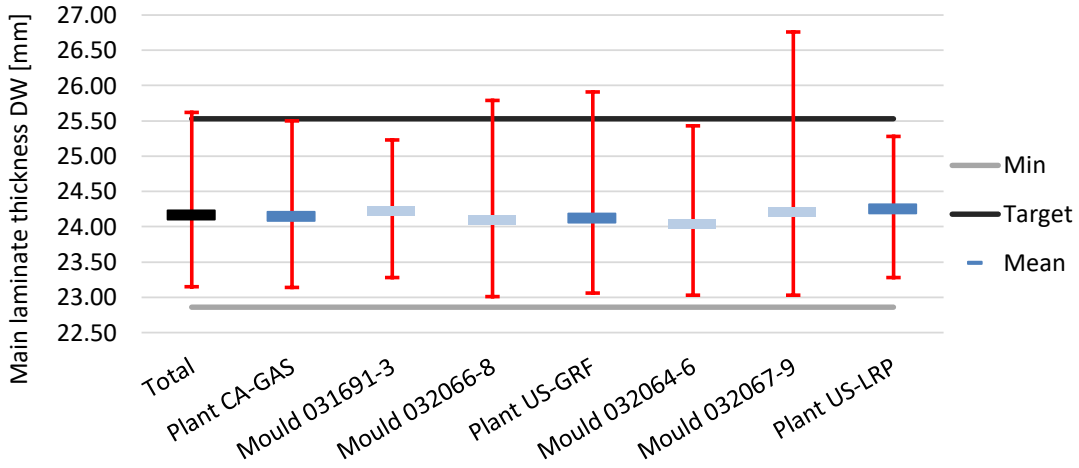

Figure D.2: Main laminate thickness comparison at 25 meters DW with a 90% tolerance confidence interval.

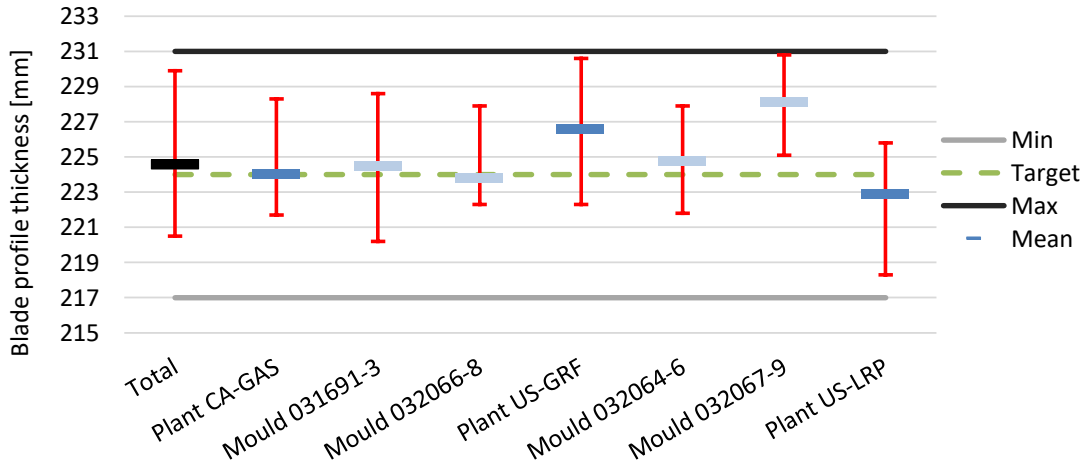

Figure D.3: Blade profile thickness comparison at 35 meters with 90% tolerance confidence interval

have the following meaning:

In black	The achieved tolerances with all factories combined
In dark blue	The achieved tolerances for that factory
In light blue	The achieved tolerances of a mould which is in the factory on the left (So mould 03169-3 and mould 032066-8 are in the CA-GAS plant) [The US-LRP plant only has one mould]

From figure D.2 it can be concluded that all the mean values are relatively close to each other, but the spread of main laminate thickness differs. See for example the results for mould 031691-3 and 032067-9. In figure D.3 a similar graph is shown which compares the blade profile thickness at 35 meters. Again, most means are relatively close to the target value. Except for one mould, which has a mean that is 4.1 mm above the target value. The spread in the main laminate thickness was largest for the same mould.

D.2. Results from the second data set

Because there where only 311 blades in the first data set, a second data set was obtained to do additional analyses. This second data set includes all LM42.1 blades being produced in the period 2013 till June 2017. So this set also includes blades that have been produced in China and India. In total about 7993 blades are in this data set. Unfortunately, not all data on each produced wind turbine blade was complete. Therefore

Shell thickness		22 - 23.49	23.5 - 24.49	24.5 - 25.49	25.5 - 40
Mould 5	average	224.01	224.34	224.20	223.84
	Stdev	0.94	0.76	0.81	1.08
Mould 6	average	224.48	224.45	224.33	224.11
	Stdev	1.77	1.47	1.20	0.84
Mould 9	average	225.45	224.66	223.80	225.93
	Stdev	2.89	2.39	1.73	2.98

Table D.4: Average and standard deviation for different blade profile thicknesses and shell thicknesses

Mould 5	Mean	Upper bound	Lower bound
All	224.28	1.32	-1.46
1:50	223.15	1.95	-0.9
51:100	223.8	1.55	-1.4
101:150	224.15	1.45	-2.1
151:200	224.15	1.51	-1.51
201:250	224.31	1.8	-2.03
251:300	224.47	1.32	-1.36
301:350	224.14	1.43	-1.26
351:400	224.43	1.11	-1.99
401:450	224.57	1.17	-1.94
451:500	224.27	1.51	-1.63
501:550	224.32	1.37	-1.52
551:600	224.46	1.18	-1.43
601:650	224.46	1.18	-1.42
651:700	224.27	1.59	-1.29
701:750	224.58	1.2	-1.47
751:800	224.27	1.38	-1.58

Table D.5: Varing in mean and 90% confidence interval

these blades could not be used in the analysis. Comparing figures D.2 and D.3 it seemes like there could be a correlation between the shell thickness and the blade profile thickness. See for example mould 032067-9, it has the highest main laminate thickness deviations (figure D.2) and also the highest mean (figure D.3).

Since the shell thickness is presumed to be effected by the vacuum level, an analyses was performed to see if correlations between the vacuum level, shell thickness and blade profile thickness could be found. The results for the shell thickness and blade profile thickness are visible in table D.4. Only for mould 6 a trend can be seen, namely that the standard deviation reduces if the shell thickness increases. However, this is not the case for the other two moulds used in this comparison. So it does not seem that there is a correlation. Further study would be required to determine if this is indeed the case. Lastly, also an attempt was made to determine if a trend could be spotted with respect to the tolerances when the moulds age. For this analysis mould 5 was used, for which the mean and upper & lower 90% confidence bounds where found for every 50 produced blades. The results are visible in table D.5. As is visible, the mean value does not change significantly over time. Also, the upper & lower 90% confidence bounds are fairly stable. So the achieved tolerances do not seem to change when the mould gets older. This could also be expected when looking at a plot of all the blades being produced within this mould, see figure D.4.

D.3. Conclusion

The North-America data set does show that most blades are produced with tolerances which are about half the width of the allowed tolerance width. From a study on the second data set it can be concluded that there is not a clear correlation between the main laminate and blade profile thickness. This is also the case for achieved tolerances and mould age. Next to that, it seems that the plants in North-America are the plants with the largest blade to blade variation (See figures D.1 & D.4).

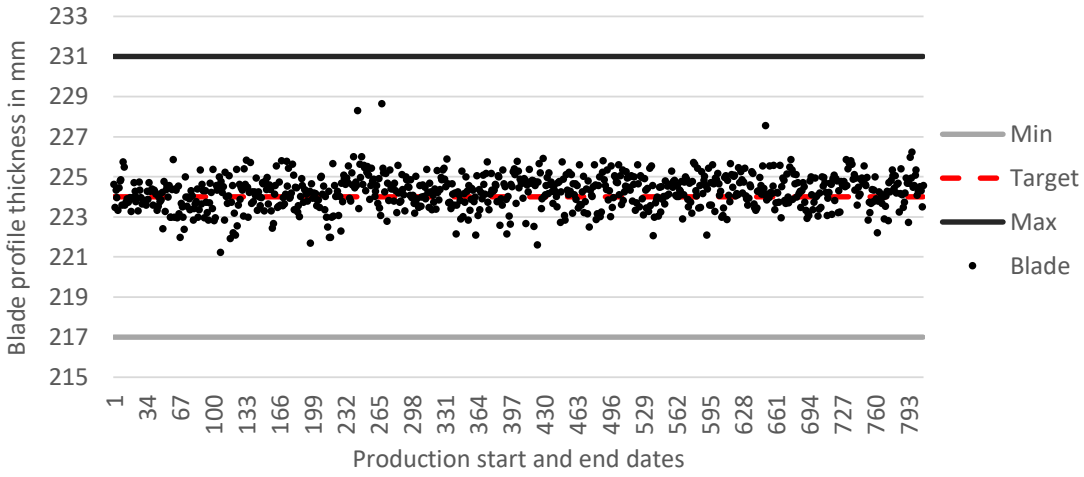

Figure D.4: Blade profile thickness comparison at 35 meters for mould 5

E

Measurement results: influence of shear web position, angle & height on profile thickness

In figures E.1, E.2 & E.3 the influences of each parameter on the profile thickness is shown. Based on the results from the measurements on 2D drawings, each parameter has a measurable influence on the profile thickness. As was noted before, the TE web position has a stronger influence on the profile thickness compared to the LE web position. The differences in profile thickness as were observed on the produced tip sections do not have a similar trend as was found in the measurements of the 2D drawings. Only in figure E.3 a trend can be observed. This shows that a higher shear web results in a lower profile thickness, a reversed relation as compared to what was found in the 2D measurements. Also, the trend line does not fit the data very well. Therefore this seemingly present relation is ignored.

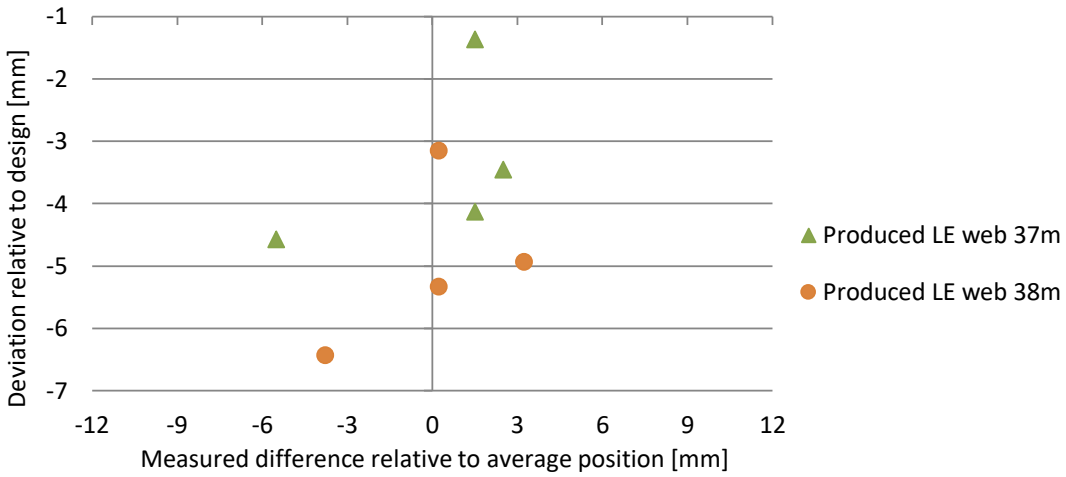

Figure E.1: Influence of LE shear web position on profile thickness in shear web region. Deviations in profile thickness are relative to the design or the average of the measured shear web position.

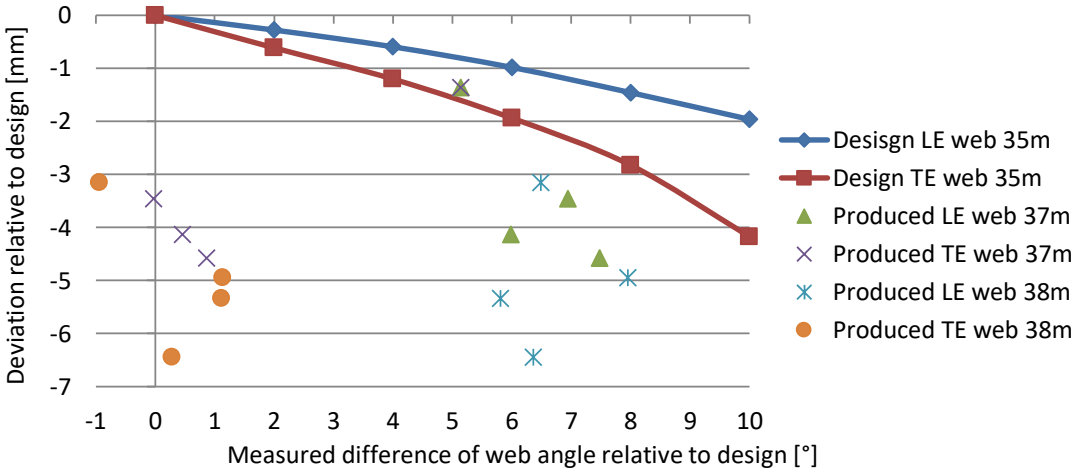

Figure E.2: Influence of LE & TE shear web angle on profile thickness relative to the model.

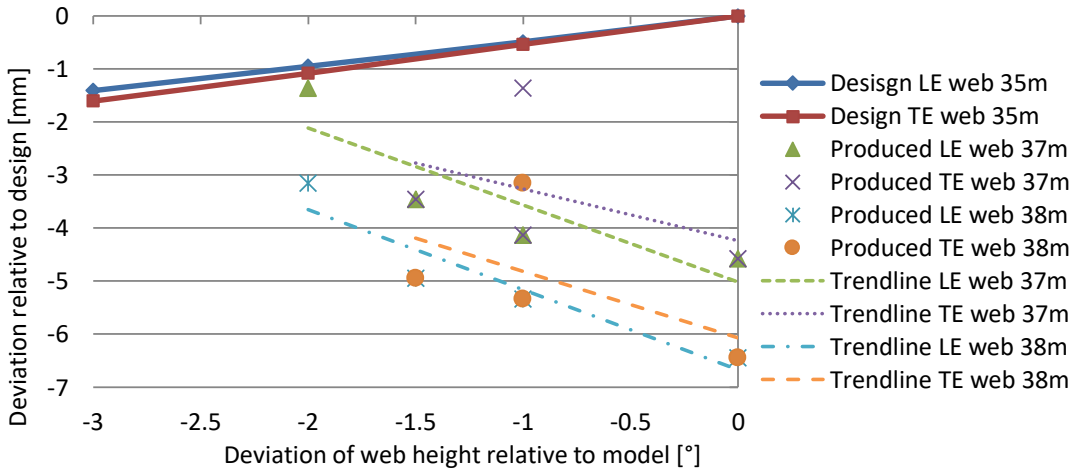

Figure E.3: Influence of LE & TE shear web height on profile thickness relative to the model.